

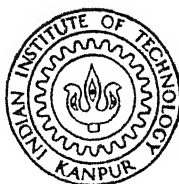
EXCHANGE - CORRELATION EFFECTS IN ATOMS : A COUPLED - CLUSTER APPROACH

By

S. SHANKAR

CHM

TH
CHM/1981/D
Sh



DEPARTMENT OF CHEMISTRY

INDIAN INSTITUTE OF TECHNOLOGY KANPUR

AUGUST, 1981

1981

D

SHA

EXC

EXCHANGE - CORRELATION EFFECTS IN ATOMS : A COUPLED - CLUSTER APPROACH

A Thesis Submitted
in Partial Fulfilment of the Requirements
for the Degree of
DOCTOR OF PHILOSOPHY

By
S. SHANKAR

to the

DEPARTMENT OF CHEMISTRY
INDIAN INSTITUTE OF TECHNOLOGY KANPUR
AUGUST, 1981

Approved - 10-2-82

70622

13 MAY 1982

TO
MY PARENTS

DEPARTMENT OF CHEMISTRY
INDIAN INSTITUTE OF TECHNOLOGY KANPUR

CERTIFICATE I

This is to certify that Mr. S. Shankar has satisfactorily completed all the courses required for the Ph.D. degree programme. These courses include :

CHM	500	Maths for Chemists I
CHM	501	Advanced Organic Chemistry I
CHM	521	Chemical Binding
CHM	523	Chemical Thermodynamics
CHM	524	Modern Physical Methods in Chemistry
CHM	534	Electronics for Chemists
CHM	541	Advanced Inorganic Chemistry I
CHM	600	Maths for Chemists II
CHM	624	Valence Bond and Molecular Orbital Theories
CHM	800	General Seminar
CHM	801	Graduate Seminar
CHM	900	Graduate Research

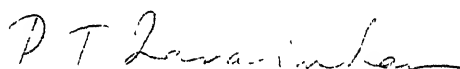
Mr. S. Shankar was admitted to the candidacy of the Ph.D. degree in October 1975 after he successfully completed the written and oral qualifying examinations.

U.C. Agarwala
(U.C. Agarwala)
Professor & Head
Department of Chemistry
I.I.T., Kanpur.

P.C. Nigam
(P.C. Nigam)
Convener
Departmental Post Graduate Committee
Department of Chemistry
I.I.T. Kanpur.

CERTIFICATE II

Certified that the work contained in this thesis entitled "Exchange-Correlation Effects in Atoms : A Coupled-Cluster Approach" has been carried out by Mr. S. Shankar under my supervision and the same has not been submitted elsewhere for a degree.



(P.T. Narasimhan)

Professor

Department of Chemistry
I.I.T. Kanpur.

Thesis Supervisor

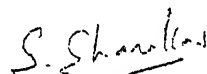
Kanpur
August, 1981

15/8/82
8

STATEMENT

I hereby declare that the matter embodied in this thesis is the result of investigations carried out by me in the Department of Chemistry, Indian Institute of Technology, Kanpur, India under the supervision of Professor P.T. Narasimhan.

In keeping with the general practice of reporting scientific observations, due acknowledgements have been made wherever the work described is based on the findings of other investigators.


S. Shankar

ACKNOWLEDGEMENTS

It gives me great pleasure to express my sincere gratitude to my supervisor Professor P.T. Narasimhan for his stimulating ideas, invaluable advice and constant encouragement. I have benefitted immensely through the several inspiring discussions, I have had with him.

I wish to record my gratitude to my teacher Professor V.R. Srinivasan, Osmania University for kindling my interest in Chemistry. Thanks are due to Dr. Debhashis Mukherjee, Indian Association for the Cultivation of Science for his interesting lectures on many-body theory. Several members of the IIT Kanpur faculty have evinced keen interest in my welfare during my stay at Kanpur; many thanks are due to them.

I am very happy to be able to record my thanks to my colleagues, Dr. Harihara Subramanian for his help and encouragement, Mr. Thankachan for his invaluable help with computation, Mr. Ramachandran and Mr. Narasimha Reddy for their timely help and Miss Amrita Tripathi without whose unflagging help the manuscript would never have attained this shape.

It is impossible to express through words my gratitude to my innumerable friends, who were instrumental in making my stay at IIT/K a memorable one. Special thanks are due to my friends, Bhat, Hollen, Kishore, Okhil, Pradeep, Prakash,

Ramaswamy, Ravichandran and Sanjeev for their companionship and help. I also owe a lot to my young friends, whom I had the privilege of tutoring, for endlessly stimulating me with creative ideas and thoughts.

I would like to place on record my thanks to Dr. Tewari and members of the staff, Computer Centre, IIT/K for providing the excellent computing facilities and to Mr. Karnal Singh for the hard copy program print out.

Many thanks are due to Professor M.V. George for kindly providing his typewriter and to my friend Abraham for performing admirably, the excruciating task of threading his way through the maze of symbols and notations while typing the thesis.

Financial assistance from the Council of Scientific and Industrial Research, India is also gratefully acknowledged.

S. Shankar

SYNOPSIS

EXCHANGE-CORRELATION EFFECTS IN ATOMS :
A COUPLED-CLUSTER APPROACH
A Thesis submitted
In Partial Fulfilment of the Requirements
for the Degree of
DOCTOR OF PHILOSOPHY
by
S. SHANKAR
Department of Chemistry
Indian Institute of Technology, Kanpur
August, 1981

This thesis attempts to study the exchange-correlation (EC) effects in atoms using the powerful coupled-cluster many-body theory. Many-electron EC effects have attracted much attention in theoretical chemistry. One of the approaches to the study of EC effects is to start from an independent particle model and introduce refinements that account for the residual inter-electron interactions. The Hartree-Fock approximation has traditionally served as the independent particle model for most of these studies. In this thesis, we use the Slater $X\alpha$ approximation, which is a local potential model, to provide the reference starting point for the study of EC effects in atoms. Our aim is to assess the effectiveness of this local potential model in representing EC effects in atoms, as compared to the Hartree-Fock model.

The coupled-cluster (CC) many-body theory of Coester, Kummel and Cizek has been used in this thesis. The CC

methodology relies on the cluster expansion of the wavefunction and uses the language of second quantisation, the associated Feynman graphology and the powerful linked-cluster theorem. Further, the methodology encompasses several sophisticated many-electron methods like, the coupled electron-pair approximation, Nesbet-Bethe-Goldstone approach and a hierarchy of approximations to many-body perturbation theory.¹ Earlier studies have used the Hartree-Fock method to provide the reference independent particle approximation for the CC expansion. Surprisingly, this expansion method has been used merely for the purpose of obtaining accurate correlation energies although its versatility extends well beyond. In fact, the method can be used to advantage for studying the independent particle approximations that serve as reference points.

^In this thesis, the CC methodology and its allied approximations are used to evaluate EC corrections to the $X\alpha$ potential and to provide an insight into the nature of the potential vis-a-vis its effectiveness in representing the true EC potential. Empirical and semi-empirical modifications to the $X\alpha$ method are also examined in this light, with a view to gauge their efficacy in improving upon the parent independent particle approximation.¹ It is hoped that a study such as that made in this thesis will provide a rational basis for the choice of local potentials that describe the EC effects in atoms more accurately.

The thesis consists of five chapters, a bibliography of the references cited in the text of the thesis and two appendices.

Chapter I of the thesis reviews the state of the art with reference to the treatment of many-electron interactions in atoms. The independent particle approximations normally in vogue and the methods to go beyond these are discussed. The linked-cluster expansion which forms the basis of the present work is discussed briefly, in the context of perturbation theory. The chapter concludes with the delineation of the scope of the thesis.

Chapter II introduces the CC methodology and its basis. With the aid of Appendix A, this chapter attempts to provide a detailed explanation of the Feynman-Goldstone graphology, which is used to derive the CC equations. Expressions for the correction to the EC energies and equations that define the cluster coefficients are explicitly given. A comparison of the CC methodology with various other many-electron theories is made with a view to highlight its powerfulness.

Chapter III presents a model calculation on beryllium atom to illustrate the application of the CC methodology and the approximations derived from it, in the context of evaluation of corrections to EC energy. Computational details are also given.

Chapter IV deals with the detailed analysis of the $X\alpha$ potential through the EC corrections obtained as described in the previous chapter. For the purpose of this analysis, the ideal many-body atomic systems, beryllium and Be-like four electron ions are studied. The role of the exchange parameter, α , in the local potential model and refinements to the $X\alpha$ potential are examined with reference to the EC corrections. Attempts are made to obtain physically meaningful insights into the nature of the $X\alpha$ approximation.

Chapter V reports the expectation values of some operators over the wavefunctions obtained through the CC expansion for the systems discussed in the previous chapter. The results are compared with the reference state expectation values.

The thesis concludes with some salient remarks on the application of the CC methodology for the study of EC effects in atoms. A few interesting features emerge from the present analysis of EC effects. Firstly, the CC methodology is seen to be extremely versatile and superior to its other many-electron counterparts. And, it can be used to assess the merit of the independent particle approximations that provide the reference states. With specific reference to the $X\alpha$ method the analysis reveals that the $X\alpha$ local potential describes very accurately the inner-shell EC effects, as is evidenced by the $1s^2$ pair corrections in Be isoelectronic series. On the other hand, the valence-shell EC effects are poorly

described by this local potential. It can be surmised from the analysis of EC effects that for obtaining accurate description of many-electron interactions in atoms with the $X\alpha$ method, it will suffice to improve upon the valence-shell description also, to achieve this correction through CI-like procedures, it will suffice to consider a very limited basis set of $X\alpha$ orbitals.

Appendix A presents a brief discussion on the language of second quantisation, Feynman-Goldstone graphology as applied to many-body perturbation theory, fourth-order Raleigh-Schrödinger perturbation theory and cancellation of the unlinked diagrams, the hole-particle formalism, Wick's theorem and contractions and illustration of the elementary Feynman-Goldstone diagrams used in this thesis.

Appendix B lists some of the computer programs used in the present study.

CONTENTS

	Page
CERTIFICATE I	i
CERTIFICATE II	ii
STATEMENT	iii
ACKNOWLEDGEMENTS	iv
SYNOPSIS	vi
CHAPTER I INTRODUCTION	1
CHAPTER II THE COUPLED-CLUSTER FORMALISM	35
CHAPTER III A MODEL CALCULATION OF EXCHANGE-CORRELATION CORRECTIONS USING COUPLED-CLUSTER METHODOLOGY	74
CHAPTER IV ANALYSIS OF EXCHANGE-CORRELATION EFFECTS IN BERYLLIUM ISOELECTRONIC SERIES	92
CHAPTER V EXPECTATION VALUES OF SOME ONE-ELECTRON OPERATORS WITH CLUSTER-EXPANDED WAVEFUNCTIONS	121
CONCLUSIONS	135
BIBLIOGRAPHY	138
APPENDIX A	144
APPENDIX B	168

For some time I have been worrying about what new developments in theoretical chemistry are likely to be most important in the next 10-15 years. One has to hazard a guess. Twenty years ago we opted for group theory, and turned out to be absolutely right:..... Today something new must be encouraged. Rightly or wrongly we have decided on diagram methods.

*C.A. COULSON
in Oxford Theoretical Chemistry
Department Progress Report
1972-73.*

CHAPTER I

INTRODUCTION

- I.1 The Schrödinger Equation
- I.2 The Independent Particle Approximation (IPA)
 - I.2.1 The Hartree and Hartree-Fock Methods
 - I.2.2 Local Potential Methods
- I.3 Exchange and Correlation
- I.4 Beyond the Independent Particle Approximation
 - I.4.1 Drawbacks in IPA
 - I.4.2 The CI Method
 - I.4.3 Electron-Pair Methods
 - I.4.4 The r_{12} Method
 - I.4.5 Perturbation Methods
 - I.4.6 Linked-Cluster Theorem and Many-Body Perturbation Theory
 - I.4.7 Other Field-Theoretic Methods
- I.5 Beyond IPA with Specific Reference to Local Potential Methods
- I.6 Scope of the Thesis

I.1 THE SCHRÖDINGER EQUATION

The non-relativistic Schrödinger equation,

$$\hat{H} |\psi\rangle = E |\psi\rangle \quad (I.1)$$

provides a theoretical framework for the quantum mechanical description of a many-electron atomic system with \hat{H} as the Hamiltonian operator[#] and E , the energy. The many-electron state function $|\psi\rangle$ in configuration space, obtained as a solution of the above equation contains, in principle, all possible information about the system. It is a function of the space and spin coordinates of all the electrons of the system. However, the equation is not exactly solvable except for the simplest case of one-electron atomic systems [1] *, owing to the presence of the interelectron interaction terms in the Hamiltonian. It becomes, therefore, necessary to resort to approximations that are mathematically tractable, physically meaningful and reasonably accurate. The problem simplifies considerably in the case of atoms due to the separability of nuclear and electronic motions. The first

[#] All quantum mechanical operators will be represented with a "▲" on top of the corresponding symbol.

* Numbers in square brackets pertain to literature references which appear at the end of this thesis.

step in the solution of the many-electron Schrödinger equation would be to reduce the N -electron equation to N one-electron equations. This is the leit motiv behind all the independent particle approximations. These approximations, however, fail to portray correctly the many-body effects that originate from simultaneous interaction between many electrons. The exact treatment of this many-body problem is complicated. Although several sophisticated methods have been developed for solving the problem, the state of the art can be said to be still in a nascent stage. An effort is made in this thesis to describe the many-body interactions between electrons in atoms using the coupled-cluster (CC) method; this appears to be the most promising in the many-body theory horizon.

I.2 THE INDEPENDENT PARTICLE APPROXIMATION (IPA).

I.2.1 The Hartree and Hartree-Fock Methods

The underlying premise in all these approximations is that every electron moves independent of the other electrons, i.e. in an averaged field produced by all other electrons and nuclei. The choice of description of the averaged field and its proximity to the exact description varies from model to model. In the case of an atom, the averaged field can be conveniently located at the centre and the ensuing spherical symmetry of the potential reduces the complexity of the problem considerably. The averaged potential, $\hat{V}(r)$, then depends on the radial part of the wavefunction, $R(r)$, which in

turn depends on $\hat{V}(r)$ and so both $\hat{V}(r)$ and $R(r)$ have to be determined together in an iterative way.

The problem of setting up a self-consistent field (SCF) was first outlined by Hartree [2]. He assumed that the field of all electrons on a particular electron can be approximated by the electrostatic action of their averaged charge density. The one-electron equations of Hartree can therefore be written as [3]

$$[-\hat{V}_i^2(1) + \hat{V}_C(1) + \hat{V}_{Xi}(1)] \phi_i(1) = \epsilon_i \phi_i(1) \quad (I.2)$$

where,

$$\hat{V}_C(1) = \frac{-2Z}{r_1} + \sum_j n_j \int \frac{\phi_j^*(2) \phi_j(2)}{|r_1 - r_2|} d\tau_2 \quad (I.3)$$

and

$$\hat{V}_{Xi}(1) = -n_i \int \frac{\phi_i^*(2) \phi_i(2)}{|r_1 - r_2|} d\tau_2 \quad (I.4)$$

Atomic units have been used alongwith the usual notation [3].

\hat{V}_C is the field arising from the nuclear charge and the total charge density of all the electrons in the system and \hat{V}_{Xi} is the term that corrects the coulombic term for the self-interaction of the electron. The decomposition of the N-electron function into a simple product of N one-electron functions is tacitly implied by the above method. This coupled with the application of the variation theorem for obtaining the energy extremum yields the one-electron equations [4], that were obtained through intuitive arguments by

Hartree. The Hartree method fails to depict the Fermion characteristic of the many-electron system; also it does not account for the instantaneous interaction of the electrons, a shortcoming inherent in all the independent particle models. The Fermi-Dirac Statistics [5], when incorporated into the SCF method through the use of determinantal wavefunction [6] yields the Hartree-Fock one-electron equations [7]

$$[-\hat{\nabla}_i^2 + \hat{V}_C(1)] \phi_i(1) - \sum_j n_j \int \phi_j^*(2) \phi_i(2) \frac{1}{|r_1 - r_2|} d\tau_2 \phi_j(1) = \epsilon_i \phi_i(1) \quad (I.5)$$

The last term on the left-hand side (LHS) of the equation (I.5) now includes in addition to the self-correction term

$$- \int \phi_i^*(2) \phi_i(2) \frac{1}{|r_1 - r_2|} d\tau_2 \phi_i(1) \text{ the terms,} \\ - \sum_{j \neq i} n_j \int \phi_j^*(2) \phi_i(2) \frac{1}{|r_1 - r_2|} d\tau_2 \phi_j(1) \quad (I.6)$$

characterised as exchange terms. The only non-vanishing contributions in eqn. (I.6) arise from the summation over the orbitals ϕ_j which have the same spin as ϕ_i , owing to the orthogonality constraints. The term can be elegantly recast in the form of a potential multiplying the orbital ϕ_i

$$\hat{V}_{HFXi}(1) = \frac{- \sum_j n_j \int \phi_i^*(1) \phi_j^*(2) \phi_j(1) \phi_i(2) (1/|r_1 - r_2|) d\tau_2}{\phi_i^*(1) \phi_i(1)} \quad (I.7)$$

This form yields greater insight into the above, since this is the potential of a charge whose magnitude is one-electronic charge removed from a hole surrounding the location of electron 1 [8]. This hole, termed as the Fermi hole, accounts for the correlation of like-spin electrons but cannot account for the correlation of unlike-spin electrons. Therefore, the last term on the LHS of eqn. (I.5) should be corrected for the coulombic correlation of unlike-spin electrons.

I.2.2 Local Potential Methods

The solution of the Hartree-Fock (HF) equations is beset by two main problems associated with the exchange-correlation (EC) potential. Firstly, the potential is different for different orbitals. Secondly, the EC potential is non-local in the sense that it cannot be written as a simple product of the type $V(r) \phi(r)$. In fact, it assumes the form $\hat{V}(r) \phi(r)$, where

$$\hat{V}(r) = \int d\tau_2 \hat{V}(r, r') \phi(r') \quad (I.8)$$

These two factors complicate the HF equation enormously and any further simplification should focus attention on these two problems. The first problem can be overcome by using the average value of the potential over all the orbitals, so that a single EC potential is common to all one-particle equations [8]. The second problem is more complicated; concomitant to the non-local nature of the potential is the

non-uniform distribution of the electron density. This non-uniformity prevents the treatment of the many-electron system as a homogeneous electron gas, a problem that has been solved elegantly by Pines [9]. However, inhomogeneous electron gas problems have been solved, albeit approximately, using local EC potentials [8,10,11].

All these methods assign a key role to one-electron density $\rho(\mathbf{r})$ and utilise a local density potential, thus eliminating the need to solve many-dimensional integrals. A rigorous theoretical justification for such local-density potential methods is provided by the theorem of Hohenberg and Kohn [12]. The theorem states that the ground-state energy of an inhomogeneous electron system is a unique functional of density $\rho(\mathbf{r})$. For a given external potential $\hat{V}(\mathbf{r})$

$$E[\rho(\mathbf{r})] = \int \hat{V}(\mathbf{r}) \rho(\mathbf{r}) d^3\mathbf{r} + F[\rho(\mathbf{r})] \quad (1.9)$$

This theorem merely proves the existence of a unique functional and offers no insight into its exact nature. However, a number of approximate functionals have been proposed to suit various types of many-electron systems [13,14]. The energy functional can be decomposed into various terms and eqn. (1.9) rewritten as

$$E[\rho(\mathbf{r})] = \int \hat{V}(\mathbf{r}) \rho(\mathbf{r}) d^3\mathbf{r} + \frac{1}{2} \int \frac{\rho(\mathbf{r}) \rho(\mathbf{r}')}{|\mathbf{r} - \mathbf{r}'|} d^3\mathbf{r} d^3\mathbf{r}' + T_S[\rho(\mathbf{r})] + E_{XC}[\rho(\mathbf{r})] \quad (1.10)$$

where in the right-hand side (RHS) the second term corresponds to the classical coulombic interaction, the third to the kinetic energy of the non-interacting many-electron system with density $\rho(\mathbf{r})$ and the last term, E_{XC} to the EC energy term. The function $E[\rho(\mathbf{r})]$ attains its minimum value for the exact ground-state density. Exploiting the formal similarity between the Hartree equation and eqn. (I.10), a set of one-particle equations can be obtained [15]

$$\left\{ \frac{\hbar^2}{2m} \nabla^2 + \hat{v}(\mathbf{r}) + \int \frac{\rho(\mathbf{r}')}{|\mathbf{r}-\mathbf{r}'|} d^3\mathbf{r}' + \hat{v}_{XC}(\mathbf{r}) \right\} \phi_i(\mathbf{r}) = \epsilon_i \phi_i(\mathbf{r}) \quad (\text{I.11})$$

The Lagrange parameters ϵ_i arise from the charge normalization constraint. In the above equation the potential v_{XC} , is the functional derivative of the EC energy

$$v_{XC}(\mathbf{r}) = \frac{\delta E_{XC}[\rho(\mathbf{r})]}{\delta [\rho(\mathbf{r})]} \quad (\text{I.12})$$

All the many-body effects are included in this EC potential, $\hat{v}_{XC}(\mathbf{r})$, which in contrast to the HF potential, is local. The construction of potentials $v_{XC}(\mathbf{r})$ is central to all local-density potential schemes.

As a first approximation, the many-electron system may be regarded as a homogeneous electron gas. The EC potential, v_{XC} in eqn. (I.12) may then be approximated as the "exchange-only" potential of the homogeneous electron gas [10,11,16]. The exchange energy of the electron gas [17]

$$E_{XC}[\rho(r)] = -\int \frac{3}{2} \left(\frac{3}{8\pi} \right)^{1/3} \rho(r)^{4/3} d^3r \quad (I.13)$$

gives the exchange potential

$$v_{XC}[\rho(r)] = -2 \left[\frac{3}{4\pi} \rho(r) \right]^{1/3} \quad (I.14)$$

The total energy equation (I.10) may then be solved variationally to determine the lowest energy [15,18]. A similar approximation to v_{XC} had earlier been obtained by Slater [8]. He replaced the exact HF potential in the one-electron equation by the free-electron exchange potential and obtained a value.

$$v_{XC} = -3 \left[\frac{3}{4\pi} \rho(r) \right]^{1/3} \quad (I.15)$$

This differs from the Gaspar, Kohn and Sham (GKS) [15,18] value by a factor of 3/2. This is so because, the order of the two steps taken, one variational in nature and the other an approximation, differ in the two methods. In the GKS method the electron gas exchange approximation is made first and then the variation is taken, while in Slater's method [8] the variation is taken before the approximation is made. Since, the two steps do not commute with each other, the potentials differ by a multiplicative constant. It is worth noting that in atomic calculations, local EC potentials mentioned above cannot be expected to reproduce the HF exchange potentials, owing to the non-uniformity of the electron density distribution in atoms.

To account for slight non-uniformities in charge density, vis-a-vis the Fermi-hole shape, in a semi-phenomenological manner, Slater [19], advocated the introduction of a parameter α , such that

$$v_{XC} = -3\alpha \left[\frac{3}{4\pi} \rho(r) \right]^{1/3} \quad (I.16)$$

There is no minimum principle associated with the dependence of the total energy on α and consequently α cannot be determined variationally. However, various methods for determining α have been postulated and a review of these methods is given by Slater [20]. The method, known as the X_α method, is non-variational to the extent of α being an arbitrary parameter. Also, it only retains the spirit of the theorem of Hohenberg and Kohn [12] and cannot be deemed to follow directly from the theorem. Nonetheless, the X_α method has numerous merits and successes to its credit [21]. At the theoretical level, the method satisfies both the Hellman-Feynman [22] and the virial theorems [23] and the energy expression rigorously leads to Fermi-Dirac Statistics [20]. At the computational level, it has decided superiority over the HF method, where the ease of computation is concerned. Also it reproduces with at least as much accuracy [24], the double-zeta basis atomic HF results of Clementi [25].

I.3 EXCHANGE AND CORRELATION

Since quantum chemical literature is replete with confusion about the definition of correlation energy and EC energy, it is necessary to clearly delineate these terms. Correlation energy is defined [26] as the energy difference between the exact non-relativistic energy, E_{NR} , and the HF single determinant energy E_{HF} ,

$$E_{corr} = E_{NR} - E_{HF} \quad (I.17)$$

The HF energy includes contributions due to the correlation between like-spin electrons originating from the Pauli exclusion principle. On the other hand, approximations to the HF potential, like that defined by eqn. (I.14) cannot be strictly termed as "exchange" potentials. By virtue of these not being variationally determined potentials, they include some correlation although a clear-cut demarcation between exchange and correlation cannot be made. Any corrections to methods using such potentials should be rightly termed as EC corrections and not as correlation energy corrections.

I.4 BEYOND THE INDEPENDENT PARTICLE APPROXIMATION

I.4.1 Drawbacks in IPA

The independent particle models satisfy admirably, most quantum chemical computational needs and are rarely in error of greater than 1%, where total energies of atoms

and molecules are concerned. However, by their very nature, they suffer from the drawback of approximating the instantaneous, inter-electron potential by an averaged one-particle potential, thereby inexactly accounting for the entire correlations between electrons [26]. This shortcoming becomes particularly serious where small energy differences between different electronic states or different geometries (for molecules) are concerned [27]. In such cases the error in energy due to electron correlation may parallel the energy differences themselves. Also, where two-electron properties are concerned, the role of electron correlation may be very important [28]. There is a need, therefore, to treat the motion and interaction of electrons exactly; and the independent particle models which so nearly mimic the actual interactions can serve as excellent starting points for more exact treatments.

As mentioned earlier, the HF method takes into account a large portion of the dynamic correlation between the electrons with like-spins, whereas it neglects entirely the correlations between unlike-spin electrons. The local density potential methods also neglect a part of electron correlation although a clear-cut distinction, like the neglect of unlike-spins electron correlation, as in the case of HF method cannot be made. In these models the correlation errors can be attributed to the approximation

of non-uniform electron density distributions by uniform density distributions; and hence this warrants a different kind of analysis of correlation effects. Besides this, there is also a non-dynamical correlation error peculiar to the HF-like models. In these models, the set of single particle basis states, may give rise to several degenerate configurations, and choice of any one configuration alone may cause the model to break down [29].

The attempts to go beyond the IPA can be broadly categorised into two divisions; viz., traditional and modern methods. These methods include (a) the method of configuration interaction (CI) involving the expansion of the wavefunction in terms of several configurations [30]; (b) the electron-pair function treatments [31]; (c) the method of incorporating the inter-particle coordinates directly into the wavefunction [32]; (d) the classical perturbation expansion methods which are derived from the CI method [33]; (e) the many-body perturbation methods [34] and (f) other field-theoretic methods like the CC [35] and Green's function methods [36]. In the ensuing discussion, no efforts are made to compartmentalize these methods and due emphasis is laid only on their conceptual development and inter-relationship.

I.4.2 The CI Method

The method of configuration interaction [37] owes its

origin to two well established principles; one, the expansion of the configuration function in terms of a complete or near complete basis of one-electron functions [32] and the other, the Ritz method of linear variations [38]. Conceptually, this implies the expansion of the cusp-like behaviour of the exact wavefunction in a Fourier series. The method employs the linear expansion ansatz for the trial wavefunction ψ ,

$$\psi = \sum_{v=1}^N C_v \phi_v \quad (I.18)$$

where ϕ_v are predetermined expansion functions and C_v are the variational parameters constrained to minimise the energy functional

$$E = \langle \psi | \hat{H} | \psi \rangle / \langle \psi | \psi \rangle \quad (I.19)$$

A formally exact solution to the N-particle problem is obtained, if and only, if all the N-tuple excitations are considered [39], i.e. ψ is chosen such that

$$\psi = \phi_0 + \sum_{\alpha} C_{\alpha}^r \phi_{\alpha}^r + \sum_{\alpha < \beta} \sum_{r < s} C_{\alpha\beta}^{rs} \phi_{\alpha\beta}^{rs} + \dots \quad (I.20)$$

All the ϕ 's are orthonormal Slater determinants. ϕ_{α}^r denotes the Slater determinant obtained by replacing the orbital α by r in ϕ_0 ; $\phi_{\alpha\beta}^{rs}$ denotes the Slater determinant obtained by replacing α and β by r and s in ϕ_0 , and so on. In general, we shall use the label $\alpha, \beta \dots$ for occupied orbitals and r, s, \dots for unoccupied orbitals.

Indices $i, j \dots$ will be used to represent either type of orbitals.

Inserting eqn. (I.18) into $H\Psi = E\Psi$ and left-multiplying by ϕ_μ yields

$$\sum_{\nu} H_{\nu\mu} C_{\nu} = EC_{\mu} \quad (\text{I.21})$$

where

$$H_{\nu\mu} = \langle \phi_{\nu} | \hat{H} | \phi_{\mu} \rangle$$

When $\phi_{\mu} = \phi_0$, it immediately follows from eqn. (I.21) that,

$$\begin{aligned} \langle \phi_0 | \hat{H} | \phi_0 \rangle C_0 + \sum_{\alpha r} \langle \phi_0 | \hat{H} | \phi_{\alpha}^r \rangle C_{\alpha}^r + \sum_{\alpha < \beta} \sum_{r < s} \langle \phi_0 | \hat{H} | \phi_{\alpha\beta}^{rs} \rangle C_{\alpha\beta}^{rs} \\ = EC_0 \end{aligned} \quad (\text{I.22})$$

This equation can be rewritten as,

$$E = E_0 + \sum_{\alpha} \epsilon_{\alpha} + \sum_{\alpha < \beta} \epsilon_{\alpha\beta} \quad (\text{I.23})$$

with $E_0 = \langle \phi_0 | \hat{H} | \phi_0 \rangle$

$$\epsilon_{\alpha} = \frac{1}{C_0} \sum_r \langle \phi_0 | \hat{H} | \phi_{\alpha}^r \rangle C_{\alpha}^r$$

$$\epsilon_{\alpha\beta} = \frac{1}{C_0} \sum_{r < s} \langle \phi_0 | \hat{H} | \phi_{\alpha\beta}^{rs} \rangle C_{\alpha\beta}^{rs}$$

The coefficients are determined by projecting the Hamiltonian with various excited states ϕ_{ν} .

With $\phi_{\nu} = \phi_{\alpha}^r$

$$\begin{aligned} \langle \phi_{\alpha}^r | \hat{H} | \phi_0 \rangle C_0 + \sum_s \sum_{\beta} \langle \phi_{\alpha}^r | \hat{H} | \phi_{\beta}^s \rangle C_{\beta}^s + \sum_{\beta} \sum_{\delta < s < u} \langle \phi_{\alpha}^r | \hat{H} | \phi_{\beta\delta}^{su} \rangle C_{\beta\delta}^{su} \\ + \sum_{\beta < \delta < \epsilon} \sum_{s < u < w} \langle \phi_{\alpha}^r | \hat{H} | \phi_{\beta\delta\epsilon}^{suw} \rangle C_{\beta\delta\epsilon}^{suw} = EC_{\alpha}^r \end{aligned} \quad (\text{I.24})$$

with $\phi_v = \phi_{\alpha\beta}^{rs}$,

$$\begin{aligned}
 & \langle \phi_{\alpha\beta}^{rs} | \hat{H} | \phi_0 \rangle C_0 + \sum_{\delta} \sum_u \langle \phi_{\alpha\beta}^{rs} | \hat{H} | \phi_{\delta}^u \rangle C_{\delta}^u \\
 & + \sum_{\delta < \epsilon} \sum_{u < w} \langle \phi_{\alpha\beta}^{rs} | \hat{H} | \phi_{\delta\epsilon}^{uw} \rangle C_{\delta\epsilon}^{uw} \\
 & + \sum_{\delta < \epsilon < \eta} \sum_{u < w < x} \langle \phi_{\alpha\beta}^{rs} | \hat{H} | \phi_{\delta\epsilon\eta}^{uwx} \rangle C_{\delta\epsilon\eta}^{uwx} \\
 & + \sum_{\delta < \epsilon < \eta < \xi} \sum_{u < w < x < y} \langle \phi_{\alpha\beta}^{rs} | \hat{H} | \phi_{\delta\epsilon\eta\xi}^{uwx y} \rangle C_{\delta\epsilon\eta\xi}^{uwx y} = EC_{\alpha\beta}^{rs}
 \end{aligned}
 \tag{I.25}$$

This projection can be continued till ϕ_v is an n-fold substituted determinant. All the coefficients are then obtained and the hierarchy of equations yields the upper bound of the exact energy. The coefficients are coupled in a complicated manner such that, even though C_0 , C_{α}^r and $C_{\alpha\beta}^{rs}$ determine the energy, a knowledge of C_{α}^r requires $C_{\alpha\beta}^{rs}$ and $C_{\alpha\beta\delta}^{rsu}$ and that of $C_{\alpha\beta}^{rs}$ requires $C_{\alpha\beta\delta}^{rsu}$ and $C_{\alpha\beta\delta\eta}^{rsuw}$. The solution of the entire hierarchy is computationally unmanageable and this necessitates the truncation of the wavefunction expansion and concomitantly the hierarchy of equations. A reasonable truncation point is the set of double excited determinants and this leads to various electron-pair theories [31,40,41]. This truncation, however, voids the separability criterion for energy. The energy of an N-particle system can be decomposed into contributions

arising from one-particle terms, simultaneous interaction of two-particles, simultaneous interaction of three particles, etc.[42]. This decomposition in terms of energies of clusters of one, two, three, etc. particles is unique. All these clusters must be linked in the sense, that an N -body cluster is not decomposable into $(N-1)$ and 1 body clusters, e.g., the energy arising from simultaneous interaction of 4-particles cannot be written down as a product of two 2-particle interactions. This is necessitated by the fact that energy, an extensive property, depends only on N , while the contribution from unlinked clusters would be proportional to higher powers of N [43]. While in complete CI this linkedness is automatically taken into account, truncated CI incorporates several of the spurious unlinked cluster terms, thereby causing a breakdown of the variational energy extremum principle [44]. This serious problem, termed size-extensivity problem common to perturbation theories as well, is highlighted with a view to emphasise on the unphysical nature of basis truncations. The magnitude of this problem becomes transparent in fourth-order perturbation theory, which is discussed later in Appendix A. Besides

the size-extensivity problems, the CI method suffers from other computational handicaps. Firstly, the number of reference functions needed to obtain meaningful results is enormous. The complexity is apparent from the fact that the number of symmetry-adapted CI configurations for a given level of excitation is approximately $\left[(n N/2)^1 / (1!)^2 s \right]$ where l is the level of excitation, n is the number of basis functions, N is the number of electrons and s is a symmetry factor that should be between 2 and 10. For a simple case of a 10-electron system with excitations upto $l = 4$, this amounts to about 10^6 configurations! Besides, the convergence of the method with increase in the level of excitations is extremely slow.

I.4.3 Electron-Pair Methods

The CI method can also be modified to deal with, instead of an N -electron problem, an $N(N-1)/2$ electron-pair problem [31,45]. A justification for this reduction originates from two reasons : (i) the Pauli Principle prevents

more than two electrons from occupying the same point in space and (ii) the many-electron Hamiltonian consists of no more than two-particle operators. In view of this, the correlation problem could be solved independently for each pair of particles in a many-particle system [46]. The correlation energy obtained in this case would be formally equivalent to that obtained with the approximation,

$$\Psi = \Phi_0 + \sum_{\alpha\beta} \sum_{rs} C_{\alpha\beta}^{rs} \Phi_{\alpha\beta}^{rs} \quad (I.26)$$

in the CI expression. Here $\Phi_{\alpha\beta}^{rs}$ represents the excitations of a pair of electrons in orbitals α, β to orbitals r, s in the reference state Φ_0 . The CI coefficients are obtained by a modified Schrödinger equation for each pair $(\alpha\beta)$. This equation for a given pair of electrons [40] takes the form :

$$[\hat{H}_{\alpha\beta}(1) + \hat{H}_{\alpha\beta}(2) + (1 - \hat{P}_{\alpha\beta})(1,2)]\Psi_{\alpha\beta}(1,2) = \epsilon_{\alpha\beta} \Psi_{\alpha\beta}(1,2) \quad (I.27)$$

where the projection operator $(1 - \hat{P}_{\alpha\beta})$ annihilates all components containing occupied orbitals ϕ_j , $j \neq \alpha, \beta$ from the orbital expansion $\Psi_{\alpha\beta}(1,2)$, an arbitrary two-particle function. The solutions of these sets of equations, referred to as the Bethe-Goldstone equations, corresponds to the exact solution of a two-particle problem, subject to the constraint that the wavefunction should be orthogonal to the remaining $(N-2)$ orbitals of an N -particle Slater determinant.

I.4.4 The r_{12} Method

Instead of trying to expand the cusp-like behaviour of the wavefunction in a Fourier-like series, as in the CI method, it is possible to incorporate it directly into the wavefunction. Slater [47] suggested the use of a factor $e^{-r_{12}/2}$ in the wavefunction to obtain the desired effect. Hylleraas [32] used an approximation to the above. For the ground-state of helium, he used the expression

$$\psi(r_1, r_2) = e^{-(r_1+r_2)/2} \sum_{n,l,m=0}^{\infty} C_{n,2l,m} (r_1+r_2)^n (r_1-r_2)^{2l} r_{12}^m \quad (I.28)$$

where n, l, m are the set of quantum numbers, r_1 and r_2 are the electronic coordinates and r_{12} are the inter-electronic distances. With a mere six-term expansion, Hylleraas obtained a near-exact energy for helium atom. Many attempts [48,49] have been made to extend the ' r_{12} -coordinate' method to many-electron systems, by multiplying the determinantal wavefunction by a correlation factor containing all the r_{ij} 's. However, these methods based on explicit use of r_{ij} coordinates are very difficult both to implement [50] and to interpret. An interesting combination of CI and Hylleraas r_{12} method has been applied to atoms with a fair amount of success [50,51]. In this method the configurations in the wavefunction are chosen to be antisymmetrised, projected products of one-electron functions with powers of inter-electronic

coordinates. Recently [52] the above method has been elegantly recast in a form suitable for the deployment of the powerful linked-cluster expansion of many-body theory.

I.4.5 Perturbation Methods

Both the CI and the Hylleraas method are beset with problems associated with large computations, for in both cases the number of parameters to be variationally determined are large. A means of reducing the computational effort, is to choose carefully limited and meaningful terms in the variational procedure. An insight into this is achieved by partitioning of the model space into appropriate subspaces [53]. Adaptations of the variational form then, leads in a straightforward manner to various forms of perturbation theory. An arbitrary partitioning of the model space into a single function ϕ_0 and a remainder χ , orthogonal to ϕ_0 yields

$$E = \langle \phi_0 | \hat{H} | \phi_0 \rangle + \langle \phi_0 | \hat{H} | \chi \rangle \langle \chi | E - \hat{H} | \chi \rangle^{-1} \langle \chi | \hat{H} | \phi_0 \rangle \quad (\text{I.29})$$

If \hat{H} is partitioned into a model Hamiltonian \hat{H}_0 and a perturbation \hat{V}

$$\hat{H} = \hat{H}_0 + \hat{V} \quad (\text{I.30})$$

$$\hat{H}_0 \phi_0 = E_0 \phi_0 \quad (\text{I.31})$$

then

$$E = E_0 + E_1 + \langle \phi_0 | \hat{V} | \chi \rangle \langle \chi | E - \hat{H}_0 - \hat{V} | \chi \rangle^{-1} \langle \chi | \hat{V} | \phi_0 \rangle \quad (I.32)$$

Expressions for various forms of perturbation theory can be obtained from eqn. (I.32) by using the operator expansion :

$$(A - B)^{-1} = A^{-1} + A^{-1} B A^{-1} + \dots \quad (I.33)$$

for the inverse term in the above equation.

When

$$A = \langle \chi | E - \hat{H}_0 | \chi \rangle \quad (I.34)$$

$$B = \langle \chi | \hat{V} | \chi \rangle \quad (I.35)$$

the Brillouin-Wigner (BW) form of perturbation theory is obtained [54]. The Raleigh-Schrodinger form of perturbation theory (RSPT) is obtained when

$$A = \langle \chi | E_0 - \hat{H}_0 | \chi \rangle \quad (I.36)$$

$$B = \langle \chi | \hat{V} - \Delta E | \chi \rangle \quad (I.37)$$

where ΔE is defined by the equation

$$\begin{aligned} \Delta E &= E - E_0 \\ &= \sum_{n=1}^{\infty} E_n \end{aligned} \quad (I.38)$$

On expanding and regrouping the terms,

$$\Delta E = \sum_{k=0}^{\infty} \langle \phi_0 | \hat{V} [(E_0 - \hat{H}_0)^{-1} \hat{P}(\hat{V} - \Delta E)]^k | \phi_0 \rangle \quad (I.39)$$

where \hat{P} is the projector for the orthogonal complement to ϕ_0 and defines the partitioned subspace

$$\hat{P} = |x\rangle\langle x|^{-1} \langle x| \quad (I.40)$$

Truncation of the summation at various k 's leads to different orders of perturbation theory and the order-by-order corrections can be obtained. For any order m ,

$$E_{m+1} = \langle \phi_0 | \hat{V} | \phi_m \rangle \quad (I.41)$$

$$\phi_m = |x\rangle\langle x| E_0 - \hat{H}_0 |x\rangle^{-1} \langle x| [(\hat{V} - E_1) | \phi_{m-1} \rangle - \sum_{k=1}^{m-2} E_{m-k} | \phi_n \rangle] \quad (I.42)$$

Defining $\hat{R} = \hat{P}/(E_0 - \hat{H}_0)$,

the energy expression upto first four orders is

$$\begin{aligned} \Delta E^{(1)} &= \langle \phi_0 | \hat{V} | \phi_0 \rangle \\ &= \langle \hat{V} \rangle \end{aligned} \quad (I.43)$$

$$\begin{aligned} \Delta E^{(2)} &= \langle \phi_0 | \hat{V} \frac{\hat{P}}{(E_0 - \hat{H}_0)} \hat{V} | \phi_0 \rangle \\ &= \langle \hat{V} \hat{R} \hat{V} \rangle \end{aligned} \quad (I.44)$$

$$\begin{aligned} \Delta E^{(3)} &= \langle \phi_0 | \hat{V} \frac{\hat{P}}{(E_0 - \hat{H}_0)} \hat{V} \frac{\hat{P}}{(E_0 - \hat{H}_0)} \hat{V} | \phi_0 \rangle - \\ &\quad \langle \phi_0 | \hat{V} | \phi_0 \rangle \langle \phi_0 | \hat{V} \frac{\hat{P}}{(E_0 - \hat{H}_0)^2} \hat{V} | \phi_0 \rangle \\ &= \langle \hat{V} \hat{R} \hat{V} \hat{R} \hat{V} \rangle - \langle \hat{V} \rangle \langle \hat{V} \hat{R}^2 \hat{V} \rangle \\ &= \langle \hat{V} \hat{R} \hat{V} \hat{R} \hat{V} \rangle - \langle \hat{V} \hat{R} \rangle \langle \hat{V} \rangle \hat{R} \hat{V} \end{aligned} \quad (I.45)$$

$$\begin{aligned}
\Delta E^{(4)} &= \langle \phi_0 | \hat{V} \hat{R} (\hat{V} - E_1) \hat{R} (\hat{V} - E_1) \hat{R} \hat{V} | \phi_0 \rangle - E_2 \langle \phi_1 | \phi_1 \rangle \\
&= \langle \hat{V} \hat{R} \hat{V} \hat{R} \hat{V} \hat{R} \hat{V} \rangle - \langle \hat{V} \hat{R} \langle \hat{V} \rangle \hat{R} \hat{V} \hat{R} \hat{V} \rangle - \\
&\quad \langle \hat{V} \hat{R} \hat{V} \hat{R} \langle \hat{V} \rangle \hat{R} \hat{V} \rangle + \langle \hat{V} \hat{R} \langle \hat{V} \rangle \hat{R} \langle \hat{V} \rangle \hat{R} \hat{V} \rangle - \\
&\quad \langle \hat{V} \hat{R} \langle \hat{V} \hat{R} \hat{V} \rangle \hat{R} \hat{V} \rangle \quad (I.46)
\end{aligned}$$

Irrespective of whether the model space is complete or finite, the energy series converges as long as the perturbation theory itself converges. When the unperturbed Hamiltonian \hat{H}_0 is chosen to be the ground-state HF operator, the Møller-Plesset [33] version of the RSPT is obtained. This form has been applied extensively by Pople [55] to carry out correlation energy calculations upto second and third order.

The Raleigh-Schrödinger perturbation theoretic method has two inherent drawbacks; firstly, it shares in common with CI, the limitation on the size of the space defined by \hat{P} . Usually, an intuitively appealing approximation like limiting $|\chi\rangle$ to single and double excitations of the reference wavefunction, $|\phi_0\rangle$, is made. For perturbation expansion upto three orders this approximation is exact, since only single and double excitations give non-vanishing matrix elements. The first-order correction to the wavefunction is then :

$$E_{ij}^{(2)} = \sum_{\alpha < \beta} \sum_{r < s} \frac{|\langle \phi | \hat{V} | \phi_{\alpha\beta} \rangle|}{\epsilon_r + \epsilon_s - \epsilon_\alpha - \epsilon_\beta} \quad (I.47)$$

$$\begin{aligned}
 |\Psi\rangle^{(1)} &= \sum_{\alpha < \beta} \sum_{r < s} \frac{\langle \phi_{\alpha\beta}^{rs} | \hat{V} | \phi_0 \rangle}{(\epsilon_r + \epsilon_s - \epsilon_\alpha - \epsilon_\beta)} |\phi_{\alpha\beta}^{rs}\rangle \\
 &= \sum_{\alpha < \beta} \sum_{r < s} c_{\alpha\beta}^{rs(1)} |\phi_{\alpha\beta}^{rs}\rangle \quad (I.48)
 \end{aligned}$$

$$\text{where } c_{\alpha\beta}^{rs(1)} = \frac{\langle \phi_{\alpha\beta}^{rs} | \hat{V} | \phi_0 \rangle}{(\epsilon_r + \epsilon_s - \epsilon_\alpha - \epsilon_\beta)} \quad (I.49)$$

where $|\phi_{\alpha\beta}^{rs}\rangle$ are obtained by substituting the occupied orbitals α and β in the HF ground-state determinant by the virtual orbitals r and s ; ϵ 's are the eigenvalues of the one-electron Fock Hamiltonian operators. Even with the restriction of the space to single and double excitations, it is not practically feasible to go beyond a few orders. The astronomical growth in the number of terms as the order of perturbation increases is the second limitation of RSPT.

I.4.6 Linked-Cluster Theorem and Many-body Perturbation Theory

The application of field-theoretic techniques to the above problem heralded a new epoch in the solution of many-body problems. The first of the genre is the famous linked-cluster theorem of Goldstone [56]. This theorem uses the time-dependent perturbation theory in the interaction representation, the language of second quantisation, and Feynman's graphology (vide Appendix A), to prove rigorously the cancellation of unlinked terms to all orders in RSPT. There are two very important features associated with the

linked-cluster theorem. Firstly, it can be formulated in an entirely time-independent framework [57,58,59]. Secondly, its applicability extends well beyond perturbation theoretic methods [60]. Numerous methods, built on this theorem, even though non-variational in nature, are devoid of the size-extensivity problems dealt with earlier. With the application of the linked-cluster theorem eqn. (I.39) becomes

$$\Delta E = \sum_{n=0}^{\infty} \langle \phi_0 | \hat{V} [(E_0 - \hat{H}_0)^{-1} \hat{V}]^n | \phi_0 \rangle_{\mathcal{L}} \quad (\text{I.50})$$

where the subscript \mathcal{L} indicates that the summation is limited only to linked terms. In other words, the projection operator \hat{P} in eqn. (I.39) which excludes the ϕ_0 component of any function it operates on, has the same effect as the restriction to summation over linked diagrams. Also, the myriad linked terms that survive are elegantly handled, with the graphical representation of Feynman [61]. The Feynman diagrams, in addition to handling the book-keeping also have provided insight for selective summation in eqn. (I.50) [62,63].

The power of the linked-cluster theorem is highlighted by the manner in which it gets rid of the size-extensivity problem mentioned earlier with reference to CI. RSPT shares the size-extensivity problem with CI. On the one hand, it is necessary to limit the basis to double-excited functions

only, while on the other this approximation introduces unphysical, spurious energy corrections. This aspect becomes transparent in the fourth-order of RSPT and has been illustrated in Appendix A. The application of the linked-cluster theorem, however, immediately solves the size-extensivity problem. There are no unlinked terms that figure at all in the summation and all the linked terms have correct behaviour for N dependence. The elimination of the size-extensivity problem portrays only one facet of the linked-cluster theorem. The theorem is much more versatile as will become apparent from the formulation of non-perturbative theories and this has been dealt with in Chapter II of this thesis. The above described many-body approach to RSPT, that goes under the name of many-body perturbation theory (MBPT) has been applied widely to atomic and molecular correlation problems [64].

I.4.7 Other Field Theoretic Methods

Notwithstanding the theoretical elegance, MBPT suffers from some major drawbacks. Firstly, the perturbation series for extended systems involving coulombic forces is itself divergent. And, despite the elimination of all the unlinked terms there still remain the numerous linked diagrams to be taken into account. However, in practice, this is not feasible in the infinite summation. Although, one of the powers of the linked-cluster theorem is to provide topological

arguments for selective summation of diagrams to infinite order [62], physical insight into the meaning of the perturbation terms is lost. Also, if only partial summation is done, infinite number of diagrams which may contribute significantly to the perturbation correction are ignored. This casts doubt on the choice of diagrams invoked in the partial summation. Lastly, the MBPT, can boast neither of the conceptual simplicity nor the physical insight into correlations of electrons provided by CI.

A method that retains all the advantages of the linked-cluster theorem, but at the same time avoids the shortcomings of the MBPT was developed by Coester and Kummel [65,66] and extended to many-electron systems by Čížek [35]. This method known as the CC or the $\exp(S)$ method [67], is based on the cluster expansion of the exact wavefunction using an exponential ansatz. The linked diagram property of the exponential operator and the effective interaction is exploited and sets of explicit CC equations for the components of the cluster operator obtained [35]. The CC method is the most powerful off-shoot of the linked-cluster theorem. Though, non-perturbative in origin, it displays the theoretical rigor of true many-body treatment and bears the conceptual simplicity of a physically meaningful theory. The details of the method and the diagrammatics are presented in Chapter II of this thesis. The other field-theoretic method, the Green's Functions method [36], has

only been sparsely used in quantum chemistry, due to its complicated nature.

I.5 BEYOND IPA WITH SPECIFIC REFERENCE TO LOCAL POTENTIAL METHODS

The methods described for going beyond the IPA, are not restrictive as far as the choice of the initial approximation is concerned. However, the HF approximation is the preferred starting point for most calculations involving these methods. This is so because, the HF operator is the exact Hamiltonian for the single determinant trial function. Besides, the terms exchange and correlation are traditionally defined with reference to the HF Hamiltonian [26], which fact is used to advantage in decomposition of the Hamiltonian into a model Hamiltonian and a well-defined perturbation. Above all, the HF solutions rigorously satisfy Brillouin's theorem,

$$\langle \phi_0 | \hat{H} | \phi_\alpha^r \rangle = 0 \quad (1.51)$$

This considerably simplifies CI and perturbation calculations with the HF basis.

The local potential methods, on the other hand, do not share the above merits of the HF method; however, they score over the HF method in the computational domain and are better suited for large system calculations [68]. Also, these methods are conceptually very attractive since they are based on a physically well-defined, measurable quantity, the one-electron density. However, unlike in the HF method a

clear-cut demarcation of the exchange and correlation effects cannot be made in these methods; nor is it clear how exactly the local potentials simulate the non-local electron-electron interaction potential. Attempts have been made to highlight the nature of these potentials by introducing local and non-local corrections to these potentials [69]. Main amongst these attempts are (a) the introduction of empirical correlation potentials based on phenomenological or conceptual arguments, (b) the incorporation of gradient corrections to kinetic and exchange energies and (c) the modification of the local potential to reproduce the correct shape of the Coulomb and Fermi holes. In the class of methods (a), the EC potential E_{XC} in eqn. (I.10) assumes the form

$$E_{XC} = \int \hat{v}_{XC}[\rho(r)] \rho(r) dr + \int \epsilon_C \rho(r) dr \quad (I.52)$$

where ϵ_C is a functional of density and defines the correlation energy per electron. ϵ_C has been variously approximated by correlation energy of a free-electron gas [70], correlation energy of a low density [71] and high density [72] electron gas obtained using perturbation theory, correlation energy of a homogeneous electron gas obtained through a dielectric formulation [73,74], correlation energy of a spin-polarised electron liquid [75], etc. All these approximations are valid only for slowly varying uniform density distributions [13] and are incapable

of taking into account density fluctuations due to atomic shell structure [15]. These potentials also have the inherent error of inclusion of self-correlation. This arises from the treatment of the electron as a continuous electron density and the subsequent calculation of the correlation between different parts of this density [76]. This self-correlation leads to a non-zero correlation energy for the hydrogen atom! [75]. Method (b) involves the incorporation of gradient corrections to kinetic energy [77] and to exchange energy [72] and leads to fairly accurate valence charge densities, but divergences are encountered in the inner regions. Also, this has the theoretical flaw of not obeying the sum rule, which states that the EC hole contains one electron [69]. The last mentioned of the methods, (c), attempts to correct for the shape of the Fermi and the Coulomb holes [75,78,79,80]. Although, these methods are conceptually very attractive, they are difficult to implement.

All the above mentioned attempts that correct the local potential approximation are still within the domain of the IPA. Zare [81] has performed a CI calculation on magnesium starting with a basis obtained from the $X\alpha$ method and has obtained excellent results. However, few attempts have been made to go beyond the local potential based IPA using the other methods described in Section I.4. In particular, it may be pointed out, that none of the more powerful approaches such as the linked-cluster methods, have been employed in this context.

I.6 SCOPE OF THE THESIS

Although the above mentioned attempts tend to refine the local potential method to higher degrees of sophistication, they fail to provide insight into the nature and efficacy of the local EC potential. In view of the growing importance of these methods for large-scale computations, it is not only desirable, but necessary to examine these models with a view to understanding the nature of and the basis for the approximations used. This thesis, an outcome of this motivation, uses the powerful CC many-body theory to study the many-body EC corrections to a member of the local potential family, namely, the $X\alpha$ method of Slater [8].

Čížek and Paldus [35,82] have employed the CC approach to study the many-body correlation effects in atoms; the HF approximation served as the starting point for their calculations. However, to the best of our knowledge, there have been no attempts made in literature to use the CC method for analysing atomic EC effects, starting from a local potential-based reference function. Such a study would, in addition to incorporating many-body correlation effects, provide an insight into the nature of the IPA chosen for the reference function.

In the present thesis, we examine in detail the role of the Slater exchange potential and the choice of the

exchange parameter α , in the treatment of many-body exchange correlation effects. The use of gradient corrections to the $X\alpha$ potential is also examined in this light. The present study entails, in addition to the use of CC approach, the use of several hierarchy of approximations derived from it, namely, variants of coupled-electron pair theories [31,46], CI [37], Sinanoglu's decoupled-pair many-electron theory [41], Nesbet-Bethe-Goldstone method [40] and RS second-order expansion [55]. Our results are compared with those of Čížek and Paldus; such a comparison provides a framework for assessing the relative merits of the HF and $X\alpha$ potentials in the description of EC effects. The use of different local potentials to generate the reference functions for the CC calculations, has permitted a detailed study of the role of these potentials vis-a-vis, the EC effects. The diagrammatic language facilitates the analysis of the importance of the terms that contribute to EC corrections and thereby provides an insight into the nature of the local potential used. An assessment of the efficacy of the potentials, in representing EC effects in various regions in the atom, has been made. It is hoped that a study such as the present one will provide a rational basis for the choice of local potentials that describe the EC effects in atoms more accurately.

Chapter II of the thesis discusses the CC method, its basis, diagrammatics and the cluster equations, in the

context of evaluation of corrections to EC energy in atoms. Chapter III presents a model calculation on beryllium atom to illustrate the application of the CC methodology and the approximations derived from it. Chapter IV presents the results of calculations of corrections to EC energies in four-electron atomic systems obtained by the CC approach. The $X\alpha$ method and its refinements have been examined through these calculations. Chapter V reports the expectation values of some operators over the wavefunctions obtained through the CC expansion for the systems discussed in the previous chapter. The results are compared with the reference state expectation values. The thesis concludes with a few salient remarks on the application of CC methodology for the study of EC effects in atoms.

Appendix A presents a brief discussion on the language of second quantisation, Feynman-Goldstone graphology as applied to MBPT, fourth-order RSPT and cancellation of the unlinked diagrams, the hole-particle formalism, Wick's theorem and contractions and illustration of the elementary Feynman-Goldstone diagrams used in this thesis. A listing of some of the computer programs used in the present study is given in Appendix B.

CHAPTER II

THE COUPLED-CLUSTER FORMALISM

- II.1 Introduction
- II.2 The Nature of \hat{T}
- II.3 The Schrödinger Equation
- II.4 Diagrammatics and CC Equations
- II.5 Relationship of the CC Method to other Many-Electron Theories

II.1 INTRODUCTION

The CC methodology, which is the most significant offshoot of the linked-cluster theorem, is used in this thesis for the analysis of EC effects in atoms. This method is based on the cluster expansion of the exact many-Fermion wavefunction in an exponential form [35,65,66]. This exponential ansatz, which is a facsimile of the linked-cluster expansion, was first inferred from the structure of many-body perturbation theory [83]. A diagrammatic Raleigh-Schrodinger expansion of the exact wavefunction elegantly proves this point. The wavefunction expansion can be equivalently expressed by diagrams that contain one or more open-linked pieces (cf. Appendix A for diagram terminology). Some of these diagrams have topologically identical linked pieces, differing only in their relative arrangement. It turns out that diagrams with n such topologically equivalent linked pieces are counted $n!$ times thanks to the various orderings of the linked pieces and independent orbital summations. It is therefore necessary to multiply the contribution from the diagram by $(n!)^{-1}$. This is illustrated for the case of a diagram containing two open-linked parts in Fig. II.1.

For the general case of a diagram with n_{r_1} linked parts of topological structure r_1 , n_{r_2} linked parts of topological structure r_2 , etc., the multiplication factor for the contribution is $[\prod_r (n_r!)]^{-1}$. The net outcome of these factors is

$$\begin{aligned}
 & \left(\text{Diagram 1} \right) + \left(\text{Diagram 2} \right) \\
 &= \frac{1}{2i} \left(\text{Diagram 3} \right)^2
 \end{aligned}$$

Fig. II.1 Example of topologically identical linked diagrams and their equivalent.

that the total wavefunction can be expressed in the form [57]

$$\Psi = e^{\hat{T}} \phi_0 \quad (\text{II.1})$$

where, \hat{T} represents the sum of all open diagrams consisting of just a single linked piece. As implied above, \hat{T} can be written in the form,

$$\hat{T} = \sum_{n=1}^N \hat{T}_n \quad (\text{II.2})$$

where, \hat{T}_n is the fully linked operator for exciting n -particles out of the Fermi sea ϕ_0 ; ϕ_0 represents the single determinantal ground state. This result can also be verified independent of perturbation theory [84]. The transformation $\exp(\hat{T})$ is non-unitary, since the expansion satisfies the intermediate normalisation condition

$$\langle \Psi | \phi_0 \rangle = 1 \quad (\text{II.3})$$

II.2 THE NATURE OF \hat{T}

The nature of the operator \hat{T} is best understood through the second quantisation formalism. The \hat{T}_n 's are defined such that,

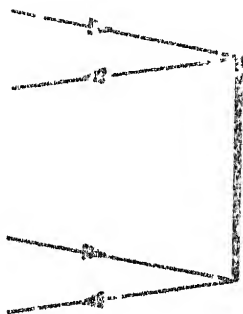
$$\begin{aligned} \hat{T}_1 &= \sum_{\alpha_1} t_{\alpha_1}^{r_1} \hat{b}_{r_1}^\dagger \hat{b}_{\alpha_1}^\dagger \\ \hat{T}_2 &= \frac{1}{2!} \sum_{\alpha_1 \alpha_2} t_{\alpha_1 \alpha_2}^{r_1 r_2} \hat{b}_{r_1}^\dagger \hat{b}_{\alpha_1}^\dagger \hat{b}_{r_2}^\dagger \hat{b}_{\alpha_2}^\dagger \\ &\dots \\ \hat{T}_k &= \frac{1}{k!} \sum_{\substack{\alpha_1 \alpha_2 \dots \alpha_k \\ r_1 r_2 \dots r_k}} t_{\alpha_1 \alpha_2 \dots \alpha_k}^{r_1 r_2 \dots r_k} \prod_{i=1}^k \hat{b}_{r_i}^\dagger \hat{b}_{\alpha_i}^\dagger \quad (\text{II.4}) \end{aligned}$$

where, the \hat{b}^\dagger 's are the particle-hole creation operators (vide Appendix A) defined on the complete set of states, $a_1 a_2 \dots$ represent hole states while $r_1, r_2 \dots$ represent particle states. The function of the operators in \hat{T}_k is to excite k particles out of the Fermi sea. In the hole-particle formalism, this is equivalent to saying that k particle-hole pairs are created. The t_k 's are the corresponding amplitudes of excitation. The following two properties of \hat{T} operators become apparent from their definition. Firstly, \hat{T} 's are non-local operators and have non-vanishing amplitudes between hole and particle states. And, the \hat{T}_n operators commute with each other, since they can only create and never annihilate particle-hole pairs. The operators \hat{T}_n can be represented graphically using Feynman-Goldstone diagrams [56]. This is shown in diagrams A-F of Fig. II.2. A solid line joining the n particle-hole lines is drawn to show that the n particle-hole pairs are created simultaneously. The arrows indicate that each upgoing line represents a Fermion creation operator and a downgoing line represents a Fermion annihilation operator. The diagrams D, E and F show the disconnected diagrams \hat{T}_1^2 , $\hat{T}_1 \hat{T}_2$ and \hat{T}_2^2 respectively.

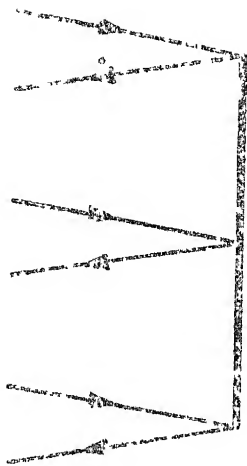
The incorporation of the many-body effects through the exponential operator becomes transparent on comparison of the cluster expansion with CI expansion [85]. Writing the CI expansion of the exact wavefunction Ψ , in the form



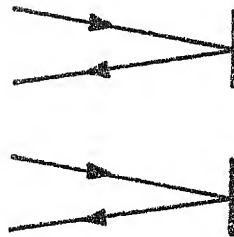
A \hat{t}_1



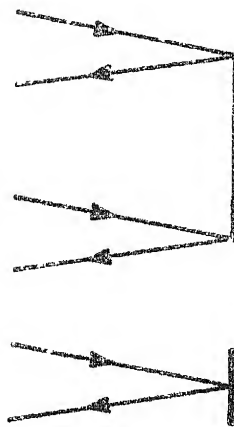
B \hat{t}_2



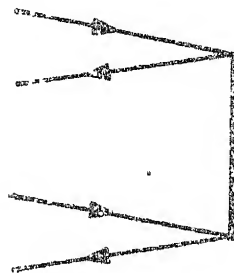
C \hat{t}_3



D \hat{t}_1^2



E $\hat{t}_1 \hat{t}_2$



F \hat{t}_2^2

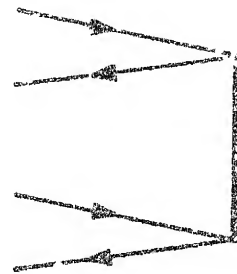


Fig.II.2 A diagrammatic representation of \hat{t} operators.

$$|\psi\rangle = |\phi_0\rangle + \sum_{s=1}^n \hat{C}_s |\phi_0\rangle \quad (\text{II.5})$$

where, \hat{C}_s is an s-fold excitation operator such that $\hat{C}_s |\phi_0\rangle$ yields the sum of all the k s-fold excited configurations,

$$\hat{C}_s |\phi_0\rangle = \sum_{k \in s} a_k |\phi^k\rangle \quad (\text{II.6})$$

It is seen on comparing eqns. (II.6) and (II.1) that, the operator \hat{C}_i can be decomposed into a connected part \hat{T}_i and a disconnected part \hat{U}_i . The \hat{U}_i 's can be written as product of \hat{T}_k 's.

$$\hat{C}_s = \hat{T}_s + \hat{U}_s \quad (\text{II.7})$$

where,

$$\hat{U}_1 = 0$$

$$\hat{U}_2 = \frac{1}{2!} \hat{T}_1^2$$

$$\hat{U}_3 = \hat{T}_1 \hat{T}_2 + \frac{1}{3!} \hat{T}_1^3$$

$$\hat{U}_4 = \hat{T}_1 \hat{T}_3 + \frac{1}{2!} \hat{T}_1^2 \hat{T}_2 + \frac{1}{4!} \hat{T}_1^4 + \frac{1}{2!} \hat{T}_2^2 \quad (\text{II.8})$$

etc. The exponential ansatz then is seen to be entirely equivalent to a CI expansion [86].

II.3 THE SCHRÖDINGER EQUATION

The Schrödinger equation, eqn. (I.1), on substituting for ψ from eqn. (II.1), assumes the form,

$$\hat{H} e^{\hat{T}} |\phi_0\rangle = E e^{\hat{T}} |\phi_0\rangle \quad (\text{II.9})$$

Left-multiplying eqn. (II.9) successively by each of the ϕ_s 's for $s \neq 0$ yields the set of eqns. (II.10), which are the constraints on \hat{T} .

$$\begin{aligned}
 \langle \phi_\alpha^r | \hat{H} | e^{\hat{T}} \phi_0 \rangle &= 0 \\
 \langle \phi_{\alpha\beta}^{rs} | \hat{H} | e^{\hat{T}} \phi_0 \rangle &= 0 \\
 &\vdots \\
 \langle \phi_{\alpha\beta}^{rs} \dots | \hat{H} | e^{\hat{T}} \phi_0 \rangle &= 0
 \end{aligned}
 \tag{II.10}$$

These constraints determine \hat{T} completely. The set of constraints yield sets of coupled non-linear equations linking the various n-body amplitudes t_n to each other. By suitably truncating the series \hat{T}_n , computationally feasible approximations are obtained. The energy E is obtained by left-multiplying eqn. (II.9) by ϕ_0 and substituting the appropriate t_n 's determined from the constraint equations. A pedestrian derivation of the constraint equations is tedious and fails to reveal the inherent properties of the CC formalism [65,86]. Use of field-theoretic methods greatly simplifies the problem and provides insight into the nature of many-electron interactions [35]. For the derivation of the CC equations, we then employ the tools of field theory, viz., the hole-particle formalism, Wick's algebra and Feynman-Goldstone diagrammatics (vide Appendix A).

The Hamiltonian can be expressed in the second quantised form as (vide Appendix A)

$$\hat{H} = \sum_{ik} \langle i | \hat{z} | k \rangle \hat{a}_i^\dagger \hat{a}_k + \gamma/2 \sum_{ijkl} \langle ij | \hat{v} | kl \rangle \hat{a}_i^\dagger \hat{a}_j^\dagger \hat{a}_l \hat{a}_k \quad (\text{II.11})$$

or alternately, in the normal product form as

$$\begin{aligned} \hat{H} = & \langle \phi_0 | \hat{H} | \phi_0 \rangle + \sum_{ik} \langle i | \hat{f} | k \rangle N [\hat{a}_i^\dagger \hat{a}_k] \\ & + \gamma/2 \sum_{ijkl} \langle ij | \hat{v} | kl \rangle N [\hat{a}_i^\dagger \hat{a}_j^\dagger \hat{a}_l \hat{a}_k] \end{aligned} \quad (\text{II.12})$$

where,

$$\langle i | \hat{f} | k \rangle = \langle i | \hat{z} | k \rangle + \langle i | \hat{g} | k \rangle \quad (\text{II.13a})$$

$$\langle i | \hat{g} | k \rangle = \sum_{\xi} \langle i \xi | \hat{v} | k \xi \rangle_A \quad (\text{II.13b})$$

\hat{z} refers to the sum of kinetic energy and nucleus-electron attraction operators and \hat{v} the electron-electron repulsion operator. The subscript A on the second term in eqn.(II.13b) stands for antisymmetrisation of the matrix element. When i, k and ξ refer to orbitals,

$$\sum_{\xi} \langle i \xi | \hat{v} | k \xi \rangle_A = \sum_{\xi} 2 \langle i \xi | \hat{v} | k \xi \rangle - \langle i \xi | \hat{v} | \xi k \rangle \quad (\text{II.13c})$$

The advantage in expressing the operators in the normal product form lies in the obviation of the need to perform contractions of the operators within the normal product (vide Appendix A).

Eqn. (II.9) can now be recast in the second quantization formalism and expressed diagrammatically. To obtain eqn. (II.9) in a compact form, the operator $\exp(\hat{T})$ is replaced by the formal Taylor series expansion,

$$e^{\hat{T}} = 1 + \hat{T} + \frac{\hat{T}^2}{2!} + \dots \quad (\text{II.14})$$

then,

$$\hat{H}(1 + \hat{T} + \frac{\hat{T}^2}{2!} + \dots) \phi_0 = E(1 + \hat{T} + \frac{\hat{T}^2}{2!} + \dots) \phi_0 \quad (\text{II.15})$$

The Hamiltonian has to be contracted with the \hat{T}_n 's of the Taylor series expansion; in other words, the creation-annihilation operators in \hat{H} are contracted with creation-annihilation operators in \hat{T}_n . After these contractions are performed, the Schrödinger equation, eqn. (II.9) assumes the form,

$$\{\hat{H} e^{\hat{T}}\}_{\mathcal{L}} \phi_0 = E \phi_0 \quad (\text{II.16})$$

The subscript \mathcal{L} implies that only topologically linked diagrams need be considered. This result, the non-perturbative analogue of the linked-cluster theorem, is easily proved [57].

On contraction with $\exp(\hat{T})$, the diagonal part of the one-body operator \hat{H} can link itself diagrammatically to no more than two of the \hat{T}_n 's. In the most general case, this can be illustrated by contracting the creation operator of the one-body operator with one of the k^{th} particle-hole pair

of \hat{T}_n and contracting the annihilation operator with one of the 1^{th} particle-hole pair of \hat{T}_n .

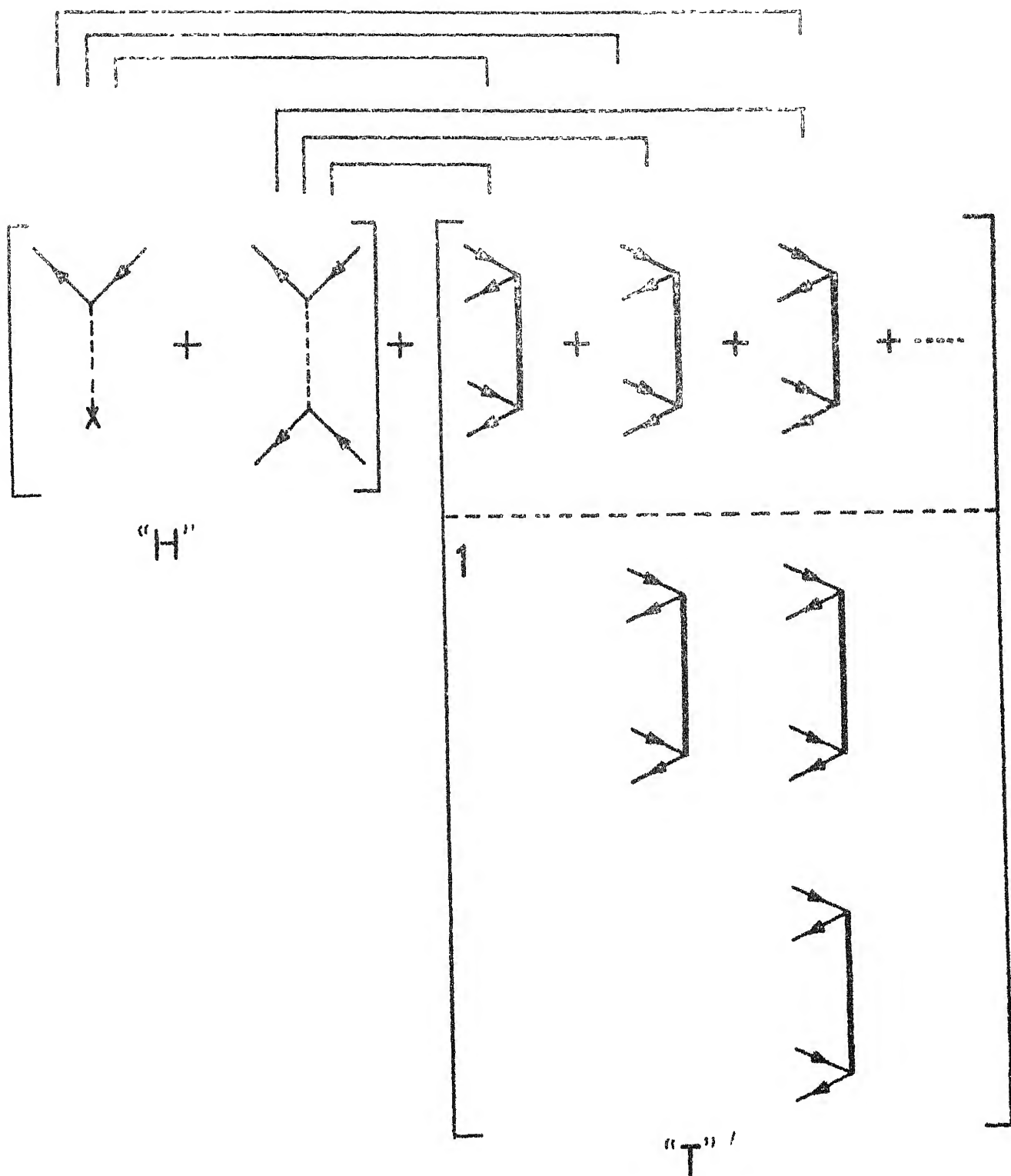
$$\begin{array}{c}
 \overbrace{(\hat{a}_i^\dagger \hat{a}_j) \{(\hat{b}_{r_1}^\dagger \hat{b}_{\alpha_1}^\dagger)(\hat{b}_{r_2}^\dagger \hat{b}_{\alpha_2}^\dagger) \dots (\hat{b}_{r_k}^\dagger \hat{b}_{\alpha_k}^\dagger) \dots (\hat{b}_{r_1}^\dagger \hat{b}_{\alpha_1}^\dagger) \dots (\hat{b}_{r_n}^\dagger \hat{b}_{\alpha_n}^\dagger)\}}^{\text{Diagrammatic representation of contraction}} \\
 \varepsilon\{\hat{H}\} \qquad \qquad \qquad \varepsilon\{\hat{T}\}
 \end{array}$$

The diagram obtained from this contracted term has none, one or two open-paths; each open-path denotes a particle-hole creation pair. The operator that corresponds to this diagram commutes with all the \hat{T}_n 's. Owing to the commutation property of the \hat{T}_n 's within themselves and the \hat{T}_n 's with operators obtained on contraction, there factors out on the left, a factor $\exp(\hat{T})$. Similarly the two-body operator of the Hamiltonian can be contracted with one, two, three or four of the \hat{T}_n 's. The diagram obtained on contraction can again have none, one or two open-paths; and the operator corresponding to this also has particle-hole creation operator pairs and hence commutes with all the \hat{T}_n 's. The result is again the factoring out of $\exp(\hat{T})$ on the left. Eqn. (II.9) can, therefore, be written as,

$$e^{\hat{T}} \{ \hat{H} e^{\hat{T}} \} \mathcal{L} \Phi_0 = e^{\hat{T}} E \Phi_0 \quad (\text{II.17})$$

Left-multiplying both sides of eqn. (II.17) with $e^{-\hat{T}}$ yields eqn. (II.16).

A diagrammatic version of the proof [87], for the case of $\hat{T} = \hat{T}_2$ is presented in Fig. II.3, for the sake of clarity.



The quantity below the dotted line yields the factor $e^{\hat{T}}$ and the combined diagram can be written as the product of $e^{\hat{T}}$ and a linked part.

Fig. II.3 A diagrammatic picturisation of the linked-cluster result.

This result can also be obtained, without the aid of diagrammatics, by rewriting eqn. (II.9) in the form,

$$e^{-\hat{T}} \hat{H} e^{\hat{T}} \phi_0 = E \phi_0 \quad (\text{II.18})$$

and using the Baker-Hausdorff-Campbell formula [88].

$$e^{-\hat{T}} \hat{H} e^{\hat{T}} = \hat{H} + [\hat{H}, \hat{T}] + \frac{1}{2!} [[\hat{H}, \hat{T}], \hat{T}] + \dots \quad (\text{II.19})$$

The commutator series terminates after the fifth term, since \hat{H} is at most a two-body operator and expansion of the resulting commutator series yields eqn. (II.17) [67]. When \hat{H} is expressed in the normal product form, eqn. (II.16) becomes an eigenvalue equation for ΔE , where

$$\Delta E = E - \langle \phi_0 | \hat{H} | \phi_0 \rangle \quad (\text{II.20})$$

The eigenvalue equation is given by,

$$\begin{aligned} \langle \phi_0 | \hat{H} | \phi_0 \rangle \phi_0 + \{\hat{H} e^{\hat{T}}\}'_{\mathcal{L}} \phi_0 &= E \phi_0 \\ \text{i.e., } \{\hat{H} e^{\hat{T}}\}'_{\mathcal{L}} \phi_0 &= \Delta E \phi_0 \end{aligned} \quad (\text{II.21})$$

The prime on LHS expression indicates that,

$$\{\hat{H} e^{\hat{T}}\}'_{\mathcal{L}} = \{(\hat{H} - \langle \phi_0 | \hat{H} | \phi_0 \rangle) e^{\hat{T}}\} \quad (\text{II.22})$$

Eqn. (II.21) can be rewritten as,

$$\langle \phi_0 | \{\hat{H} e^{\hat{T}}\}'_{\mathcal{L}} | \phi_0 \rangle = \Delta E \quad (\text{II.23})$$

Since, the RHS in eqn. (II.23) is a scalar, only closed-linked diagrams of the expression $\{\hat{H} e^{\hat{T}}\}'_{\mathcal{L}}$ need be taken into account for ΔE evaluation; the open-linked diagrams correspond to particle-hole pair creation operators. The diagrams

corresponding to eqn. (II.23) are presented in Fig. II.4.

To obtain explicit expressions for ΔE , the normal product form of the Hamiltonian may be rewritten as,

$$\begin{aligned}
 (\hat{H} - \langle \Phi_0 | \hat{H} | \Phi_0 \rangle) = & \sum_{ik} \langle i | \hat{h}_0 | k \rangle N[\hat{a}_i^\dagger \hat{a}_k] + \sum_{ik} \langle i | \hat{g} - \hat{v}_s | k \rangle N[\hat{a}_1^\dagger \hat{a}_k] \\
 & + \frac{1}{2} \sum_{ijkl} \langle ij | \hat{v} | kl \rangle N[\hat{a}_1^\dagger \hat{a}_j^\dagger \hat{a}_l \hat{a}_k] \quad (II.24)
 \end{aligned}$$

where \hat{h}_0 is any one-particle operator diagonal in the given orbital basis

$$\begin{aligned}
 \hat{h}_0 |i\rangle &= (\hat{z} + \hat{v}_s) |i\rangle \\
 &= \epsilon_i |i\rangle \quad (II.25)
 \end{aligned}$$

The potential \hat{v}_s is any single particle operator and in the present study it is defined through the X^α local potential (vide Chapter I). The one-body part of the operator in the LHS of eqn. (II.21), \hat{f} , is given by the first two terms on the RHS of eqn. (II.24), while the two-body part of the operator is given by the last term. Using this definition for \hat{H} and the standard rules for constructing Feynman-Goldstone graphs, an explicit equation for ΔE is obtained.

If \hat{h}_0 happens to be the Fock operator, ΔE represents the correlation energy. In our case, ΔE actually represents the corrections to EC energy (vide Section I.3). The expression for ΔE from Fig. II.4 is then,

$$\begin{aligned}
 \Delta E = & \sum_{\alpha r} \langle \alpha | \hat{g} - \hat{v}_s | r \rangle t_\alpha^r + \sum_{\alpha\beta rs} \langle \alpha\beta | \hat{v} | rs \rangle_A t_\alpha^r t_\beta^s \\
 & + \sum_{\alpha\beta rs} \langle \alpha\beta | \hat{v} | rs \rangle_A t_{\alpha\beta}^{rs} \quad (II.26)
 \end{aligned}$$

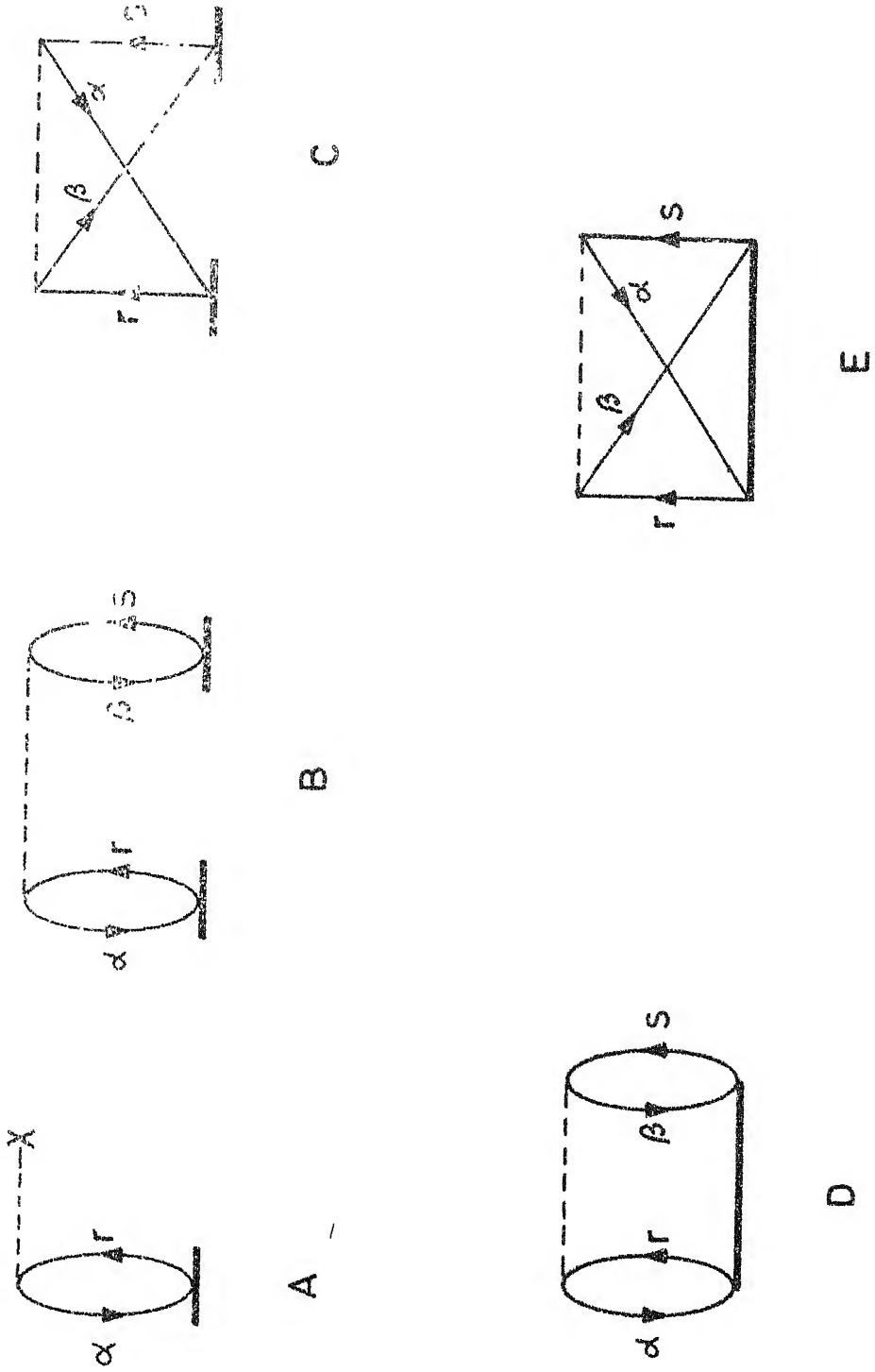


Fig. II-4 Diagrams for ΔE

Diagram A of Fig. II.4 corresponds to the first term in the RHS of eqn. (II.26), B and C correspond to the second term and D and E to the last term. A knowledge of the amplitudes, which are the cluster coefficients, t_{α}^r and $t_{\alpha\beta}^{rs}$, is necessary and sufficient to obtain ΔE . The amplitudes t_{α}^r and $t_{\alpha\beta}^{rs}$ are obtained from the cluster equations, that result from projection of eqn. (II.21) with ϕ_{α}^r and $\phi_{\alpha\beta}^{rs}$ as functions

$$\begin{aligned} \langle \phi_{\alpha}^r | \{ \hat{H} e^{\hat{T}} \}'_{\mathcal{L}} | \phi_0 \rangle &= 0 \\ \langle \phi_{\alpha\beta}^{rs} | \{ \hat{H} e^{\hat{T}} \}'_{\mathcal{L}} | \phi_0 \rangle &= 0 \end{aligned} \quad (\text{II.27})$$

II.4 DIAGRAMMATICS AND CC EQUATIONS

The closed-linked diagrams of the LHS of eqn. (II.21) provide expressions for the correlation energy; on the other hand, their open counterparts with one, two, ... etc. open-paths represent one or more particle-hole pair creation operators and therefore have no corresponding terms on the RHS of the equation. Hence, they must independently be equal to zero. Eqns. (II.27), therefore, may be expressed diagrammatically and the resulting diagram topologies provide meaningful insight into the nature of the diagrams. In the ensuing description Feynman-Goldstone diagrammatics, which represent non-antisymmetrized matrix elements, are employed. The rules for obtaining these linked diagrams are simple (vide Appendix A). The "H" diagrams are linked with the "T" diagrams of each term in $\exp(\hat{T})$ in accordance with the

contraction rules for the creation-annihilation and particle-hole pair creation operators. The resulting diagrams are referred to as "R" diagrams by Čížek [35,89] .

The R diagrams have connected lines, free lines, closed loops and H and T vertices. The rules for obtaining matrix element expressions with proper weight factors and signs are the same as that employed in Goldstone perturbation theory (vide Appendix A). However, since there is no projection operator implied in these diagrams, energy denominators don't arise. By virtue of contraction rules for creation-annihilation operators, the following assignment can be made for the lines in the R diagrams; connecting lines that begin from a H vertex and enter a T vertex carry hole labels and those that begin from a T vertex and enter a H vertex carry particle labels. In the case of free lines, those entering the vertices of T or H diagrams carry hole labels, while those leaving the vertices carry particle labels. The amplitudes t_{α}^r , $t_{\alpha\beta}^{rs}$ are also referred to, as the t matrix elements $\langle \alpha | t | r \rangle$, $\langle \alpha \beta | t | rs \rangle$ to preserve a Goldstone-like diagram correspondence.

Diagrams with one open-path :

All the topologically distinct one open-path linked diagrams obtained by linking H and T diagrams are given in Figs. II.5 and II.6. The diagrams, each representing a particle-hole creation operator pair are obtained by the PUK

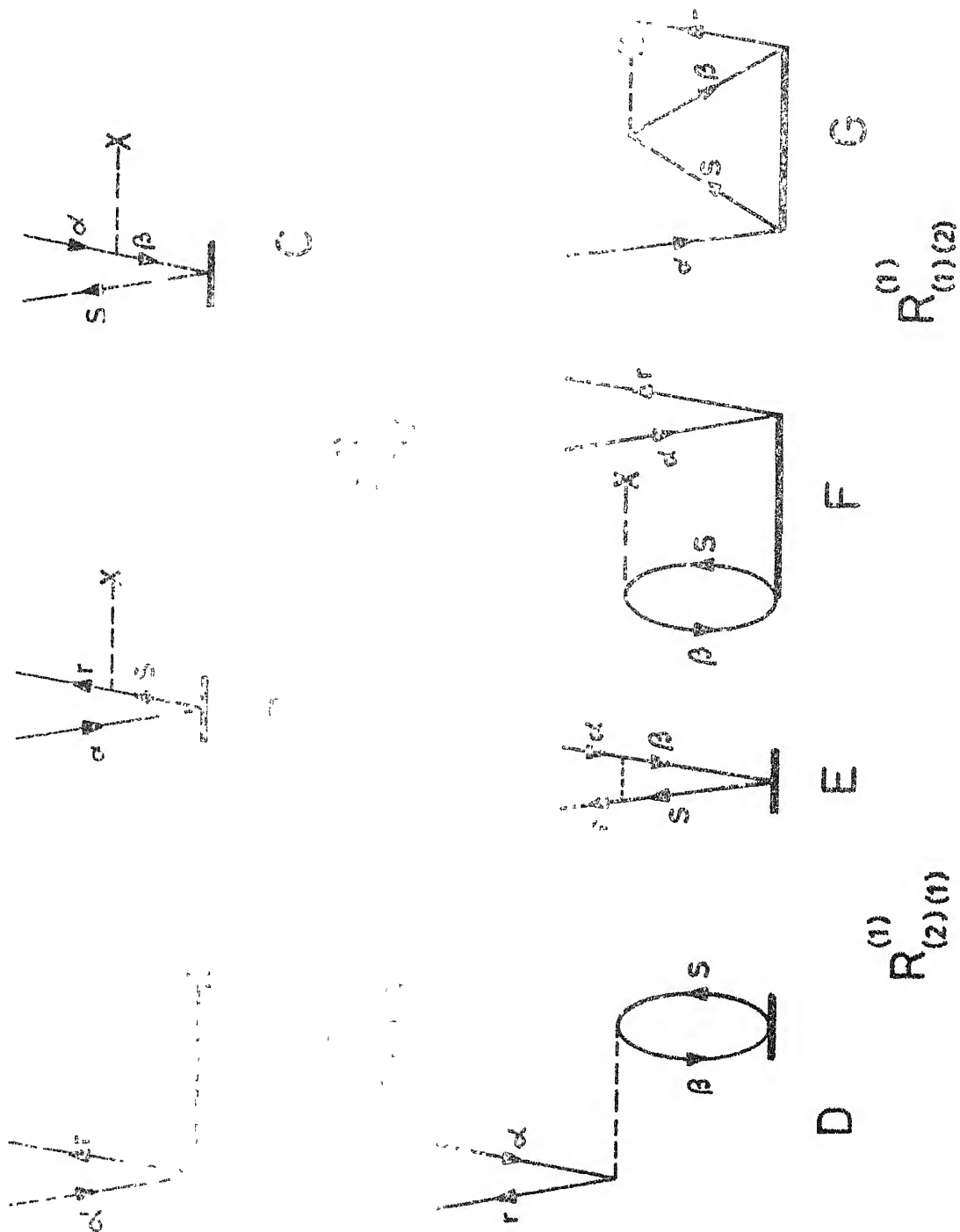
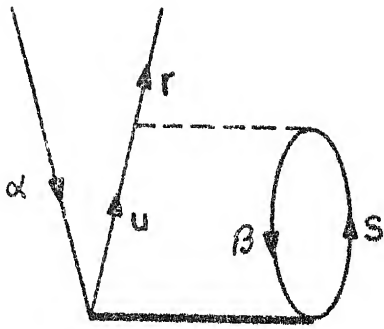
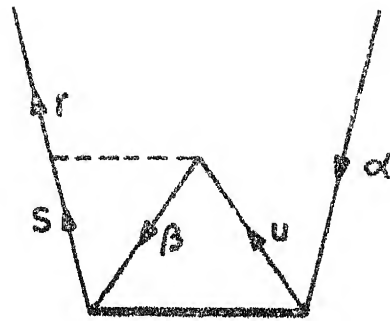


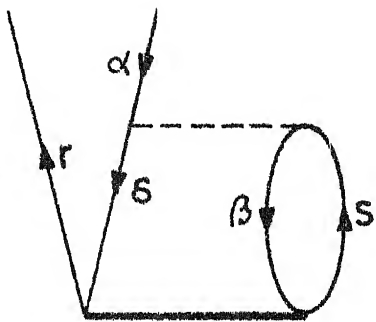
Fig. 11.5 (continued)



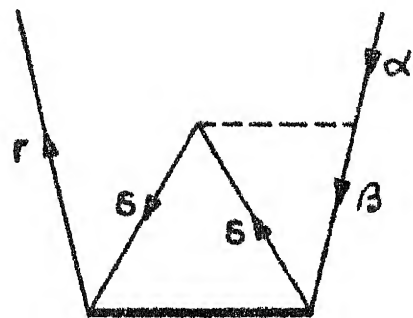
H



I



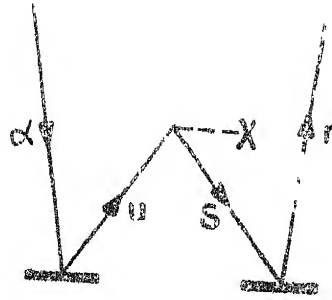
J



K

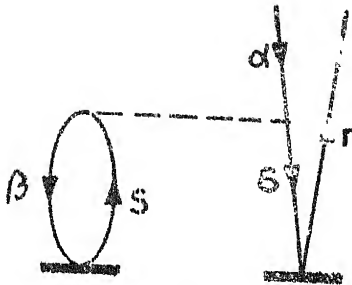
$$R_{(2)(2)}^{(1)}$$

Fig.II.5 One open-path diagrams yielding terms linear in "t".

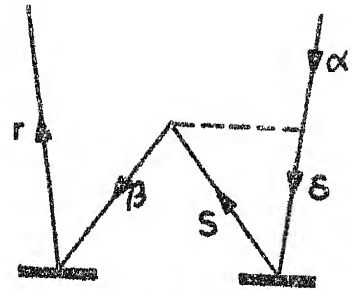


A

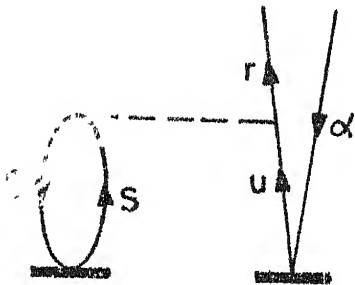
$$R_{(1)(1,1)}^{(1)}$$



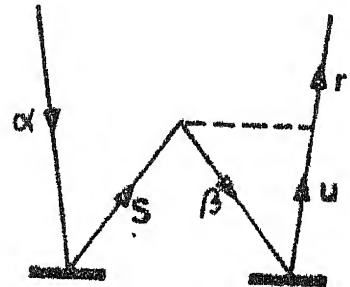
B



C



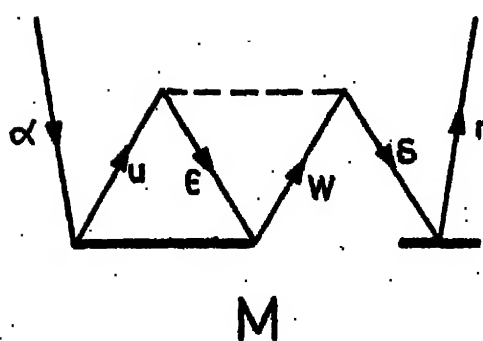
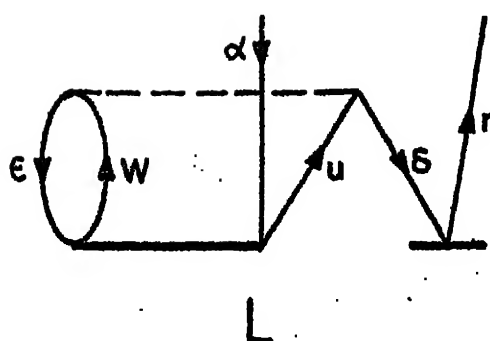
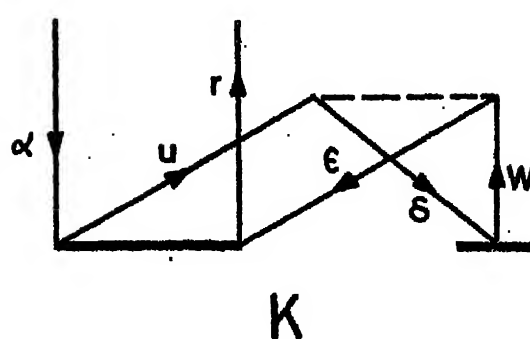
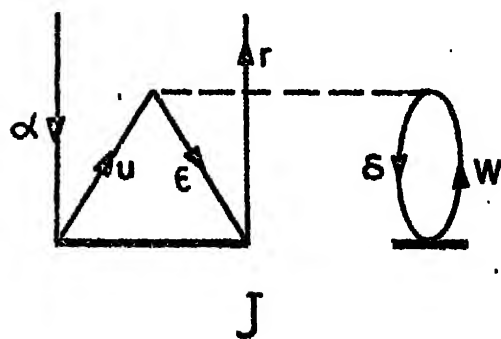
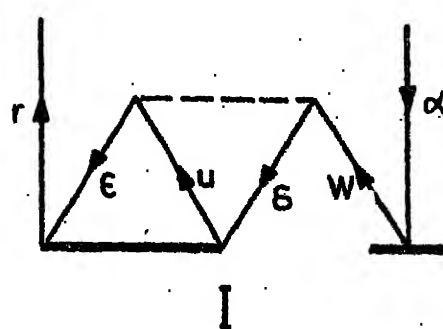
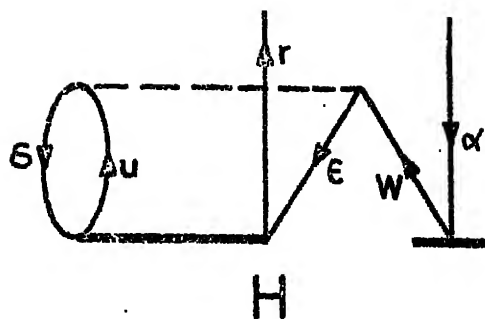
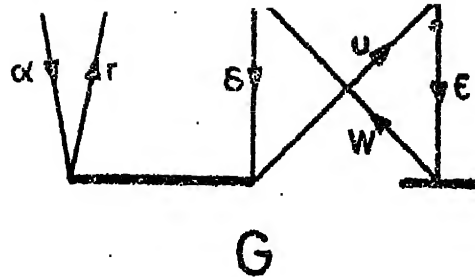
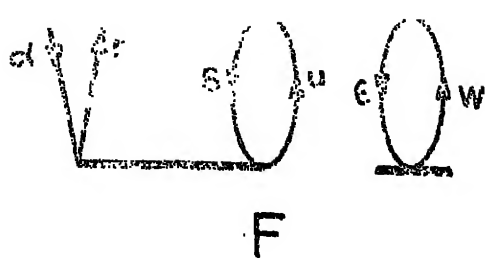
D



E

$$R_{(2)(1,1)}^{(1)}$$

Fig. II. 6 (continued)



$$R_{(2)(2,1)}^{(2)}$$

Fig.II.6 One open-path diagrams yielding terms non-linear in 't'

following linking between H and T diagrams :

- a) \hat{f} diagrams with none of the T diagrams (diagram A of Fig. II.5)
- b) \hat{f} with a T_1 diagram (diagrams B and C of Fig. II.5)
- c) \hat{v} with a T_1 diagram (diagrams D and E of Fig. II.5)
- d) \hat{f} with a T_2 diagram (diagrams F and G of Fig. II.5)
- e) \hat{v} with a T_2 diagram (diagrams H-K of Fig. II.5)
- f) \hat{f} with two T_1 diagrams (diagram A of Fig. II.6)
- g) \hat{v} with two T_1 diagrams (diagrams B-E of Fig. II.6)
- h) \hat{v} with a T_1 and a T_2 diagram (diagrams F-M of Fig. II.6).

The contributions to the one open-path linked diagrams from T_1 are represented by diagrams A-E of Fig. II.5, while those for T_2 are represented by diagrams F-K of Fig. II.5. All these terms are linear in the coefficients and give the linear contributions to the cluster equation. Diagrams A-E of Fig. II.6 arise from linking T_1^2 (two T_1 diagrams) with \hat{f} and \hat{v} diagrams, while diagrams F-M of Fig. II.6 arise from linking of $T_1 T_2$ (a T_1 and a T_2 diagram) with \hat{v} diagrams. These give the non-linear contributions to the equations containing one open-path linked diagrams. No other 'one open-path' diagrams result owing to the linked-cluster theorem represented by eqn. (II.21). The equations corresponding to these diagrams are given in Eqn. (II.28).

$$\begin{aligned}
R_{(2)(2,1)}^{(1)} = & \sum_{\delta \in uw} (4 \langle \epsilon \delta | \hat{V} | wu \rangle - 2 \langle \epsilon \delta | \hat{V} | uw \rangle) t_{\epsilon}^w t_{\delta \alpha}^{ur} - \\
& \sum_{\delta \in uw} (2 \langle \delta \epsilon | \hat{V} | uw \rangle - \langle \delta \epsilon | \hat{V} | wu \rangle) t_{\alpha}^w t_{\delta \epsilon}^{ur} - \\
& \sum_{\delta \in uw} (2 \langle \delta \epsilon | \hat{V} | wu \rangle - \langle \delta \epsilon | \hat{V} | uw \rangle) t_{\delta}^w t_{\alpha \epsilon}^{ur} + \\
& \sum_{\delta \in uw} (2 \langle \delta \epsilon | \hat{V} | uw \rangle - \langle \delta \epsilon | \hat{V} | wu \rangle) t_{\delta}^r t_{\alpha \epsilon}^{uw} .
\end{aligned}$$

The following notation is used to label the terms from the various R diagrams. Each class is represented by $R_{(i)(k)}^{(r)}$ the superscript indicating the number of open-paths, the subscripts indicating the elementary diagrams involved in the linking; i is equal to 1 or 2 depending on whether an \hat{f} or a \hat{v} diagram is involved in the linking; k indicates the T_k operator involved in the linking process. If more than one \hat{T} operator is involved in the linking it is indicated in the second subscript as $(k,1)$, etc.

The one-particle operator \hat{f} (eqn. II.13a) is diagonal if HF basis is used and the matrix elements automatically vanish if \hat{f} connects different single-particle states. For any other basis \hat{f} is not diagonal and the matrix elements connecting different states are given by

$$\begin{aligned}
\langle i | \hat{f} | j \rangle &= \langle i | \hat{g} - \hat{v}_s | j \rangle & \text{for } i \neq j \\
\langle i | \hat{f} | i \rangle &= \epsilon_i + \langle i | \hat{g} - \hat{v}_s | i \rangle
\end{aligned} \tag{II.29}$$

The single-particle states i, j in this case are the eigenfunctions of eqn. (II.25).

Diagrams with two open-paths :

All the topologically distinct two open-path linked diagrams obtained by linking H and T diagrams are given in Figs. II.7, II.8 and II.9. Each diagram represents a pair of particle-hole creation operators. These diagrams are obtained by the following linking between H and T diagrams.

- a) \hat{v} with none of the T diagrams (diagram A of Fig. II.7)
- b) \hat{v} with a T_1 diagram (diagrams B and C of Fig. II.7)
- c) \hat{f} with a T_2 diagram (diagrams D and E of Fig. II.7)
- d) \hat{v} with a T_2 diagram (diagrams F-K of Fig. II.7)
- e) \hat{v} with a T_1^2 (two T_1 's) (diagrams A-C of Fig. II.8)
- f) \hat{v} with a T_2^2 (two T_2 's) (diagrams D-N of Fig. II.8)
- g) \hat{v} with a T_1 and a T_2 (diagrams A-N of Fig. II.9)

Diagrams B and C of Fig. II.7 arise from T_1 diagram linkings while diagrams D-K of Fig. II.7 arise from T_2 diagram linkings. All terms represented by these diagrams are linear in T_1 and T_2 . Diagrams A-C of Fig. II.8 originate from linking of T_1^2 diagrams, D-N of Fig. II.8 from linking of T_2^2 diagrams and A to N of Fig. II.9 from linking of $T_1 T_2$ diagrams. These give the non-linear contributions to the cluster equation with two open-paths. The corresponding equations are given in eqn. (II.30). The topologically identical diagrams with the index permutations $\alpha \longleftrightarrow \beta$, $r \longleftrightarrow s$ are not drawn

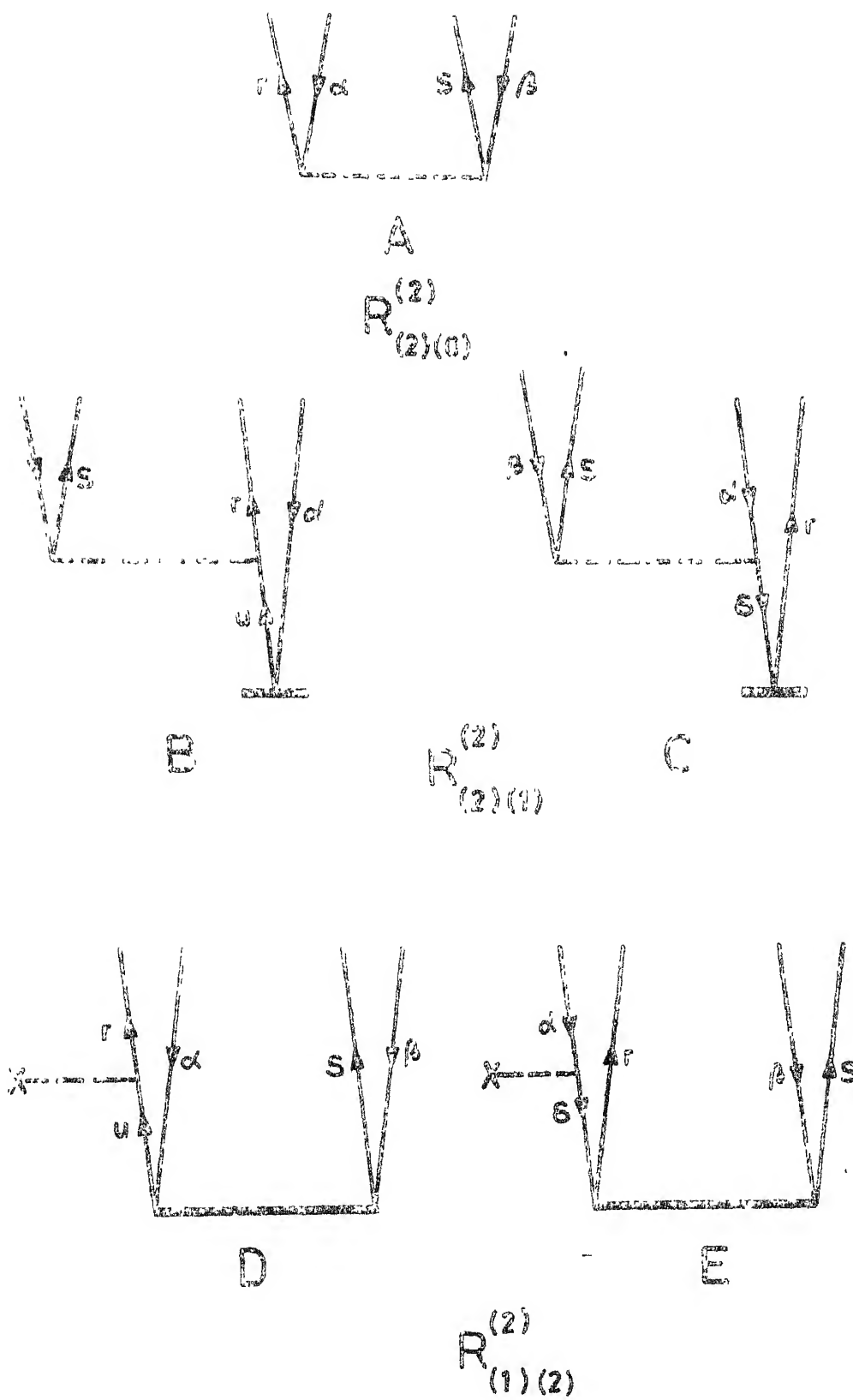
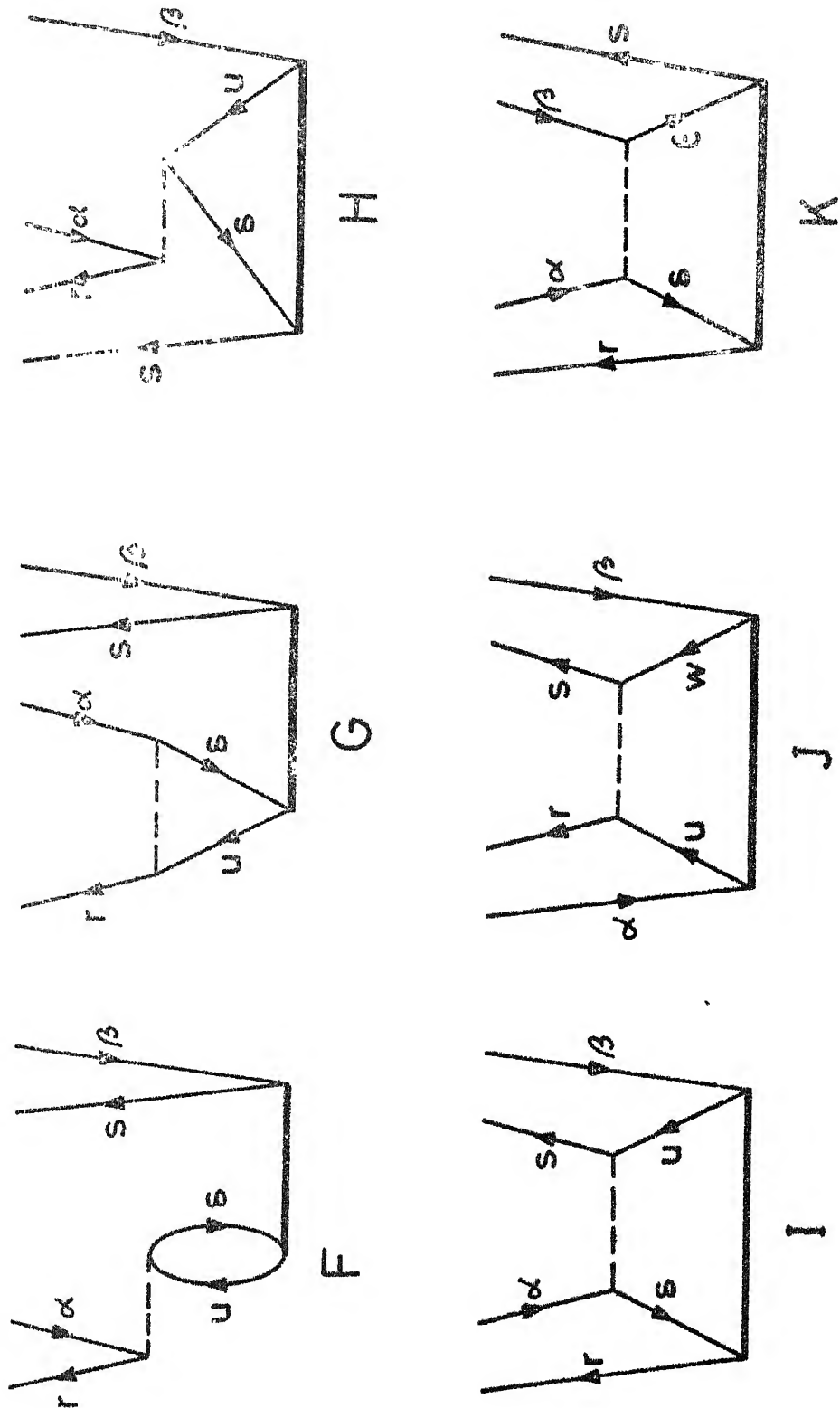
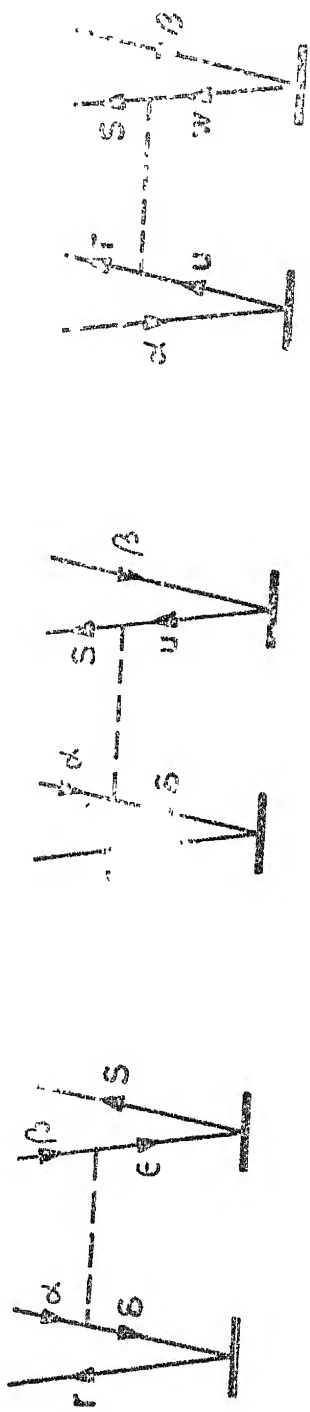


Fig. II.7 (continued)



$$R_{(2)(2)}^{(2)}$$

Fig. II.7 Two open-path diagrams yielding terms linear in t .



A

B

C

$$R_{(2)}^{(2)}(1)$$

Fig. II.8 (continued)

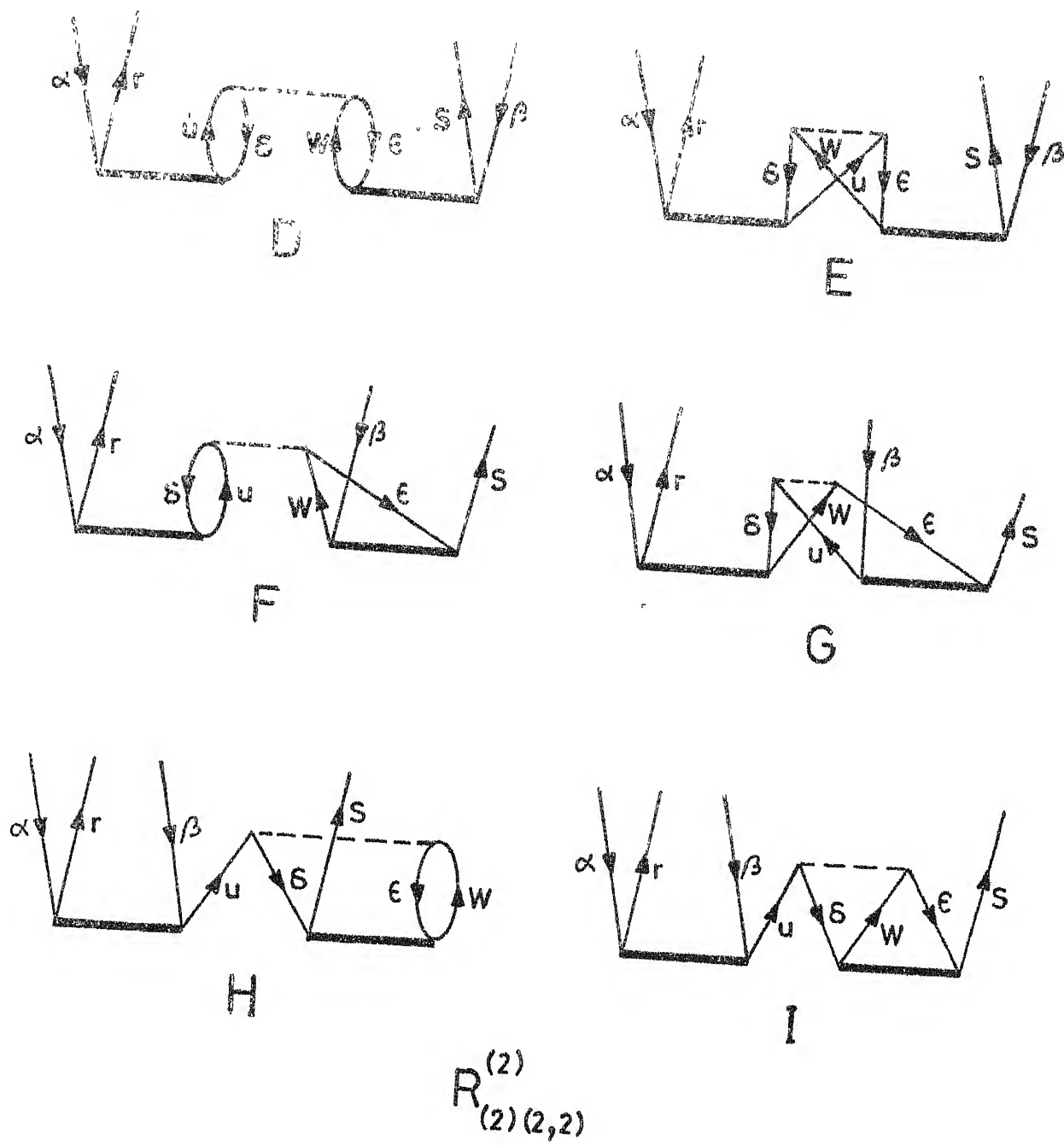


Fig.II.8 (continued)

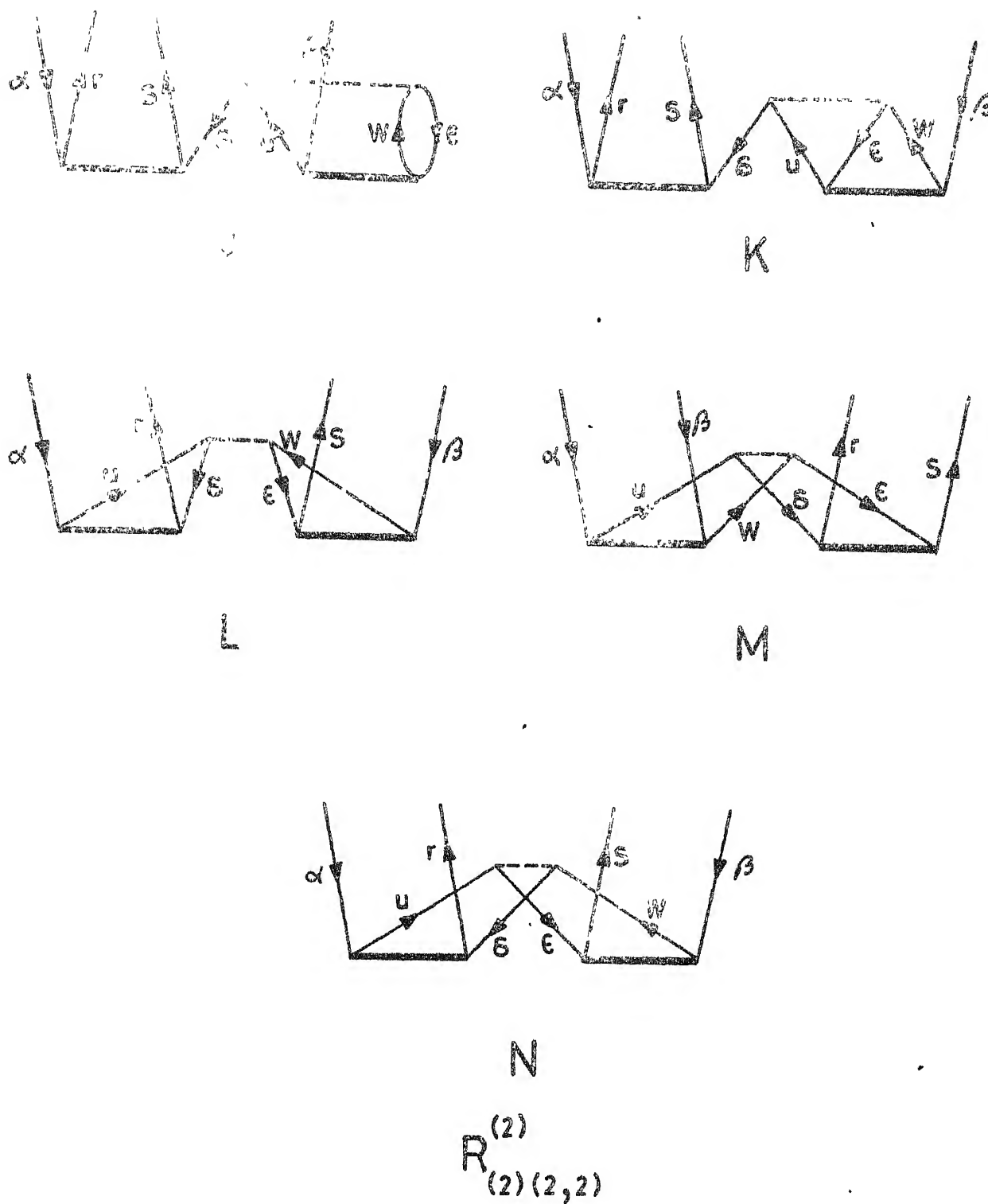
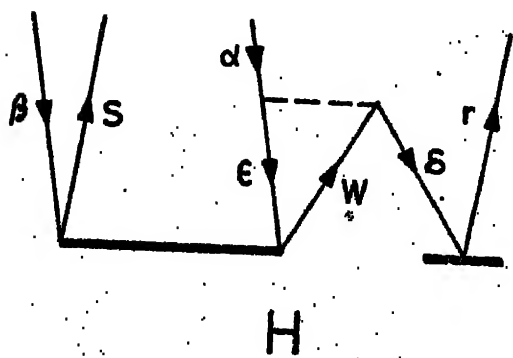
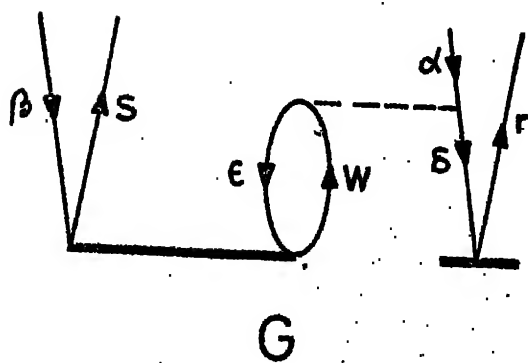
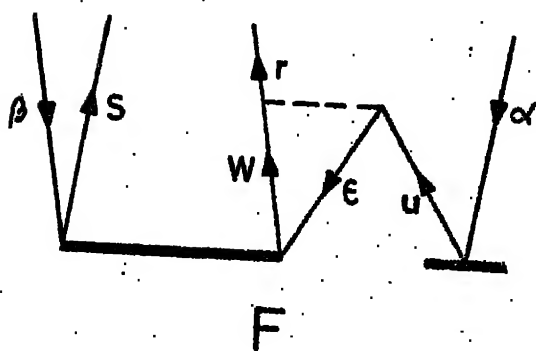
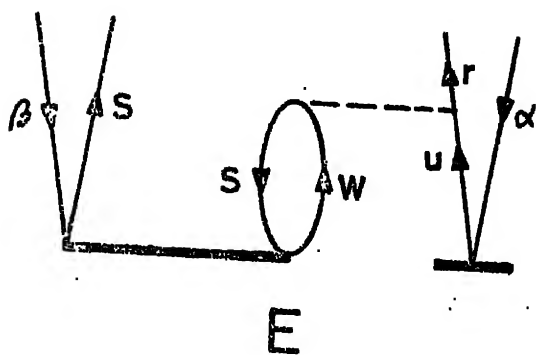
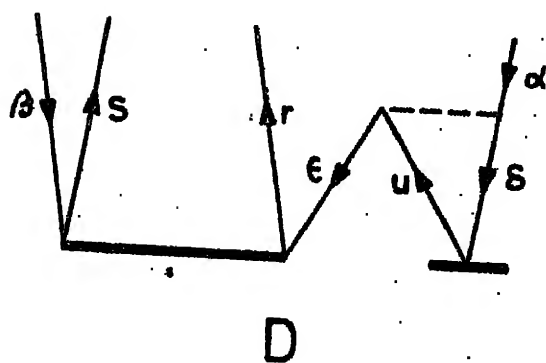
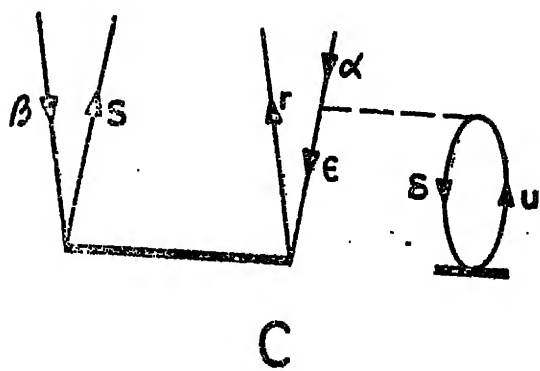
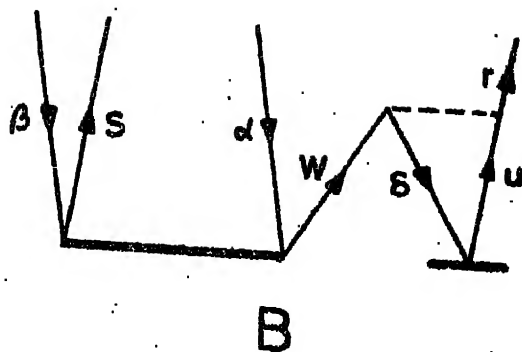
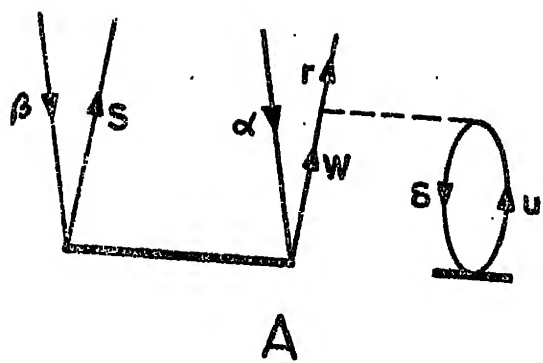


Fig.II.8 Two open-path diagrams (involving T_2^2) yielding terms non-linear in 't'



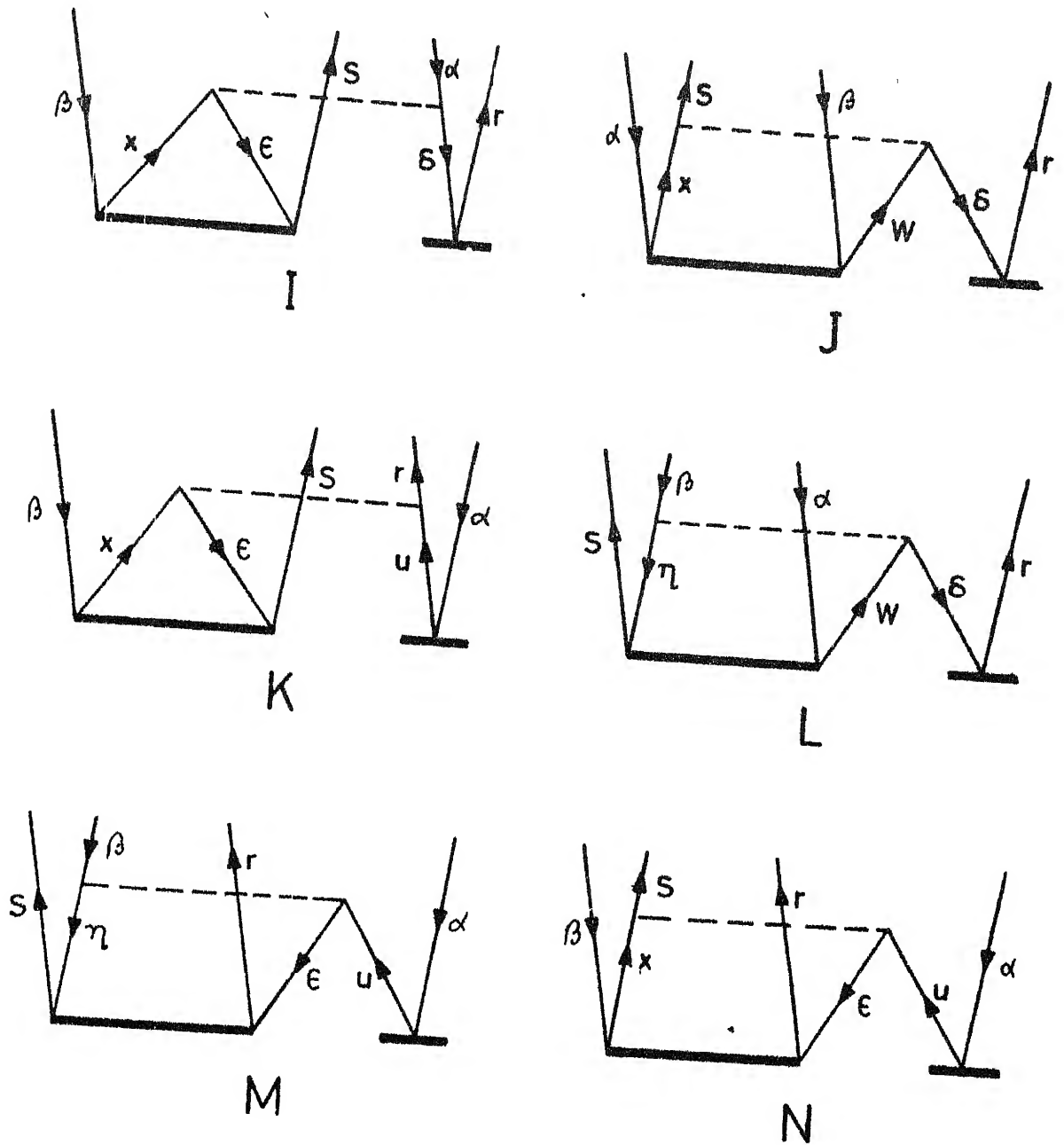


Fig. II.9 Two open-path diagrams (involving $T_1 T_2$) yielding terms non linear in t .

explicitly; however, the terms arising from these diagrams are written explicitly in eqn. (II.30).

The two open-path cluster equations are given by :

$$R_{(2)(0)}^{(2)} + R_{(2)(1)}^{(2)} + R_{(1)(2)}^{(2)} + R_{(2)(2)}^{(2)} + R_{(2)(1,1)}^{(2)} + \\ R_{(2)(2,2)}^{(2)} + R_{(2)(1,2)}^{(2)} = 0 \quad (\text{II.30})$$

where,

$$R_{(2)(0)}^{(2)} = \langle rs | \hat{V} | \alpha \beta \rangle$$

$$R_{(2)(1)}^{(2)} = \sum_u [\langle \beta u | \hat{V} | sr \rangle t_{\alpha}^u + \langle \alpha u | \hat{V} | rs \rangle t_{\beta}^u - \\ \sum_{\delta} [\langle \beta \alpha | \hat{V} | s \delta \rangle t_{\delta}^r + \langle \alpha \beta | \hat{V} | r \delta \rangle t_{\delta}^s].$$

$$R_{(1)(2)}^{(2)} = \sum_u [\langle r | \hat{f} | u \rangle t_{\alpha \beta}^{us} + \langle s | \hat{f} | u \rangle t_{\beta \alpha}^{ur}] - \\ \sum_{\delta} [\langle \alpha | \hat{f} | \delta \rangle t_{\delta \beta}^{rs} + \langle \beta | \hat{f} | \delta \rangle t_{\delta \alpha}^{sr}].$$

$$R_{(2)(2)}^{(2)} = \sum_{u \delta} [(2 \langle r \delta | \hat{V} | \alpha u \rangle - \langle r \delta | \hat{V} | u \alpha \rangle) t_{\delta \beta}^{us} + \\ (2 \langle s \delta | \hat{V} | \beta u \rangle - \langle s \delta | \hat{V} | u \beta \rangle) t_{\delta \alpha}^{ur} - \langle r \delta | \hat{V} | \alpha u \rangle t_{\delta \beta}^{su} - \\ \langle s \delta | \hat{V} | \beta u \rangle t_{\delta \alpha}^{ru} - \langle s \delta | \hat{V} | \beta u \rangle t_{\delta \alpha}^{ru} - \langle \delta r | \hat{V} | \beta u \rangle t_{\delta \alpha}^{su}] + \\ \gamma_2 \sum_{uw} [\langle rs | \hat{V} | uw \rangle t_{\alpha \beta}^{uw} + \langle sr | \hat{V} | uw \rangle t_{\beta \alpha}^{uw}] + \\ \gamma_2 \sum_{\delta \epsilon} [\langle \alpha \beta | \hat{V} | \delta \epsilon \rangle t_{\delta \epsilon}^{rs} + \langle \beta \alpha | \hat{V} | \delta \epsilon \rangle t_{\delta \epsilon}^{sr}].$$

$$R_{(2)}^{(2)}(1,1) = \sum_{\delta \epsilon} \langle \delta \epsilon | \hat{V} | \alpha \beta \rangle t_{\delta}^r t_{\epsilon}^s - \sum_{\delta u} \langle \delta s | \hat{V} | \alpha u \rangle t_{\delta}^r t_{\beta}^u +$$

$$\sum_{uw} \langle uw | \hat{V} | rs \rangle t_{\alpha}^u t_{\beta}^w$$

$$R_{(2)}^{(2)}(2,2) = \sum_{\delta \epsilon uw} [(2 \langle \delta \epsilon | \hat{V} | uw \rangle - \langle \delta \epsilon | \hat{V} | wu \rangle)$$

$$(t_{\alpha \delta}^{ru} t_{\beta \epsilon}^{sw} + t_{\beta \delta}^{su} t_{\alpha \epsilon}^{rw} - t_{\alpha \delta}^{ru} t_{\beta \epsilon}^{ws} - t_{\beta \delta}^{su} t_{\alpha \epsilon}^{wr} - t_{\alpha \beta}^{ru} t_{\delta \epsilon}^{sw} -$$

$$t_{\beta \alpha}^{su} t_{\delta \epsilon}^{rw} - t_{\alpha \delta}^{rs} t_{\beta \epsilon}^{uw} - t_{\beta \delta}^{sr} t_{\alpha \epsilon}^{uw}) +$$

$$1/2 \langle \delta \epsilon | \hat{V} | uw \rangle (t_{\alpha \delta}^{ur} t_{\epsilon \beta}^{sw} + t_{\alpha \beta}^{uw} t_{\delta \epsilon}^{rs} + t_{\alpha \delta}^{ur} t_{\epsilon \beta}^{sw} +$$

$$t_{\beta \delta}^{us} t_{\epsilon \alpha}^{rw} + t_{\beta \alpha}^{uw} t_{\delta \epsilon}^{sr} + t_{\beta \delta}^{us} t_{\epsilon \alpha}^{rw})].$$

$$R_{(2)}^{(2)}(1,2) = \sum_{\delta uw} [(2 \langle r \delta | \hat{V} | wu \rangle - \langle r \delta | \hat{V} | uw \rangle) t_{\delta}^u t_{\alpha \beta}^{ws} +$$

$$(2 \langle s \delta | \hat{V} | wu \rangle - \langle s \delta | \hat{V} | uw \rangle) t_{\delta}^u t_{\beta \alpha}^{wr}] -$$

$$\sum_{\delta \epsilon u} [(2 \langle \epsilon \delta | \hat{V} | \alpha u \rangle - \langle \epsilon \delta | \hat{V} | u \alpha \rangle) t_{\delta}^u t_{\epsilon \beta}^{rs} +$$

$$(2 \langle \epsilon \delta | \hat{V} | \beta u \rangle - \langle \epsilon \delta | \hat{V} | u \beta \rangle) t_{\delta}^u t_{\epsilon \alpha}^{sr}] +$$

$$\sum_{\epsilon uw} [(2 \langle r \epsilon | \hat{V} | uw \rangle - \langle r \epsilon | \hat{V} | wu \rangle) t_{\alpha}^u t_{\epsilon \beta}^{ws} +$$

$$(2 \langle s \epsilon | \hat{V} | uw \rangle - \langle s \epsilon | \hat{V} | wu \rangle) t_{\beta}^u t_{\epsilon \alpha}^{wr}] -$$

$$\sum_{\delta \epsilon w} [(2 \langle \delta \epsilon | \hat{V} | \alpha w \rangle - \langle \delta \epsilon | \hat{V} | w \alpha \rangle) t_{\delta}^r t_{\epsilon \beta}^{ws} +$$

$$(2 \langle \delta \epsilon | \hat{V} | \beta w \rangle - \langle \delta \epsilon | \hat{V} | w \beta \rangle) t_{\delta}^s t_{\epsilon \alpha}^{wr}] +$$

$$\sum_{\epsilon x} [\langle \delta \epsilon | \hat{V} | \alpha x \rangle t_{\delta}^r t_{\epsilon \beta}^{sx} + \langle \delta \epsilon | \hat{V} | \beta x \rangle t_{\delta}^s t_{\epsilon \alpha}^{rx}] -$$

$$\begin{aligned}
& \sum_{\delta w x} [\langle s\delta | \hat{V} | xw \rangle t_{\delta}^r t_{\alpha\beta}^{wx} + \langle r\delta | \hat{V} | xw \rangle t_{\delta}^s t_{\beta\alpha}^{wx}] - \\
& \sum_{\epsilon u x} [\langle r\epsilon | \hat{V} | ux \rangle t_{\alpha}^u t_{\epsilon\beta}^{sx} + \langle s\epsilon | \hat{V} | ux \rangle t_{\beta}^u t_{\epsilon\alpha}^{sx}] + \\
& \sum_{\delta \eta w} [\langle \delta\eta | \hat{V} | w\beta \rangle t_{\delta}^r t_{\alpha\eta}^{ws} + \langle \delta\eta | \hat{V} | w\alpha \rangle t_{\delta}^s t_{\eta\alpha}^{wr}] + \\
& \sum_{\epsilon \eta u} [\langle \epsilon\eta | \hat{V} | u\beta \rangle t_{\alpha}^u t_{\epsilon\eta}^{rs} + \langle \epsilon\eta | \hat{V} | u\alpha \rangle t_{\beta}^u t_{\epsilon\eta}^{sr}] - \\
& \sum_{\epsilon u x} [\langle s\epsilon | \hat{V} | xu \rangle t_{\alpha}^u t_{\epsilon\beta}^{rx} + \langle r\epsilon | \hat{V} | xu \rangle t_{\beta}^u t_{\epsilon\alpha}^{sx}] .
\end{aligned}$$

The coupled non-linear equations, eqns. (II.28) and (II.30) yield as solutions the cluster coefficients, which can then be substituted in eqn. (II.26) to obtain ΔE .

II.5 RELATIONSHIP OF THE CC METHOD TO OTHER MANY-ELECTRON THEORIES

The relationship of the CC coefficients to the CI coefficients was outlined in Sec. II.2. The CC method is an extremely elegant way of incorporating the many-electron correlations. In contrast to CI, the method is rigorously size-extensive and avoids the messy problem of dealing with Slater determinants. However, the method is non-variational and can lead to energies lower than the exact energies [90]. Variational counterparts of the CC method, although, are very complicated, still involve less computational effort than full CI methods [31].

The relationship of the CC method to the perturbative methods is even more obvious; after all, as shown in Sec.II.1, the basic form of the wavefunction in the CC method is a direct result from RSPT. The perturbative flavor of the method becomes apparent from the comparison of the Goldstone diagrams in the two versions of the theory. The cluster equations, eqns. (II.28) and (II.30) can be written in such a manner that a diagrammatic expansion is obtained for each t . When this is substituted into the energy diagrams (vide Fig. II.4) taking into account the appropriate label matching of the lines, a Goldstone-like expansion is obtained for the energy. Iteration of the equations leads to generation of Goldstone diagrams to higher orders. For instance, inclusion of the diagram K of Fig. II.7 in cluster equations is equivalent to performing an MBPT partial summation to all orders of the corresponding ladder diagram [62]. Similarly, the diagram F of Fig. II.7 generates the corresponding ring diagrams of perturbation theory to all orders. This is illustrated in Fig. II.10. Alternatively, this can also be pictured from perturbation theory. Snipping off the top-most vertices of the Goldstone perturbation energy diagrams results in the open-path diagrams that have topological structures similar to the diagrams in Figs. II.6 - II.9 [60]. It is obvious from this that the ΔE obtained by solution of the coupled equations, eqns. (II.26), (II.28) and (II.30), invokes perturbation theory diagrams that far exceed the

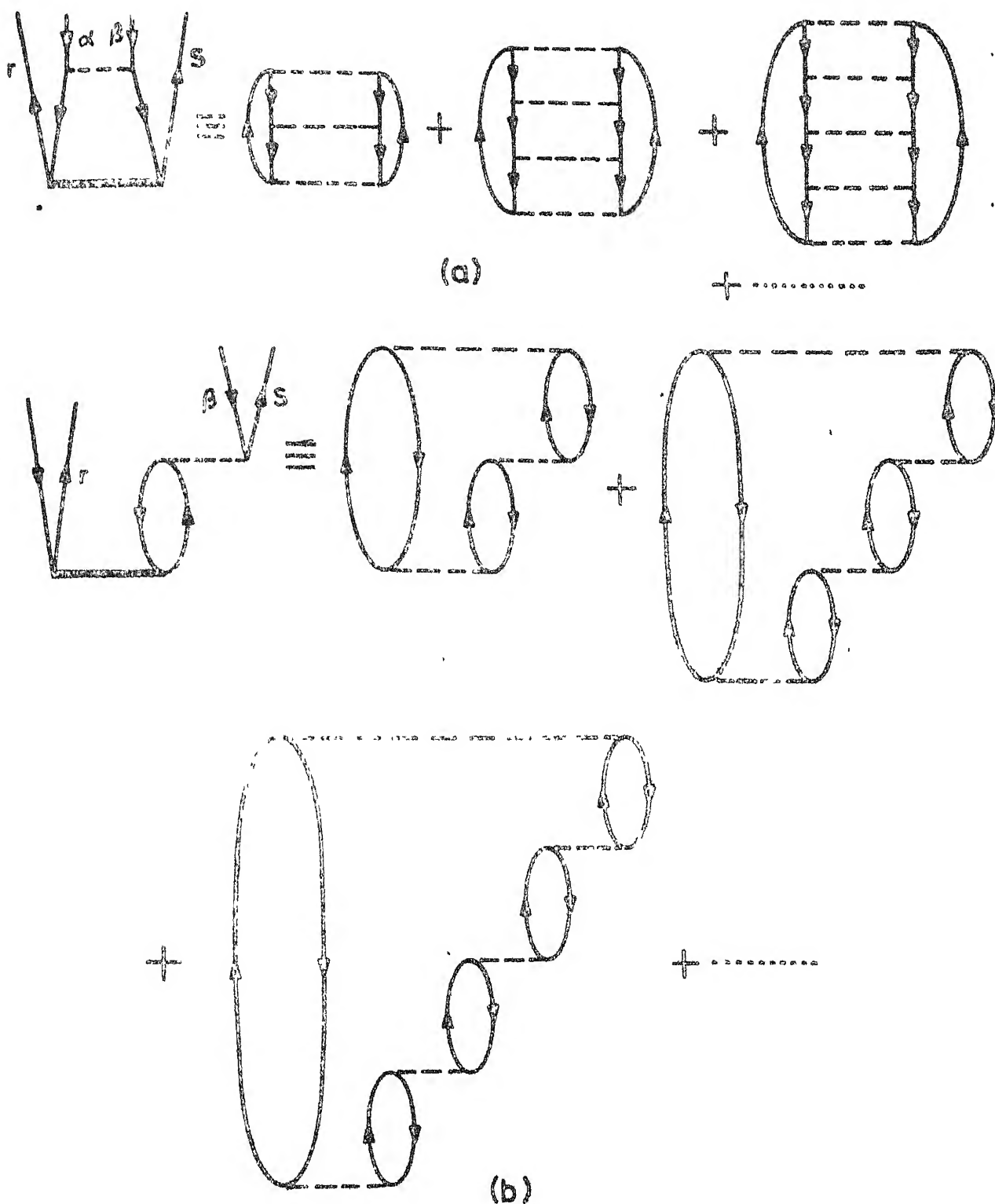


Fig. II 10 Classes of energy diagrams generated by the R diagrams. (a) Ladder diagrams (b) ring diagrams.

number that can be included by MBPT calculations. Also, by choosing only certain diagrams in eqns. (II.28) and (II.30) it is possible to obtain selective perturbation summations to infinite orders. For instance, retaining only the diagrams A and K of Fig. II.7 leads to a result equivalent to selective summation of particle-particle ladder diagrams to all orders in perturbation theory. Likewise, consideration of all ladder diagrams in this theory yields equations similar to the Bethe-Goldstone equations of nuclear many-body theory [91]. On the other hand, retention of only the diagrams D of Fig. II.5, A and F of Fig. II.7 and D of Fig. II.8 in the cluster equations yields solutions equivalent to those obtained by inclusion of ring diagrams to all orders in perturbation theory.

As shown by Paldus et al. [89], the T_2 approximation to the CC method is a generalisation of Sinanoglu's decoupled-pair many-electron theory (DPMET). When the occupied orbitals in the CC equations for the ' T_2 only' approximation are restricted to a pair of spin-orbitals, and the inter-pair neglected, each surviving term assumes the form of a product of a pair correlation energy and the corresponding t_2 amplitude. The CC equations, therefore, reduce to a number of independent equations one for each pair of occupied orbitals. These equations are exactly those of Sinanoglu's DPMET theory.

The CC method, it is apparent from the above discussion, is superior to both CI and MBPT methods at least for many-

electron systems. The closed-shell version described here has been generalised with the aid of graphical methods of angular momentum to open-shell systems by a number of workers [59,60,92,93]. This open-shell version of the theory has also been shown to be very superior to all the existing open-shell many-electron theories. An excellent review of the CC method and its applications has been presented by Kümmel et al [67]. The applications have included the analysis of correlation effects in atoms and molecules [35,89,94], analysis of exchange effects via inclusions of ring diagrams in electron gas [95], and the analysis of long-range forces in nuclear matter [67].

In the next chapter, we present as an example of the application of the CC methodology, the calculation of EC corrections in beryllium atom.

CHAPTER III

A MODEL CALCULATION OF EXCHANGE-CORRELATION CORRECTIONS USING COUPLED-CLUSTER METHODOLOGY

III.1 General

III.2 Details of Computational Method

III.2.1 The Atomic Orbitals

III.2.2 Matrix Elements and the Total Energy

III.2.3 The CC Equations

III.2.4 Numerical Methods

III.3 Hierarchy of Approximations to the CC Equations

III.4 Results of the Calculation and Discussion

III.1 GENERAL

This chapter presents the procedural details of the computations performed in this thesis and a model calculation to illustrate the CC methodology. The $X\alpha$ approximation of Slater[8] is our starting point. The self-consistent field orbitals obtained by this method are used to generate the matrix elements and to calculate the total electronic energy of the atom. The CC equations for various hierarchy of approximations are set-up and solved using iterative algorithms. For all the cases a partial wave analysis of the EC energy corrections is presented.

The beryllium atom has been chosen as the model system for this study in view of the following : beryllium is the simplest example of a true many-electron system. Almost every tool in the theoretical chemists' repertoire has been employed for the study of this atom with the result that it is the best understood many-electron system [96] . And the tour de force calculations that have been performed on beryllium [97,98] make it an ideal probe to test new theories and determine their range of validity. Above everything else, the spherical symmetry coupled with the presence of a mere four electrons renders it the most attractive choice for model studies.

III.2 DETAILS OF COMPUTATIONAL METHOD

III.2.1 The Atomic Orbitals

The occupied and virtual atomic orbitals of the beryllium atom are obtained as solutions to the self-consistent field equations of the $X\alpha$ Hamiltonian.

$$\left\{ -\frac{\hbar^2}{2m} \nabla^2 + \hat{V}(r) + \int \frac{\rho(r')}{|r-r'|} dr' - 3\alpha \left[\frac{3}{4\pi} \rho(r) \right]^{1/3} \right\} \phi_i(r) = \epsilon_i \phi_i(r) \quad (\text{III.1})$$

In this study, the virtual orbital basis is chosen to consist of the three 2p, the 3s and the three 3p orbitals bounded by the self-consistent local potential of the occupied orbitals 1s and 2s. Slater's exchange parameter α is chosen to be 0.768, keeping in view the observation, that orbitals obtained with this α in eqn. (III.1) closely mimic the corresponding HF orbitals [24]. The orbitals ϕ_i , which are functions of coordinate space are written in the central field approximation as

$$\phi_i = R_{n_i l_i}(r_i) Y_{l_i m_{l_i}}(\theta, \phi) \quad (\text{III.2})$$

The $R_{nl}(r)$ form the radial part of the wavefunction and $Y_{lm}(\theta, \phi)$ are the normalised spherical harmonics : n, l, m_l are respectively the principal, orbital and magnetic quantum numbers. Within the central field approximation, the radial part of eqn. (III.1) assumes the form,

$$\left[-\frac{d}{dr^2} + \frac{l(l+1)}{r^2} + v(r) \right] P_{nl}(r) = E_{nl} P_{nl}(r) \quad (\text{III.3})$$

where,

$$P_{nl}(r) = r R_{nl}(r) \quad (\text{III.4})$$

are the normalised radial wavefunctions. The potential $v(r)$ in eqn. (III.3) is given by

$$v(r) = -\frac{2Z}{r} + \frac{2}{r} \int_0^r \sum_{nl} [P_{nl}(t)]^2 dt + 2 \int_r^\infty \sum_{nl} \frac{[P_{nl}(t)]^2}{t} dt -$$

$$3\alpha \left\{ \frac{3}{4\pi r^2} \sum_{nl} [P_{nl}(r)]^2 \right\}^{1/3} \quad \text{for } r < r_0 \quad (\text{III.5})$$

and

$$v(r) = -\frac{2(Z-N+1)}{r} \quad \text{for } r > r_0 \quad (\text{III.6})$$

Z being the atomic number and N the total number of electrons. Eqn. (III.6) defines the Latter modification to the $X\alpha$ potential [99], introduced to correct the unphysical behaviour of the local potential $v(r)$ of eqn. (III.3) at large r values. In the absence of Latter correction the virtual orbitals remain unbounded. A modified Herman-Skillman program [100] is used to obtain the solutions to eqn. (III.3). In this program a linearly scaled 441-point mesh is used to obtain the numerical wavefunction at these points.

III.2.2 Matrix Elements and the Total Energy

The total ground-state electronic energy of the atom is determined with the basis set of orbitals ϕ_i of

eqn. (III.2) whose radial part is obtained as solutions to eqn. (III.3). The Fock Hamiltonian is constructed with these $X\alpha$ orbitals for determining the total energy

$$E = \sum_a I(a) + \sum_{\substack{a,b \\ \text{pairs}}} [J(a,b) - K(a,b)] \quad (\text{III.7})$$

where,

$$I(a) = \int \phi_a^*(1) \hat{f}(1) \phi_a(1) d\tau_1 \quad (\text{III.8})$$

where $f(1)$ defines the sum of one-electron kinetic energy and nucleus-electron attraction energy operator, and

$$J(a,b) = \int \int \phi_a^*(1) \frac{e^2}{|r_1 - r_2|} \phi_b^2(2) d\tau_1 d\tau_2 \quad (\text{III.9})$$

$$K(a,b) = \int \int \phi_a^*(1) \phi_b^*(2) \frac{e^2}{|r_1 - r_2|} \phi_a(2) \phi_b(1) d\tau_1 d\tau_2 \quad (\text{III.10})$$

are the Fock matrix elements that represent the coulomb and the exchange energies. The matrix elements $J(a,b)$ and $K(a,b)$ are given by the usual expressions [3,101]

$$J(a,b) = \sum_k a^k(a,b) F^k(a,b) \quad (\text{III.11})$$

$$K(a,b) = \delta(m_{s_a}, m_{s_b}) \sum_k b^k(a,b) G^k(a,b) \quad (\text{III.12})$$

where the factors a^k and b^k can be expressed in terms of the Wigner 3-j symbols

$$a^k(a,b) = (-1)^{(m_a+m_b)} (2l_a+1)(2l_b+1) \begin{pmatrix} 1_a & 1_a & k \\ 0 & 0 & 0 \end{pmatrix} \begin{pmatrix} 1_b & 1_b & k \\ 0 & 0 & 0 \end{pmatrix} \\ \times \begin{pmatrix} 1_a & 1_a & k \\ -m_a & m_a & 0 \end{pmatrix} \begin{pmatrix} 1_b & 1_b & k \\ -m_b & m_b & 0 \end{pmatrix} \quad (\text{III.13})$$

$$b^k(a,b) = (2l_a+1)(2l_b+1) \begin{pmatrix} 1_a & 1_b & k \\ 0 & 0 & 0 \end{pmatrix}^2 \begin{pmatrix} 1_a & 1_b & k \\ -m_a & m_b & m_a-m_b \end{pmatrix}^2 \\ (\text{III.14})$$

and F^k and G^k are the Slater-Condon parameters,

$$F^k(a,b) = e^2 R^k(a,b; a,b) \quad (\text{III.15})$$

$$G^k(a,b) = e^2 R^k(a,b; b,a) \quad (\text{III.16})$$

The radial matrix elements $R^k(a,b; c,d)$ are given by,

$$R^k(a,b; c,d) = \int_0^\infty \int_0^\infty \frac{r_1^k}{r_1^{k+1}} P_a(1) P_c(1) P_b(2) P_d(2) dr_1 dr_2 \\ (\text{III.17})$$

The general r_{12} matrix elements are given by

$$\langle a b | \frac{e^2}{|r_1-r_2|} | cd \rangle = \delta(m_{s_a}, m_{s_c}) \delta(m_{s_b}, m_{s_d}) (-1)^{(m_a+m_d)} e^2 \\ \times \sum_k [(2l_a+1)(2l_b+1)(2l_c+1)(2l_d+1)]^2 \\ \times \begin{pmatrix} 1_a & 1_c & k \\ 0 & 0 & 0 \end{pmatrix} \begin{pmatrix} 1_d & 1_b & k \\ 0 & 0 & 0 \end{pmatrix} \begin{pmatrix} 1_a & 1_c & k \\ m_a & m_c & m \end{pmatrix} \begin{pmatrix} 1_d & 1_b & k \\ -m_d & m_b & m \end{pmatrix} \\ \times R^k(a,b; c,d) \quad ; \text{ where } m = (m_a - m_c) = (m_d - m_b). \quad (\text{III.18})$$

The F^k and G^k integrals are evaluated with a modified version of the computer program of Zare [102] and the ground-state energy of the atom is computed. Programs have also been developed for the evaluation of the general matrix element given by eqn. (III.18). An extended Simpson's rule integration formula [103], is used for the evaluation of the R^k integrals. A FORTRAN listing of the relevant program is presented in Appendix B. All calculations presented in this thesis have been performed with a DEC 1090 system.

III.2.3 The CC Equations

The CC equations described in eqns. (II.28) and (II.30) are coupled non-linear equations, whose unknowns are the excitation coefficients, t 's (vide Chapter II). These equations define the full CC many-electron theory, where the operator T contains T_1 terms, T_2 terms and all the non-linear terms involving the products and squares of these. The non-linear CC equations are very complicated and tedious to solve. As is true of any system of non-linear equations, existence of multiple minima can cause innumerable computational difficulties and lead to spurious solutions. Keeping this in view, we first attempted the solution of the linear part of the equations.

The linear CC equations contain terms arising from T_1 and T_2 operators. The diagrammatic representation of these equations has been given in Figs. II.5 and II.7. The one

open-path and two open-path diagram equations independently equal zero, but are coupled due to the presence of t_{α}^r and $t_{\alpha\beta}^{rs}$ occurring in both the equations, eqns. (II.28) and (II.30). The linear part of these equations is given in eqns. (III.19) and (III.20).

$$\begin{aligned}
 < r | \hat{f} | \alpha > + \sum_s < r | \hat{f} | s > t_{\alpha}^s - \sum_{\beta} < \beta | \hat{f} | \alpha > t_{\beta}^r \\
 & - \sum_{\beta s} (2 < r \beta | \hat{V} | \alpha s > - < r \beta | \hat{V} | s \alpha >) t_{\beta}^s \\
 & + \sum_{\beta s} (2 < \beta | \hat{f} | s > t_{\beta\alpha}^{sr} - < \beta | \hat{f} | s >) t_{\alpha\beta}^{sr} \\
 & + \sum_{\beta su} (2 < r \beta | \hat{V} | us > - < r \beta | \hat{V} | su >) t_{\beta\alpha}^{su} \\
 & - \sum_{\beta\delta s} (2 < \delta \beta | \hat{V} | \alpha s > - < \delta \beta | \hat{V} | s \alpha >) t_{\beta\delta}^{sr} = 0 \quad (\text{III.19})
 \end{aligned}$$

$$\begin{aligned}
 < rs | \hat{V} | \alpha \beta > + \sum_u [< \beta u | \hat{V} | sr > t_{\alpha}^u + < \alpha u | \hat{V} | rs > t_{\beta}^u] - \\
 & \sum_{\delta} [< \beta \alpha | \hat{V} | s \delta > t_{\delta}^r + < \alpha \beta | \hat{V} | r \delta > t_{\delta}^s] + \\
 & \sum_u [< r | \hat{f} | u > t_{\alpha\beta}^{us} + < s | \hat{f} | u > t_{\beta\alpha}^{ur}] - \\
 & \sum_{\delta} [< \alpha | \hat{f} | \delta > t_{\delta\beta}^{rs} + < \beta | \hat{f} | \delta > t_{\delta\alpha}^{sr}] + \\
 & \sum_{u\delta} [(2 < r \delta | \hat{V} | \alpha u > - < r \delta | \hat{V} | u \alpha >) t_{\delta\alpha}^{us} + \\
 & (2 < s \delta | \hat{V} | \beta u > - < s \delta | \hat{V} | u \beta >) t_{\delta\alpha}^{ur} - \\
 & < r \delta | \hat{V} | \alpha u > t_{\delta\beta}^{su} - < \delta s | \hat{V} | \alpha u > t_{\delta\beta}^{ru} - \\
 & < s \delta | \hat{V} | \beta u > t_{\delta\alpha}^{ru} - < \delta r | \hat{V} | \beta u > t_{\delta\alpha}^{su}] +
 \end{aligned}$$

$$\begin{aligned}
& + \frac{1}{2} \sum_{uw} [\langle rs | \hat{V} | uw \rangle t_{\alpha\beta}^{uw} + \langle sr | \hat{V} | uw \rangle t_{\beta\alpha}^{uw}] + \\
& \frac{1}{2} \sum_{\delta\epsilon} [\langle \alpha\beta | \hat{V} | \delta\epsilon \rangle t_{\delta\epsilon}^{rs} + \langle \beta\alpha | \hat{V} | \delta\epsilon \rangle t_{\delta\epsilon}^{sr}] \\
& = 0 \qquad \qquad \qquad (III.20)
\end{aligned}$$

where $\alpha, \beta \dots$ represent the occupied 1s and 2s orbitals while r, s, \dots represent the virtual 2p, 3s and 3p orbitals.

III.2.4 Numerical Methods

The linear equations, eqn. (III.19) and (III.20) contain, besides the unknown CC coefficients, the general r_{12} matrix elements and the orbital energies, which have been evaluated as described in Section III.2.2. For our calculation on Be, we chose a basis consisting of the three 2p, 3s and three 3p orbitals in addition to the ground-state 1s and 2s orbitals. The number of cluster coefficients, i.e. unknowns of eqns. (III.19) and (III.20), total 210. These contain the 14 single excitation coefficients, t_{α}^r and 196 double excitation coefficients, $t_{\alpha\beta}^{rs}$. The $t_{\alpha\beta}^{rs}$ possess the permutational symmetry $t_{\alpha\beta}^{rs} = t_{\beta\alpha}^{sr}$ and, therefore, the number of unknowns reduces further to 119. Our linear equations then are of the form,

$$\underline{A} \underline{x} = \underline{B} \qquad \qquad \qquad (III.21)$$

where \underline{A} has the dimension 119×119 , These equations are solved using the triangular decomposition procedure [104].

The matrix \underline{A} is decomposed into an upper triangular and a lower triangular matrix such that

$$\underline{A} = \underline{L} \underline{U} \quad (\text{III.22})$$

The system of eqns. (III.21), is then solved through the solution of the system,

$$\underline{L} \underline{y} = \underline{B} \quad (\text{III.23})$$

and then the system

$$\underline{U} \underline{x} = \underline{y} \quad (\text{III.24})$$

since,
$$\underline{A} \underline{x} = \underline{L} \underline{U} \underline{x} = \underline{L} \underline{y} = \underline{B} \quad (\text{III.25})$$

Since both \underline{L} and \underline{U} are triangular, eqns. (III.23) and (III.24) are much more easily solved than eqn. (III.22). A routine to improve the solutions has also been introduced. The entire solution takes less than 10 secs of CPU time in the DEC 1090 computer. A listing of the computer program is presented in Appendix B.

While the linear equations were well-behaved and yielded solutions accurate to within 1 in 10^{-8} , the solution of the full non-linear equations turned out to be computationally very complicated. Several efficient algorithms [105] were used in an attempt to solve the non-linear equations. The Newton-Raphson procedure, which has quadratic convergence, yielded solutions which however corresponded to incorrect minima. We then used a modification of the Newton's method,

the powerful Brown's algorithm [106], with the hope of obtaining the correct minima. In Newton's iterative method, all members of the system of equations are expanded simultaneously about a point, x^n , assumed to be close to the solution. For the system

$$f(x) = 0 \quad (\text{III.26})$$

the expansion is,

$$f(x) = f(x^n) + J(x^n)(x-x^n) \quad (\text{III.27})$$

where J is the Jacobian matrix; the higher order terms in the expansion are neglected. The expansion is iterated to convergence. In Brown's algorithm a successive substitution scheme is used rather than the simultaneous treatment of all f_i as in Newton's method; i.e., the modified root of f_1 is used in f_2 and that of f_2 in f_3 , etc. The derivative-free version, where the derivatives in the Jacobian were replaced by first-difference quotients, was used. The search based on Brown's method also failed to converge. Further work is in progress. Only results obtained from the solution of the linear equations are reported in this thesis.

III.3 HIERARCHY OF APPROXIMATIONS TO THE CC EQUATIONS

A. In this approximation the entire linear part of the cluster equations, eqns. (III.19) and (III.20) is set-up and solved. These equations result from inclusion of all the

diagrams involving the linear T_1 and T_2 terms. This procedure is formally equivalent to performing a CI calculation with all single- and double- excited determinants.

B. In this set of approximations only the terms arising from the linear part of T_2 diagrams have been retained in the CC equation. In the first case one and two open-path diagrams of the above mentioned type (diagrams F-K of Fig. II.5 and diagrams A and D-K of Fig. II.7) have been retained, while in the second case only two open-path diagrams of the above mentioned type have been retained (diagrams A and D-K of Fig. II.7). Both cases lead to almost identical results and, therefore, the results of only one of these has been presented. The procedure is equivalent to a variant of the coupled electron pair approximation [31].

C. In this approximation all the one and two open-path ladder diagrams (diagrams A-C of Fig. II.5 and diagrams A,D,E and J of Fig. II.7) arising from the T_1 and T_2 approximation have been included in the CC equation. The procedure is equivalent to solving the generalised Nesbet-Bethe-Goldstone equations [46].

D. In this approximation, only the terms arising from the two open-path ladder diagrams (diagrams A,D,E and J of Fig. II.7) have been included in the CC equation. This procedure is equivalent to a partial summation of ladder diagrams to all orders in MBPT [62].

E. In this approximation only the particle-particle ladder diagram given by diagram J of Fig. II.7 is included. This result is equivalent to a selective summation of the corresponding particle-particle ladder diagram in perturbation theory to all orders.

F. In this approximation, the CC equivalent of the second-order RSPT equations are set up and solved. This is achieved by taking into consideration only the diagram A of Fig. II.7 into account for generating the terms of the equation.

III.4 RESULTS OF THE CALCULATION AND DISCUSSION

Table III.1 presents the pair-wise contribution to the energy corrections and the total EC energy corrections for the Approximations A to F mentioned above. In Table III.2, we present a partial wave analysis of the EC energy corrections wherein the ss and pp excitation contributions to $1s^2$, $1s\ 2s$ and $2s^2$ pairs are determined separately. In Table III.3, we give the individual contributions to the EC corrections.

A cursory analysis of the results presented in Tables III.1 and III.2, reveals the following : In all the approximations used, the contribution to EC correction energies comes mainly from the $2s^2$ pair, whereas in the calculations of Paldus et al [90], where the HF method is used as the starting point, $1s^2$ pair contributions are found to be

Table III.1 EC Energy Corrections in Beryllium Atom

Approximation	Pair-wise Contribution to the			Total Correction*	Total Energy ⁺
	$1s^2$	$1s\ 2s$	$2s^2$		
A	- 4.4198	-57.0836	-9628.1753	-9746.7623	-14.663598
B	- 4.6022	-60.0177	-10115.6070	-10240.2450	-14.668532
C	-11.6494	-163.5081	-13440.0790	-13778.7920	-14.703918
D	-11.3484	-155.7249	-12875.2480	-13198.0470	-14.698110
E	- 2.3098	-11.8982	-1944.2400	-1958.4480	-14.585715
F	- 2.3945	- 6.4007	-4435.2347	-4450.4306	-14.610634

*All values in units of 10^{-5} Hartree

+ All values in units of Hartree

Table III.2 Partial Wave Analysis of the EC Energy Corrections
in Beryllium Atom

Approximation	Partial Wave Contribution	1s	2s	2s ²
A		- 0.5343	2.5563	-244.8591
B		- 0.5916	3.0287	-289.5595
C		- 0.1319	- 0.7042	57.6863
D	ss	- 0.2248	- 0.1287	4.6673
E		- 0.2483	- 0.0459	- 39.1784
F		- 0.2522	- 0.0460	- 64.2064
A		- 3.8855	-116.7235	-9383.3161
B		- 4.0107	-123.0641	-9826.0477
C	pp	-11.5644	-326.3120	-13497.7650
D		-11.1236	-311.3212	-12879.9160
E		- 2.0616	-11.8523	-1905.0616
F		- 2.1422	-12.7554	-4371.0283

All values in units of 10^{-5} Hartree.

Table III.3 Individual Contributions to EC
Corrections in Beryllium Atom

virtual occupied	$2p^2$	$2p\ 3p$	$3s^2$	$3p^2$
$1s^2$	-8.1063	2.5304	-0.5343	1.6906
$1s\ 2s$	-316.0383	134.4522	2.5562	64.8626
$2s^2$	-16263.1236	4920.8812	-244.8591	1958.9266

All values in units of 10^{-5} Hartree.

equally important. The EC effects seem to be well represented in the $1s^2$ orbital by the $X\alpha$ method. Tong and Sham [107] have observed that the uniform gas model leads to over-estimation of correlation energy and the under-estimation of exchange energy in the inner regions. Our results seem to indicate that these two opposing effects balance each other, with the net result that EC corrections in the inner orbital are negligible. The $2s^2$ orbital, on the other hand, seems to be poorly represented by the $X\alpha$ model. It is a well-known fact, that valence regions in atoms are not correctly represented by this model [75]. The local-density potential, therefore, appears to be well-suited for mimicing the exact electron-electron interaction potential in the inner regions of atoms only. The partial wave analysis given in Table III.2 reveals that the dominant contribution to the energy corrections come from the pp excitations, amongst these the most important are the $2s^2 \rightarrow 2p^2$ excitations (see Table III.3). This is due to the near-degeneracy of the 2p orbital, and its spatial distribution nearly parallelling that of the 2s distribution.

Table III.1, also reveals the fact that T_1 terms play a crucial role in the evaluation of EC corrections. In the calculation of Paldus et al. [90], with linear coupled-pair many-electron approximation, only the T_2 diagrams with two open-paths were considered. By virtue of - - using the HF basis which obeys the Brillouin's theorem, they could

neglect all the single excitations. However, our calculation uses the $X\alpha$ orbitals as the basis; these orbitals do not obey Brillouin's theorem and the T_1 excitations survive. Also, the matrix elements of the type $\langle i|f|j \rangle$ are non-vanishing, since $X\alpha$ orbitals are used in the calculation. The T_1 terms however contribute only indirectly through their coupling with the T_2 terms. The approximations which neglect the T_1 terms tend to over-estimate the EC corrections. This is similar to the results obtained by Paldus et al [90] where the quasi-degeneracy of the 2s, 2p orbitals has been shown to cause over-estimation of correlation energies. An interesting feature apparent from our calculations, is that contributions from ring diagrams are found to be very important for a proper estimation of the EC corrections. Approximations C and D, where only contributions of ladder diagrams are considered, tend to over-estimate the energy corrections. The importance of ring diagrams in representation of EC in electron gas approximations is well known [71,95] and is reflected in our calculations as well. For the purpose of comparison, we performed the second-order RSPT calculation (vide Approximation F). This accounts for only about 50% of the corrections. In the following chapter, we present a detailed discussion on these and other results obtained by us in our CC analysis of the EC effects.

CHAPTER IV

ANALYSIS OF EXCHANGE-CORRELATION EFFECTS IN BERYLLIUM ISOELECTRONIC SERIES

- IV.1 General
- IV.2 Some Comments on the CC Equations
- IV.3 Results
- IV.4 Discussion
 - IV.4.1 $X\alpha$ and the Electron Gas Model :
An Analysis
 - IV.4.2 General Trends in EC Corrections
 - IV.4.3 The Role of the Exchange Parameter α
 - IV.4.4 Variation of Z - Isoelectronic Series
 - IV.4.5 Gradient Corrections to Exchange
- IV.5 Conclusions

IV.1 GENERAL

This chapter presents the analysis of the many-body EC effects in beryllium atom and the ions B^+ , C^{+2} and N^{+3} , which are isoelectronic with Be. The CC formalism and the hierarchy of approximations derived from it have been employed for this purpose. The $X\alpha$ local potential model has been used to generate the reference functions for the CC expansion. The computational methods employed have been already outlined in the previous chapter. The analysis presented in this chapter entails the study of the EC effects, for various choices of α in the $X\alpha$ potential, with gradient corrections to the $X\alpha$ potential and for Z-variation along the isoelectronic series. The results are discussed in the light of the electron gas approximation which serves as the basis of the $X\alpha$ model. As has been shown through variational arguments [15], the use of the uniform electron gas potential in the $X\alpha$ model leads to a value of $2/3$ for α . Use of any different value of α in the $X\alpha$ potential would imply deviation from uniform charge description. In view of this, the role of α in the portrayal of EC effects, is examined. The use of gradient corrections to account for the inhomogeneities in the charge distribution is also examined from this view point.

After commenting briefly on the CC equations in the

next section, we present the results of our calculations in Sec. IV.3. The results are discussed in Sec. IV.4 after a brief resume of the theoretical framework concerning many-body effects in electron gas models. The conclusions are then summarized in the background of this theoretical presentation.

IV.2 SOME COMMENTS ON THE CC EQUATIONS

The CC equations, eqns. (III.19) and (III.20) in full, and under a hierarchy of approximations, have been solved for the Be isoelectronic series using the numerical methods outlined in Chapter III. The structure of the equations, eqns. (III.19) and (III.20) becomes clear if they are recast in the following manner :

$$\langle \alpha | \hat{f} | r \rangle + (\epsilon_\alpha - \epsilon_r) t_\alpha^r + A t_\alpha^r + K_1 = 0 \quad (\text{IV.1})$$

and

$$\langle \alpha\beta | \hat{V} | rs \rangle + (\epsilon_\alpha + \epsilon_\beta - \epsilon_r - \epsilon_s) t_{\alpha\beta}^{rs} + B t_{\alpha\beta}^{rs} + K_2 = 0 \quad (\text{IV.2})$$

Eqn. (IV.1) corresponds to eqn. (III.19) where A is the coefficient of the diagonal term, t_α^r , and K_1 stands for all the non-diagonal terms with their coefficients. Likewise, eqn. (IV.2) corresponds to eqn. (III.20) where B is the coefficient of the diagonal term, $t_{\alpha\beta}^{rs}$, and K_2 stands for all the non-diagonal terms with their coefficients. A, B, K_1 and K_2 contain the hole-hole, hole-particle and particle-particle ladder and ring diagram terms (vide

Figs. II.5 and II.7). These diagrams represent hole state interactions occurring via creation of particle-hole pairs, and interactions arising from scattering between hole-hole, hole-particle and particle-particle states. In Brueckner's electron gas theory [71,72] ring diagrams contribute dominantly to the correlation energy correction while in Sinanoglu's many-electron theory [41] ladder diagrams contribute dominantly. In the work of Singal and Das [74] the non-diagonal terms were replaced by a constant times the diagonal coefficient and the resulting equations were solved. The importance of ring diagrams was again gleaned from their calculation. In our calculations, we have solved the linear part of eqns. (IV.1) and (IV.2) with no approximation to the non-diagonal terms. The effect of various diagrams on EC corrections is studied through the various Approximations (vide Chapter III). For instance, Approximation B neglects the T_1 excitations altogether, while Approximations C, D and E neglect ring diagrams entirely and include some of the ladder diagrams. A comparison is made with the second-order RSPT calculation made by us to highlight the importance of higher order corrections.

IV.3 RESULTS

Tables IV.1 to IV.3 present the results of pair EC corrections in beryllium atom for the choice of various α values and under the different Approximations outlined. Total EC corrections and the calculated total energy values for

Table IV.1 $1s^2$ Pair EC Corrections in Be - Effect of α Variation

α	Approximation				
	A	B	C	D	E
0.6667	*	*	*	-25.9352	-1.8797
0.6800	*	*	-20.0796	-22.2620	-1.9296
0.7000	*	*	-18.3112	-19.2835	-2.0078
0.7200	-10.8603	-6.5470	-16.4984	-15.5164	-2.0909
0.7400	-6.3165	-5.4481	-14.1296	-13.4533	-2.1787
0.7600	-4.7676	-4.7909	-12.7378	-11.8816	-2.2712
0.7800	-4.0520	-4.3758	-10.8954	-10.6422	-2.3691
0.8000	-3.6901	-4.1110	-9.8008	-9.6597	-2.4724
0.8200	-3.5121	-3.9456	-8.9389	-8.8694	-2.5811
0.8400	-3.4458	-3.8524	-8.2468	-8.2221	-2.6964
0.8600	-3.4531	-3.8120	-7.6986	-7.6963	-2.8167
0.8800	-3.5142	-3.8125	-7.2258	-7.2728	-2.9421
0.9200	-3.7916	-3.9127	-6.5620	-6.6455	-3.3126
0.9600	*	-4.1156	-6.1639	-6.2514	-3.5078
1.0000	-4.3425	-4.4016	-5.9531	-6.0316	-3.8269
					-1.9468
					-1.9986
					-2.0800
					-2.1664
					-2.2579
					-2.3543
					-2.4563
					-2.5639
					-2.6773
					-2.7977
					-2.9233
					-3.0543
					-3.3371
					-3.6460
					-3.9804

All energy values in units of 10^{-5} Hartree

*Instabilities encountered in the solution.

Table IV.2 1s 2s Pair EC Corrections in Be - Effect of α Variation

α	Approximation				
	A	B	C	D	E
0.6667	*	*	*	-739.1090	-9.9658
0.6800	*	*	-565.1330	-633.5020	-10.1894
0.7000	*	*	-519.0712	-555.6860	-10.5402
0.7200	-356.6420	-211.2582	-475.9328	-437.0638	-10.9132
0.7400	-190.1192	-161.3270	-403.7798	-375.6220	-11.3082
0.7600	-129.0206	-129.7320	-357.3394	-327.9208	-11.7340
0.7800	-97.3366	-107.9452	-301.0632	-289.3678	-12.1650
0.8000	-78.1844	-92.2700	-264.7930	-257.9208	-12.6298
0.8200	-65.5642	-80.4460	-235.3234	-231.7486	-13.1182
0.8400	-56.9078	-71.2586	-210.6876	-209.3384	-13.6388
0.8600	-51.0288	-63.9622	-190.3194	-190.1884	-14.1794
0.8800	-47.4452	-58.0376	-172.0258	-173.9344	-14.7400
0.9200	-51.5438	-49.0876	-143.2488	-146.8592	-15.9500
0.9600	*	-42.7406	-121.6126	-125.1630	-17.3644
1.0000	-15.8880	-38.0566	-104.8716	-108.7740	-18.6756

All energy values in units of 10^{-5} Hartree

*Instabilities encountered in the solution.

Table IV.3 $2s^2$ Pair EC Corrections in Be - Effect of α Variation

α	Approximation					
	A	B	C	D	E	F
0.6667	*	*	*	-28267.9020	-1877.8319	-4280.0411
0.6800	*	*	-21818.8320	-24473.6610	-1885.6737	-4297.8278
0.7000	*	*	-20361.2990	-21679.7540	-1897.8849	-4325.8249
0.7200			-18809.9340	-17408.1930	-1910.7531	-4355.7442
0.7400	-28496.3550	-16867.1500	-16210.1230	-15192.5830	-1924.2713	-4387.5510
0.7600	-15558.8740	-13182.1440	-14698.7260	-13471.5890	-1938.3578	-4421.1117
0.7800	-10793.4080	-10834.7440	-12501.3570	-12076.2010	-1953.1887	-4456.8527
0.8000	-8302.2965	-9205.0500	-11187.1670	-10936.4640	-1968.6795	-4494.6250
0.8200	-6777.3690	-8011.0609	-10118.0090	-9987.0502	-1984.7963	-4534.3518
0.8400	-5754.3557	-7096.3583	-9218.6811	-9169.0401	-2001.8538	-4576.8210
0.8600	-5032.5150	-6370.1130	-8475.9193	-8471.0709	-2019.4049	-4621.0365
0.8800	-4523.5477	-5781.7732	-7789.0664	-7880.0167	-2037.4168	-4666.8826
0.9200	-4190.533	-5292.8783	-6707.7166	-6889.4339	-2075.8071	-4765.9743
0.9600	-4402.6231	-4516.6316	-5894.1246	-6110.9176	-2116.7611	-4873.7090
1.0000	-1220.9281	-3916.8977	-5267.4043	-5490.8236	-2159.9146	-4989.2388

All energy values in units of 10^{-5} Hartree

*Instabilities encountered in the solution.

various α 's are presented in Table IV.4 and Table IV.5. Similar results for B^+ , C^{+2} and N^{+3} are presented in Tables IV.6, IV.7 and IV.8 respectively. The EC corrections obtained with the gradient-corrected $X\alpha$ potentials for a pair of α values, viz. 0.768 and 0.6667 in the case of Be atom are given in Tables IV.9 and IV.10.

IV.4 DISCUSSION

IV.4.1 $X\alpha$ and the Electron Gas Model : An Analysis

The basic tenet of the $X\alpha$ and like methods is the approximation of the electron density distribution in atoms by the uniform charge density of an electron gas. In atoms the electron density distribution is non-uniform and the validity of the above approximations is, therefore, subject to question. However, the electron gas model can be extended to non-uniform charge distributions, as well, provided the density is either high [71] or slowly varying[72]. This is true for the bulk of the electron distribution in atoms. Regions which are neither too near the nucleus nor far removed can be described as possessing a slowly varying charge distribution and the electron gas approximation would have reasonable validity in these regions. In regions very close to the nucleus the electron density is high, but the density gradient is large and the changes are rapid. In this region of large negative potential energy, the electron gas approximation leads to spurious densities, thus causing an unphysical behaviour of the

Table IV.4 Total EC Corrections in Be - Effect of α Variation

α	Approximation				
	A	B	C	D	E
0.6667	*	*	*	-29032.9460	-1889.6775
0.6800	*	*	-22404.0450	-25129.4250	-1897.7925
0.7000	*	*	-20898.6820	-22254.7230	-1910.4329
0.7200	-28863.8570	-17084.9550	-19302.3650	-17860.7830	-1923.7571
0.7400	-15755.3090	-13348.8190	-16628.0230	-15581.6580	-1937.7581
0.7600	-10927.1970	-10969.1670	-15068.8020	-13811.3910	-1952.3531
0.7800	-8403.6854	-9317.3712	-12813.3150	-12376.2110	-1967.7228
0.8000	-6859.2434	-8107.4418	-11461.7600	-11204.0440	-1983.7816
0.8200	-5823.4319	-7180.7499	-10362.2720	-10227.6680	-2000.4956
0.8400	-5092.8685	-6445.2239	-9437.6154	-9386.6006	-2018.1891
0.8600	-4578.0296	-5849.5474	-8673.9372	-8668.9555	-2036.4010
0.8800	-4241.4928	-5354.7283	-7968.3180	-8061.2239	-2055.0989
0.9200	-4457.9586	-4569.6320	-6857.5275	-7042.9386	-2094.9697
0.9600	*	-3963.7540	-6021.9010	-6242.8321	-2137.5332
1.0000	-1241.1588	-3462.1602	-5378.2290	-5605.6193	-2182.4171
					-4292.7014
					-4310.7810
					-4339.2381
					-4369.6467
					-4401.9718
					-4436.0788
					-4472.3993
					-4510.7829
					-4551.1528
					-4594.3078
					-4639.2363
					-4685.8230
					-4786.5156
					-4895.9938
					-5013.4015

All energy values in units of 10^{-5} Hartree

* Instabilities encountered in the solution.

Table IV.5 Total Ground State Energy in Be - Effect of α Variation

α	Approximation					
	A	B	C	D	E	F
0.6667	*	*	*	-14.847849	-14.576417	-14.600447
0.6800	*	*	-14.782995	-14.810249	-14.577933	-14.602063
0.7000	*	*	-14.769932	-14.783492	-14.580049	-14.604337
0.7200		*	-14.755714	-14.741298	-14.581928	-14.606387
0.7400	-14.851329	-14.733540	-14.730565	-14.720102	-14.583663	-14.608305
0.7600	-14.721838	-14.697773	-14.716338	-14.703764	-14.585173	-14.610011
0.7800	-14.674922	-14.675342	-14.694913	-14.690542	-14.586457	-14.611504
0.8000	-14.650817	-14.659954	-14.682328	-14.679750	-14.587548	-14.612818
0.8200	-14.636302	-14.648785	-14.672028	-14.670682	-14.588410	-14.613917
0.8400	-14.626639	-14.640213	-14.663226	-14.662716	-14.589032	-14.614793
0.8600	-14.619779	-14.633302	-14.655814	-14.655765	-14.589439	-14.615467
0.8800	-14.614855	-14.627571	-14.648733	-14.649662	-14.589601	-14.615908
0.9000	-14.611465	-14.622597	-14.636835	-14.638689	-14.589210	-14.616125
0.9200	-14.612840	-14.613956	-14.626604	-14.628813	-14.587760	-14.615345
0.9600	*	-14.606023	-14.617307	-14.619581	-14.585349	-14.613659
1.0000	-14.575937	-14.598147				

All energy values in units of Hartree

*Instabilities encountered in the solution.

Table IV.6 Pair-wise and Total EC Corrections
and Total Ground State Energies in B⁺

Contri- bution	α	Approximation*			
		C	D	E	F
1s ² pair ⁺	0.6667	-24.2430	-23.7216	-12.2316	-12.7395
	0.7200	-22.7720	-22.6367	-12.9635	-13.5037
	0.7600	-22.1115	-22.0534	-13.5459	-14.1124
	0.8200	-21.4717	-21.4796	-14.4633	-15.0719
	1.0000	-21.1873	-21.2350	-17.3843	-18.1332
1s 2s pair ⁺	0.6667	-315.2612	-307.2124	-47.2238	-51.1420
	0.7200	-278.5920	-274.7944	-49.2000	-53.2940
	0.7600	-255.2404	-253.5426	-50.8184	-55.0512
	0.8200	-225.5220	-225.7670	-53.4224	-57.8912
	1.0000	-162.4568	-164.1172	-62.1176	-67.4096
2s ² pair ⁺	0.6667	-7356.0910	-7151.8010	-2981.7319	-6771.9813
	0.7200	-6750.1579	-6647.6688	-3010.3846	-6869.8808
	0.7600	-6357.8803	-6309.7828	-3033.9545	-6950.0663
	0.8200	-5852.1823	-5859.6859	-3072.5932	-7080.4938
	1.0000	-4784.1236	-4852.1684	-3210.5439	-7536.3983
Total Corre- lation energy ⁺	0.6667	-7695.3764	-7482.7350	-3041.1873	-6835.8627
	0.7200	-7051.5219	-6945.0998	-3072.5524	-6936.6784
	0.7600	-6635.2321	-6585.3787	-3098.3189	-7019.2298
	0.8200	-6099.1759	-6106.9325	-3140.4789	-7153.4568
	1.0000	-4967.7677	-5037.5205	-3290.0548	-7621.9410
Total energy in Hartree	0.6667	-24.299134	-24.297007	-24.252592	-24.290539
	0.7200	-24.297950	-24.296886	-24.258161	-24.296802
	0.7600	-24.296782	-24.296284	-24.261413	-24.300622
	0.8200	-24.294232	-24.294309	-24.264645	-24.304775
	1.0000	-24.278033	-24.278730	-24.261256	-24.304574

*In Approximations A and B instabilities encountered in the solution

⁺All energy values in units of 10^{-5} Hartree.

Table IV.7 Pair-wise and Total EC Corrections
and Total Ground-State Energies in C⁺2

Contri- bution	α	Approximation*			
		C	D	E	F
1s ² pair ⁺	0.6667	-38.9484	-38.7947	-26.4460	-27.4872
	0.7200	-38.3067	-38.2308	-27.4584	-28.5407
	0.7600	-37.9967	-37.9603	-28.2444	-29.3591
	0.8200	-37.7481	-37.7498	-29.4475	-30.6126
	1.0000	-37.9537	-37.9930	-33.0034	-34.3225
1s 2s pair ⁺	0.6667	-334.6036	-330.7684	-85.2072	-91.8206
	0.7200	-308.5242	-306.5632	-87.3006	-94.0788
	0.7600	-290.9968	-290.0350	-88.9916	-95.9062
	0.8200	-267.4646	-267.5098	-91.6882	-98.8252
	1.0000	-211.4250	-212.4394	-100.3378	-108.2128
2s ² pair ⁺	0.6667	-6569.9495	-6480.7426	-3778.8860	-8478.3847
	0.7200	-6273.5244	-6224.8707	-3808.4640	-8598.5605
	0.7600	-6071.9774	-6046.8764	-3832.6371	-8695.4047
	0.8200	-5800.2808	-5801.5575	-3872.2675	-8851.3829
	1.0000	-5179.1428	-5217.4015	-4011.1085	-9372.6277
Total corre- lation energy ⁺	0.6667	-6943.5014	-6850.3057	-3890.5391	-8597.6926
	0.7200	-6620.3550	-6569.6645	-3923.2230	-8721.1798
	0.7600	-6400.9709	-6374.8716	-3949.8733	-8820.6700
	0.8200	-6105.4934	-6106.8170	-3993.4032	-8980.8207
	1.0000	-5428.5215	-5467.8338	-4144.4496	-9515.1630
Total energy in Har- tree	0.6667	-36.462605	-36.461673	-36.432076	-36.479147
	0.7200	-36.464643	-36.464137	-36.437672	-36.485651
	0.7600	-36.465460	-36.465199	-36.440949	-36.489657
	0.8200	-36.465360	-36.465373	-36.444239	-36.494113
	1.0000	-36.453685	-36.454079	-36.440845	-36.494552

*In Approximations A and B instabilities encountered in the solution

⁺All energy values in units of 10^{-5} Hartree.

Table IV.8 Pair-wise and Total EC Corrections
and Total Ground-State Energies in $N+3$

Contri- bution	α	Approximation*			
		C	D	E	F
$1s^2$ pair ⁺	0.6667	-53.4573	-53.3448	-40.5062	-41.9643
	0.7200	-53.0404	-52.9797	-41.6216	-43.1201
	0.7600	-52.8562	-52.8236	-42.4780	-44.0079
	0.8200	-52.7432	-52.7396	-43.7732	-45.3515
	1.0000	-53.0161	-53.0502	-47.4550	-49.1742
$1s\ 2s$ pair ⁺	0.6667	-362.9558	-360.2948	-116.7482	-124.9784
	0.7200	-340.1164	-338.6610	-118.6924	-127.0574
	0.7600	-324.3942	-323.6072	-120.2622	-128.7394
	0.8200	-302.8232	-302.7378	-122.7762	-131.4266
	1.0000	-248.6758	-249.3746	-130.6930	-139.9506
$2s^2$ pair ⁺	0.6667	-6717.2496	-6655.0769	-4504.8491	-10012.7630
	0.7200	-6512.0927	-6475.7992	-4537.9332	-10157.5890
	0.7600	-6370.5758	-6349.9286	-4564.6477	-10272.9550
	0.8200	-6177.3783	-6174.9527	-4607.9412	-10456.5670
	1.0000	-5728.9502	-5755.2325	-4757.6843	-11060.9780
Total Corre- lation energy ⁺	0.6667	-7133.6626	-7068.7165	-4662.1036	-10179.7050
	0.7200	-6905.2496	-6867.4398	-4698.2472	-10327.7660
	0.7600	-6747.8262	-6726.3593	-4727.3879	-10445.7030
	0.8200	-6532.9445	-6530.4300	-4774.4806	-10633.3450
	1.0000	-6030.6421	-6057.6573	-4935.8323	-11250.1030
Total energy in Har- tree	0.6667	-51.138337	-51.137687	-51.113621	-51.1687970
	0.7200	-51.141303	-51.140924	-51.119232	-51.1755280
	0.7600	-51.142778	-51.142564	-51.122574	-51.1797570
	0.8200	-51.143579	-51.143554	-51.125995	-51.1845830
	1.0000	-51.133556	-51.133826	-51.122608	-51.1857510

*In Approximations A and B instabilities encountered in the solution

⁺All energy values in 10^{-5} Hartree.

Table IV.9 Pair-wise and Total EC Corrections and Total Ground-State Energies in Be for $\alpha = 0.667$ - Effect of β Variation

Contribution	β	Approximation				
		A	B	C	D	E
1s pair ⁺	0.0016	-1.5142	-1.8887	-7.7329	-8.1248	-1.3380
	0.0023	-0.9795	-1.4111	-5.3830	-5.4226	-1.1822
	0.0030	-0.9041	-1.1731	-4.0228	-3.9463	-1.0717
1s 2s pair ⁺	0.0016	-25.9802	-31.6138	-251.8826	-267.4408	-7.7304
	0.0023	2.8642	-15.2314	-183.8532	-185.6034	-7.0782
	0.0030	2.3912	-7.7742	-142.4038	-138.6674	-6.6268
2s pair ⁺	0.0016	-3251.0010	-4092.4381	-13118.7670	-13938.1160	-1830.1273
	0.0023	-659.6687	-2616.0358	-10838.9450	-10943.7260	-1816.3697
	0.0030	-506.5419	-1825.9071	-9367.0971	-9116.2502	-1808.2460
Total	0.0016	-3278.4954	-4125.9437	-13378.3820	-14213.6810	-1839.1958
Correlation energy ⁺	0.0023	-657.7841	-2632.6784	-11028.1810	-11134.7520	-1824.6300
	0.0030	-505.0548	-1834.8544	-9513.5238	-9258.8639	-1815.9446
Total	0.0016	-14.592580	-14.601054	-14.6935790	-14.7019320	-14.578187
energy in Har-	0.0023	-14.566538	-14.586287	-14.6702420	-14.6713080	-14.578206
tree	0.0030	-14.565001	-14.578299	-14.6550850	-14.6525390	-14.578109

⁺ All energy values in units of 10^{-5} Hartree.

Table IV.10 Pair-wise and Total EC Corrections and Total Ground-State Energies in Be for $\alpha = 0.768$ - Effect of β Variation

Contribution	β	Approximation				
		A	B	C	D	E
$1s^2$ pair ⁺	0.0016	-1.5854	-1.9181	-5.1178	-5.0824	-1.6609
	0.0023	-1.4050	-1.5928	-3.8335	-3.7904	-1.4627
	0.0030	1.2936	-1.4017	-2.9979	-2.9612	-1.3159
$1s 2s$ pair ⁺	0.0016	-1.8522	-17.9768	-155.8068	-153.3800	-9.4128
	0.0023	-0.7544	-9.0726	-120.4580	-117.8522	-8.6278
	0.0030	-2.5438	-4.6678	-95.9228	-92.1966	-8.0638
$2s^2$ pair ⁺	0.0016	-825.3516	-2543.9992	-8826.1468	-8710.7555	-1901.6073
	0.0023	-409.6589	-1659.5577	-7801.3143	-7608.2314	-1889.2792
	0.0030	61.1886	-1111.2602	-7031.2170	-6807.4331	-1882.4824
Total correlation energy ⁺	0.0016	-828.7893	-2563.8942	-8987.0716	-8869.2180	-1912.6811
	0.0023	-410.3095	-1670.2231	-7925.6058	-7728.8740	-1899.3797
	0.0030	59.9383	-1117.3397	-7130.1377	-6902.5808	-1891.8719
Total energy in Hartree	0.0016	-14.574513	-14.591864	-14.656096	-14.654917	-14.585352
	0.0023	-14.569403	-14.582002	-14.644556	-14.642589	-14.584294
	0.0030	-14.564564	-14.575138	-14.635266	-14.632991	-14.582884
tree						
+ All energy values in units of 10^{-5} Hartree.						

+ All energy values in units of 10^{-5} Hartree.

distribution [108]. Nonetheless, this is not a serious shortcoming, for the kinetic energy term dominates the inter-electron interaction term close to the nucleus and if the kinetic energy is treated exactly as is done in the $X\alpha$ method, the use of electron gas-like local potential approximation is reasonable. However, this justification is of no avail at large distances from the nucleus. In these regions the electron density is low and the inter-electron term becomes significant in comparison to the kinetic energy term and the electron gas approximation breaks down. Besides, the use of the electron gas approximation entails two serious shortcomings. Firstly, the uniform charge description has the effect of smoothening the density variations throughout the atom and therefore is incapable of depicting correctly the atomic-shell structure. Also, the approximation fails to portray correctly the effect of the long range of the coulomb interaction. This is due to its inability to account for the shielding of the interactions between the particles [109].

Several corrections to the electron gas approximation have been made in order to take into account the non-uniformity of the charge distributions in atoms [14]. The $X\alpha$ method itself is an outcome of this. Use of any α value other than $2/3$ in the $X\alpha$ potential takes it beyond the electron gas approximation [110]; values of α higher than the Gaspar-Kohn-Sham (GKS) limit of $2/3$, characterise more

non-uniformity of the charge distribution. For systems with higher Z , better description is obtained with α values nearer to $2/3$. As Z increases, the high density region in the atom expands and the uniform charge approximation finds greater justification [111]. In the limit of high Z the uniform charge distribution GKS value of $\alpha = 2/3$ is obtained. Although, higher values of α may account for non-uniformity of charge distribution there are no rigorous theoretical grounds for choosing α . Due to the absence of a variational bound on α , the energy decreases with increasing α . Several prescriptions have been given for the choice of α , the main amongst these being the choice for which the X_α energy reaches the HF limit or the total energy limit [20]. The resulting self-consistent potential is an EC potential although a demarcation of the "exchange-only" and "correlation-only" parts cannot be made.

The electron gas system most relevant to atomic problems is the high density electron gas subject to a uniform positive field. This has been studied by Gell-Mann and Brueckner [71] through MBPT techniques. The uniform electron gas study gives very inaccurate estimates for atomic correlation energies [112]. To account for the discrepancy, the effect of non-uniform charge density was treated as a perturbation to high density electron gas by Ma and Brueckner [72]. Their analysis was based on the treatment of the electron-electron interaction to all orders in the ring

diagrams and the external field producing the non-uniform density to second-order. The ring diagrams yield terms which take into account the coulombic screening and are therefore extremely important for non-uniform charge distributions. The slow density variation was accounted for by expansion of the EC potential in powers of density gradient. For atoms where regions near the nucleus with high density gradients exist, this expansion leads to infinite energies. The gradient-corrected EC potential also fails to account for the sum rule [69], which is a very stringent criterion on EC potentials. Brueckner has also shown, that at intermediate electron densities the perturbation theories diverge, and the electron gas approximation becomes unacceptable. An extremely interesting result of Brueckner's electron gas study is the observation that the ring diagram terms are the most divergent terms in the perturbation series. This is in contrast to the many-electron theory result of Sinanoglu [41], which discusses the relative unimportance of the third and higher order rings. Our model which is a superior version of Sinanoglu's many-electron theory has overtones of Brueckner's theory by virtue of the use of electron gas-like local potential approximations to provide the reference functions. In the light of this it would be worthwhile to examine the many-body EC effects in the $X\alpha$ model vis-a-vis Brueckner's electron gas theory and Sinanoglu's many-electron theory.

The studies of Singal and Das [74] and Freeman [95], using the CC methodology provide an excellent insight into the many-body correlation effects in electron gas models. The importance of the ring diagrams in accounting for pair-correlation energy of an electron gas has been re-emphasized in their study. In view of the extensive studies on electron gas and their relevance in atomic problems we have undertaken this study of the $X\alpha$ model with specific reference to EC effects.

IV.4.2 General Trends in EC Corrections

The EC values reported in the previous chapter portray the general trends of diagonal diagrams-wise and pair-wise contributions for beryllium atom (vide Tables III.1 and III.2). Firstly, as depicted by the EC corrections in all the Approximations A to F, the inner-shells in beryllium atom are best described by the $X\alpha$ local potential approximation. Secondly, the electrons in the inner regions appear to be well localized as depicted by the small value of inter-pair EC corrections. However, the outer regions in the atom, which in the case of beryllium atom represent the valence 2s orbitals are poorly represented by the $X\alpha$ local potential approximation and need to be corrected. This is in contrast to the results reported in the literature with reference to the HF method (vide Table IV.11). All the calculations that have gone beyond the HF method, including the

Table IV.11 Comparison of EC Energy Corrections
in Be Atom

Pair-wise Contribution to the Correction*			Total Correction*	Total Energy+ [#]	Ref.
$1s^2$	$1s\ 2s$	$2s^2$			
-4395.00	-648.00				107
-4212.00	-497.00	-4488.00	-9197.0000		108
-4208.30	-497.00	-4438.10	-9143.4000		109
-4182.70	-586.40	-4535.10	-9304.2000		110
-3758.00	-457.00	-4357.00	-9572.0000		35
-4031.00	-547.00	-3050.00	-7628.0000		111
			-9400.0000	-14.66700	112
-4.41980	-57.0836	-9628.1753	-9746.7623	-14.663598	Present Work

^{1/2} Experimental non-relativistic Total energy = -14.668452 Hartree
Reference [98]

* All values in units of 10^{-5} Hartree

+ Values in Hartree.

CC calculations of Čížek [35] have indicated the importance of both $1s^2$ and $2s^2$ pair correlation corrections. Comparison of our results with the exact experimental non-relativistic energy reveals that with the inclusion of all the pair excitations an accuracy of 99.967% (for the α value of 0.768) is achieved. With the exclusion of the $1s^2$ and $1s2s$ pair corrections an accuracy of 99.962% is still obtained; this suggests that it will be sufficient to consider only valence-shells in the many-electron treatments based on the $X\alpha$ model.

The hierarchy of Approximations C, D and E all involve selective summations of various ladder diagrams. In Approximations C and D the EC correction is over-estimated. As is well-known in the electron gas approximation to atoms, non-inclusion of higher order ring diagrams leads to over-estimation of correlation energy. The experimental correlation energies for oxygen and potassium are about 60% of that obtained from the perturbation result which does not include higher order ring diagrams [112]. A similar result has been reported by Singal and Das [74]. Inclusion of ring diagrams introduces the right trend in the EC corrections as is seen from the values obtained in Approximation A which includes rings and ladders to all orders. Also as expected, the second-order RSPT results give about 50% of the correction obtained by the full calculation. It is worth noting that for the $\alpha = 0.768$, the higher order ring diagrams seem to be well-behaved.

IV.4.3 The Role of the Exchange Parameter α

The result of our calculations provide some insight into the role of the exchange parameter α . With increasing α the EC corrections are generally seen to decrease in magnitude in all the Approximations except in those of E and F. The total energy with the EC corrections tends to decrease in magnitude with increase in α , although for higher orders of α , the corrected total energy remain almost a constant. These results are again entirely in consonance with the electron gas results. The work of Herman et al [113] indicates that inhomogeneity causes the local one-electron potential to increase in magnitude and hence drive the α value above the GKS limit. Conversely, higher α values provide descriptions reflecting larger inhomogeneities which in turn decrease the total energy. Therefore, use of higher α values imply incorporation of more correlation corrections and this causes a decrease in EC corrections. However, in Approximation E, only the particle-particle ladder summation is involved and this leads to incorrect energies and trends. The same is true of second-order RSPT corrections. Approximations C and D overestimate the EC corrections, as expected. The inclusion of ring diagrams rectifies this problem and like in the electron gas model correctly accounts for the screening of the charge at large distances.

The effect of α on the description of the EC potential merits a brief discussion. With the use of values of α higher than $2/3$, the EC potential in the X^α model can be written as,

$$v_{XC} = -3\left(\frac{2}{3} + x\right) \left[\frac{3}{4\pi} \rho(r)\right]^{1/3} \quad (\text{IV.3})$$

As x increases, the EC potential becomes more negative and the repulsive interactions between electrons are decreased. In other words, the electrons tend to get correlated. This is reflected by the decrease in EC corrections with increase in α . However, there is no method for estimating the limit to which the negative potential can be carried to and therefore, any quantification of α with reference to non-uniformity is devoid of meaning. An interesting feature that emerges from our calculations is the ill-conditioning of the solutions for the cases where α values approach the GKS limit. This parallels the divergence behaviour of correlation energy of electron gas in perturbation theory. As in perturbation theory, the origin of this erratic behaviour rests with the most divergent terms arising from the ring diagrams. Exclusion of the ring diagrams stabilises the equations, but leads to over-estimation of EC corrections.

In all these calculations, the Latter correction potential [99] has been used for obtaining the SCF X^α orbitals. The effect of the inclusion of the Latter correction potential

on the wavefunctions is to push the outer maxima slightly outward, as well as to increase the amplitude of the tails. This tends to inhomogenise the charge distribution in the outer regions further, with the concomitant need to use higher α values [114]. It can be surmised from the above discussion that α plays a very important role in determining the structure of such local potential models. From the comparison of the EC corrected total energies with the exact non-relativistic experimental energies, it appears that the best EC corrected energy value is obtained for an α value near 0.768. This value of α has also been reported to yield the reference state energies which are closest to the HF energies [24].

IV.4.4 Variation of Z - Isoelectronic Series

Tables IV.6 to IV.8 give the results of our calculations of EC corrections in the Be isoelectronic series, B^+ , C^{+2} and N^{+3} , under all the Approximations outlined earlier. Five different α values have been used in the $X\alpha$ potential. The trends displayed appear to be similar. Approximations A and B display an ill-conditioned behaviour for most cases. Approximations C,D,E and F, though better behaved, under-estimate the EC corrections. In all the later mentioned Approximations a consistent increase in the magnitude of EC corrections with increase in the atomic number, Z, is observed. Once again with increasing α a decrease in the magnitude of the EC corrections is observed.

As mentioned earlier, an increase in Z along this series causes the contraction of the orbitals and homogeneises the charge density distribution to some extent. This tends to favour lower α values; however, the large density fluctuations encountered in the inner-most regions coupled with the incorrect description of regions farther away from the atom tend to undermine the local potential approximation. The divergence of the ring diagrams in perturbation theory manifests itself through the ill-conditioned behaviour of the cluster-coefficients and energies as portrayed by the results of Approximations A and B in Tables IV.6 to IV.8. The exclusion of these divergent terms arising from the ring diagram as in Approximations C,D,E and F assumes well-behavedness of the coefficients and energies. The EC corrections obtained in the second-order RSPT approximation seem to display the correct trend. This fortuitious result is a consequence of the highly restricted nature of the summation and bears no theoretical justification. The important point that emerges from these calculations is the total dominance of the valence-shell EC corrections. That the electrons in the inner-shells are well-correlated in the local potential model is borne out in all the cases discussed.

IV.4.5 Gradient Corrections to Exchange

Herman et al [113,115] have suggested the use of a gradient correction for exchange within the $X\alpha$ method. In

this method the exchange potential has the form

$$\hat{v}_{XC}(r) = \{\alpha + \beta G(\rho)\} \hat{v}_{X1}(\rho) \quad (\text{IV.4})$$

where

$$G(\rho) = \frac{1}{\rho^{2/3}} \left[\frac{4}{3} \left(\frac{\hat{v}_\rho}{\rho} \right)^2 - 2 \frac{\hat{v}_\rho^2}{\rho} \right] \quad (\text{IV.5})$$

The potential \hat{v}_{X1} is the $X\alpha$ potential for $\alpha = 1$ and β is an adjustable parameter. The introduction of gradient correction into the $X\alpha$ potential was studied in the case of beryllium atom for three different values of β at $\alpha = 0.667$ and $\alpha = 0.768$. and the results are presented in Tables IV.9 and IV.10. As can be seen from these tables, the gradient correction does seem to stabilise the equations for $\alpha = 0.667$, although poor estimates of the EC correction are obtained. As pointed out by Herman et al [113], lower β values are seen to be favoured for beryllium atom. Although the gradient corrections provide little improvement where EC corrections are concerned, they are found to be absolutely necessary to assure well-behavedness of the solutions for the case of $\alpha = 2/3$. Use of higher α values appears to partially account for the atomic density gradients in these models. The presence of the $(\hat{v}_\rho^2) \rho^{-4/3}$ term in the gradient expansion (varies as $1/r$ as $r \rightarrow 0$) would cause divergence of energies. We have taken into account this problem, through the introduction of a convergence factor [115], so that the product of the convergence factor and $G(\rho)$ remains equal to $G(\rho)$ for a much larger range of r

than before. This is especially important at very low values of r , where there is a delicate balance between very large kinetic energies and potential energies and even a small change in the EC potential causes divergences. After incorporation of the convergence factor, eqn. (IV.4) assumes the form,

$$\hat{v}_{XC} = \alpha \left[1 + \tanh \left\{ \frac{\beta}{\alpha} G(\rho) \right\} \right] \hat{v}_{XS} \quad (\text{IV.6})$$

where the hyperbolic tangent plays the role of a convergence factor, restricting the inhomogeneity term in the square brackets to the range ± 1 . At very large values of r , $\tanh \left\{ \frac{\beta}{\alpha} G(\rho) \right\}$ approaches -1 , such that \hat{v}_{XC} approaches 0 as $r \rightarrow \infty$. At very small values of r , $\tanh \left\{ \frac{\beta}{\alpha} G(\rho) \right\}$ approaches $+1$ such that \hat{v}_{XC} approaches $2\alpha \hat{v}_{X1}$ as $r \rightarrow 0$. At intermediate values of r , including the entire effective range of the $1s$ orbitals, the deviations of $\left\{ \frac{\beta}{\alpha} G(\rho) \right\}$ from 0 are sufficiently small that $\tanh \left\{ \frac{\beta}{\alpha} G(\rho) \right\} = \left\{ \frac{\beta}{\alpha} G(\rho) \right\}$ to a high degree of approximation. For the cases involving higher α values in the $X\alpha$ potential, gradient corrections do not give any significant EC corrections. The results of our calculations (Approximations A, B, C and D of Tables IV.9 and IV.10) emphasize the importance of ring diagram terms for gradient-corrected potentials as well. The inherent shortcomings of the electron gas model are shared to some extent by the $X\alpha$ method as revealed by the instabilities encountered in the cluster equations for $\alpha \rightarrow 2/3$. However,

the exact treatment of the kinetic energy coupled with an appropriate scaling of the EC potential removes the divergences characteristic of the electron gas approximation to non-uniform charge distributions.

IV.5 CONCLUSIONS

The import of our study rests on the analysis of the local potential $X\alpha$ approximation. Owing to the use of the uniform charge density approximation, the $X\alpha$ model shares the problems inherent in the electron gas theories. The ill-behaved terms arising from the ring diagrams indicate the inappropriateness of the unmodified electron gas approximation for atomic structure studies. However, with a proper scaling of the local potential all the divergences inherent in the modified electron gas approximation can be eliminated. Our study prescribes the limits of validity of the $X\alpha$ local potential with reference to α variations and gradient corrections. In this context, it may be pointed out that, unlike in Brueckner's study where only ring diagrams were found to be important, or in Sinanoglu's study where only ladder diagrams were found to be important, in our study with the $X\alpha$ model, it has been found necessary to take into account both the ladder and the ring diagram terms. Also, in contrast to Sinanoglu's studies with HF reference functions, where all the pair correlation corrections were found to be important, our study reveals that the

only important pair corrections are the valence-shell EC corrections. This coupled with the simplicity achieved at the computational level, strongly recommends the use of the $X\alpha$ local potential model for many-body atomic structure calculations.

CHAPTER V

EXPECTATION VALUES OF SOME ONE-ELECTRON OPERATORS WITH CLUSTER-EXPANDED WAVEFUNCTIONS

- V.1 General
- V.2 The Expectation Values
- V.3 Results and Discussion

V.1 GENERAL

This chapter reports the results of our preliminary investigation on the evaluation of one-electron operators for Be isoelectronic series obtained over the cluster-expanded wavefunctions. Two of the hierarchy of approximations to the full CC equations are examined in this context. The expectation values of r, r^2 and $1/r$ are obtained over these wavefunctions.

The calculation of the expectation values can be done in either of two ways. In the first method, the cluster-expanded wavefunctions are obtained first and the expectation value of the operator is evaluated over these functions. Alternately, as in MBPT, it is possible to incorporate into the Goldstone diagrams the operator directly, by replacing one interaction vertex by the corresponding operator in all orders [116,117]. This later method, when adapted to CC methodology has the drawback of invalidating the basis for the truncation of the expansion series after a few terms. In the limit of ultimate sophistication both methods are expected to yield identical results. In the following we use the simpler of the two methods, viz., evaluation of the property over the cluster expanded functions, with a view to gauge the effect of inclusion of higher order terms on the properties.

V.2 THE EXPECTATION VALUES

The CC expansion in the Approximations E and F outlined in the previous chapter is used to obtain the refined wavefunctions. It may be recalled that in Approximation E, the particle-particle ladder diagram term is included resulting in a procedure equivalent to the selective ladder diagram summation to all orders in MBPT. Approximation F corresponds to the simple second-order RSPT expansion. Taking into consideration that only the cluster coefficients, $t_{\alpha\beta}^{rs}$, are significant in the expansion, the exact wavefunction may be written in terms of the cluster expansion formalism as

$$|\psi\rangle = |\phi\rangle + \sum_{\alpha\beta rs} t_{\alpha\beta}^{rs} \hat{a}_{\alpha}^{\dagger} \hat{a}_{\beta}^{\dagger} \hat{a}_s \hat{a}_r |\phi\rangle \quad (V.1)$$

where ϕ is the reference wavefunction and ψ the wavefunction obtained through the cluster expansion. The CI expansion,

$$|\psi\rangle = |\phi\rangle + \sum_{\alpha\beta rs} c_{\alpha\beta}^{rs} |\phi_{\alpha\beta}^{rs}\rangle \quad (V.2)$$

may be compared with eqn. (V.1) in order to obtain the relationship between $c_{\alpha\beta}^{rs}$ and $t_{\alpha\beta}^{rs}$. As can be seen

$$c_{\alpha\beta}^{rs} = (2!)^{-2} t_{\alpha\beta}^{rs} \quad (V.3)$$

For any operator \hat{O} , the expectation value expression assumes the form

$$\begin{aligned}
\frac{1}{N_0} \langle \Psi | \hat{O} | \Psi \rangle = & \frac{1}{N_0} [\langle \Phi | \hat{O} | \Phi \rangle + \sum_{\alpha\beta rs} c_{\alpha\beta}^{rs} \langle \Phi | \hat{O} | \Phi_{\alpha\beta}^{rs} \rangle \\
& + \sum_{\alpha\beta rs} c_{\alpha\beta}^{rs} \langle \Phi_{\alpha\beta}^{rs} | \hat{O} | \Phi \rangle \\
& + \sum_{\alpha\beta rs} \sum_{\alpha' \beta' r' s'} c_{\alpha\beta}^{rs} c_{\alpha' \beta'}^{r' s'} \langle \Phi_{\alpha\beta}^{rs} | \hat{O} | \Phi_{\alpha' \beta'}^{r' s'} \rangle] \quad .
\end{aligned}
\tag{V.4}$$

where, the c 's are defined through eqn. (V.2) and N_0 is the normalisation factor given by,

$$N_0 = \langle \Psi | \Psi \rangle \tag{V.5}$$

For one-electron operators \hat{O} , the second and the third terms on the RHS of eqn. (V.4) vanish owing to orthogonality of the orbitals; the first term in the equation corresponds to the ground state expectation value of the operator, i.e.

$$\langle \hat{O} \rangle_0 = \langle \Phi | \hat{O} | \Phi \rangle \tag{V.6}$$

The last term in eqn. (V.4) can be written for the three cases, where the index sets $\{\alpha\beta rs\}$ and $\{\alpha' \beta' r' s'\}$ may differ by none, one or more index labels.

Case i) the index sets, $\{\alpha\beta rs\}$ and $\{\alpha' \beta' r' s'\}$ are identical; the last term in eqn. (V.4) assumes the form,

$$\begin{aligned}
\langle \Phi_{\alpha\beta}^{rs} | \hat{O} | \Phi_{\alpha\beta}^{rs} \rangle & = \langle \hat{O} \rangle_0 - \langle \alpha | \hat{O} | \alpha \rangle - \langle \beta | \hat{O} | \beta \rangle + \\
& \quad \langle r | \hat{O} | r \rangle + \langle s | \hat{O} | s \rangle .
\end{aligned}
\tag{V.7}$$

Case ii) the index sets, $\{\alpha\beta rs\}$ and $\{\alpha'\beta'r's'\}$ differ by one label;

Let the differing labels be identified as i in the first set and j in the second set. The matrix element then has the form,

$$\langle \phi_{\alpha\beta}^{rs} | \hat{O} | \phi_{\alpha'\beta'}^{r's'} \rangle = \langle i | \hat{O} | j \rangle \quad (V.8)$$

Case iii) the index sets differ in more than one label; the matrix elements vanish by virtue of the orbitals being orthogonal.

$$\langle \phi_{\alpha\beta}^{rs} | \hat{O} | \phi_{\alpha'\beta'}^{r's'} \rangle = 0 \quad (V.9)$$

The expressions in eqns. (V.7) and (V.8) are used to evaluate the expectation values after taking into consideration appropriate numerical factors corresponding to spin summations.

V.3 RESULTS AND DISCUSSION

Tables V.1 to V.8 present the one-electron expectation values obtained in the two Approximations E and F for Be, B⁺, C⁺² and N⁺³ systems. As can be seen from the tables, all the expectation values obtained over the cluster-expanded wavefunctions are uniformly higher than the reference function expectation values. It is well known that the theorem of Møller and Plesset [33], which states that one-electron properties calculated from the HF wavefunctions are correct to "first order" can be extended to X α wavefunctions as well.

Table V.1 $\langle r^2 \rangle$, $\langle r \rangle$ and $\langle 1/r \rangle$ Values for Be (Approximation E)

α	$\langle r^2 \rangle$			$\langle r \rangle$		$\langle 1/r \rangle$	
	Ground State	All configurations included	Ground State	All configurations included	Ground State	All configurations included	
0.667	21.6007	21.9559	6.7475	6.7949	8.2110	8.2343	
0.720	20.8800	21.2349	6.6365	6.6841	8.3662	8.3899	
0.768	20.1421	20.4788	6.5260	6.5720	8.4230	8.4466	
0.840	19.0384	19.3458	6.3584	6.4020	8.5089	8.5327	
1.000	16.6958	16.9327	5.9927	6.0300	8.7013	8.7254	

All values in atomic units.

Table V.2 $\langle r^2 \rangle$, $\langle r \rangle$ and $\langle 1/r \rangle$ Values for Be (Approximation F)

n	< r ² >			< r >			< 1/r >		
	Ground State	All configurations included	Ground State	All configurations included	Ground State	All configurations included	Ground State	All configurations included	
0.667	21.6007	23.2083	6.7475	6.9758	8.2110	8.3308			
0.720	20.8800	22.4940	6.6365	6.8659	8.3662	8.4875			
0.768	20.1421	21.6775	6.5260	6.7484	8.4230	8.5447			
0.840	19.0384	20.4497	6.3584	6.5700	8.5089	8.6317			
1.000	16.6958	17.8134	5.9927	6.1783	8.7013	8.8283			

All values in atomic units.

Table V.3 $\langle r^2 \rangle$, $\langle r \rangle$ and $\langle 1/r \rangle$ Values for B^+ (Approximation E)

c	$\langle r^2 \rangle$			$\langle r \rangle$			$\langle 1/r \rangle$	
	Ground State	All configurations included	Ground State	All configurations included	Ground State	All configurations included	Ground State	All configurations included
0.66	9.0445	9.0879	4.4991	4.8141	10.7178	10.7433		
0.72	8.8600	8.9017	4.4544	4.4690	10.7782	10.8038		
0.76	8.7157	8.7560	4.4194	4.4337	10.8242	10.8500		
0.84	8.4141	8.4517	4.3461	4.3599	10.9179	10.9439		
1.00	7.7811	7.8131	4.1914	4.2041	11.1097	11.1361		

All values in atomic units.

Table V.4 $\langle r^2 \rangle$, $\langle r \rangle$ and $\langle 1/r \rangle$ Values for B^+ (Approximation F)

α	$\langle r^2 \rangle$			$\langle r \rangle$			$\langle 1/r \rangle$		
	Ground State	All configurations included	Ground State	All configurations included	Ground State	All configurations included	Ground State	All configurations included	All configurations included
0.66	9.0445	9.2547	4.4991	4.5733	10.7178	10.8490			
0.72	8.8600	9.0636	4.4544	4.5275	10.7782	10.9113			
0.76	8.7157	8.9142	4.4194	4.4917	10.8242	10.9588			
0.84	8.4141	8.6018	4.3461	4.4168	10.9179	11.0557			
1.00	7.7811	7.9457	4.1914	4.2586	11.1097	11.2544			

All values in atomic units.

Table V.5 $\langle r^2 \rangle$, $\langle r \rangle$ and $\langle 1/r \rangle$ Values for C^{+2} (Approximation E)

a	$\langle r^2 \rangle$			$\langle r \rangle$			$\langle 1/r \rangle$	
	Ground State	All configurations included	Ground State	All configurations included	Ground State	All configurations included	Ground State	All configurations included
0.667	5.0739	5.0883	3.4177	3.4260	13.2197	13.2477	13.2197	13.2477
0.720	4.9978	5.0117	3.3926	3.4007	13.2802	13.3084	13.2802	13.3084
0.760	4.9378	4.9515	3.3729	3.3809	13.3263	13.3547	13.3263	13.3547
0.840	4.8111	4.8241	3.3312	3.3391	13.4203	13.4490	13.4203	13.4490
1.000	4.5396	4.5513	3.2422	3.2497	13.6127	13.6421	13.6127	13.6421

All values in atomic units.

Table V.6 $\langle r^2 \rangle$, $\langle r \rangle$ and $\langle 1/r \rangle$ Values for C^{+2} (Approximation F)

α	$\langle r^2 \rangle$			$\langle r \rangle$			$\langle 1/r \rangle$	
	Ground State	All configurations included	Ground State	Ground State	All configurations included	Ground State	Ground State	All configurations included
0.667	5.0739	5.1413	3.4177	3.4575	13.2197	13.3602		
0.720	4.9978	5.0639	3.3926	3.4322	13.2802	13.4234		
0.760	4.9378	5.0030	3.3729	3.4124	13.3263	13.4717		
0.840	4.8111	4.8743	3.3312	3.3706	13.4203	13.5703		
1.000	4.5396	4.5984	3.2422	3.2812	13.6127	13.7723		

All values in atomic units.

Table V.8 $\langle r^2 \rangle$, $\langle r \rangle$ and $\langle 1/r \rangle$ Values for N^{+3} (Approximation F)

α	$\langle r^2 \rangle$			$\langle r \rangle$			$\langle 1/r \rangle$		
	Ground State	All configurations included	Ground State	All configurations included	Ground State	All configurations included	Ground State	All configurations included	All configurations included
0.667	3.2701	3.3016	2.7667	2.7930	15.7202	15.8719			
0.720	3.2310	3.2622	2.7505	2.7768	15.7807	15.9359			
0.760	3.2002	3.2312	2.7377	2.7642	15.8269	15.9848			
0.840	3.1346	3.1652	2.7106	2.7373	15.9211	16.0848			
1.000	2.9924	3.0219	2.6523	2.6794	16.1141	16.2897			

All values in atomic units.

Whereas, two-electron properties are expected to be influenced considerably by EC corrections, most one-electron properties are not expected to show a marked deviation from the reference state expectation values. In view of this, it appears that the inclusion of ladder diagrams to all orders (Approximation E) corrects the higher estimates obtained in second-order RSPT approximation (Approximation F). As can be seen from the tables, with increasing α values the $\langle r \rangle$ and $\langle r^2 \rangle$ values decrease, while the $\langle 1/r \rangle$ values increase steadily. At higher values of α a more contracted charge density description is provided by the $X\alpha$ model and this results in the above mentioned trends.

Due to the importance of these operator expectation values in the estimation of magnetic susceptibility and diamagnetic shielding, it will be of interest to examine the relative importance of contributions of various diagram terms in the evaluation of these expectation values. For this purpose, the direct method of incorporating the one-electron operator into the diagrammatic expansion is likely to be superior [118] and further work in this direction is in progress.

CONCLUSIONS

The work presented in this thesis represents an attempt to describe many-electron interactions more accurately. It is different from other attempts, in the sense that it starts from a local potential-based model for studying these interactions and that it uses the CC method which originates from the powerful linked-cluster theorem. This rigorously size-extensive, CC method, has provided an extremely useful framework for assessing the merits of local potential IPA's. The diagrammatic language employed in the method has facilitated the understanding and analysis of the terms encountered. Selective inclusion of diagrams has also enabled a comparison with various many-electron models.

The CC method based analysis of the X_α local potential model has revealed interesting facets of the underlying electron gas-like approximation. The limits of validity of the X_α approximation with reference to α variation and gradient correction have been outlined. It has been shown that by appropriate scaling of the uniform electron gas potential, through the parameter α , it is possible to obtain independent particle descriptions that serve as good starting points for many-electron treatments. It has been found that the best α -valued potential is the one that

mimics closely the HF potential; this is perhaps no mere coincidence, since the HF potential is the true potential of an independent particle approximated many-electron function. The superiority of the $X\alpha$ model over the HF model in the computational realm is retained in the many-electron treatment as well.

An interesting feature revealed by our study is the relative unimportance of the inner-shell EC corrections in beryllium atom. It appears from this that in many-electron treatments based on local potential models, consideration of valence-shell EC corrections alone would provide a good representation of many-electron interactions in atoms. It is hoped that recognition of this fact will be particularly useful for large system calculations. The study also reveals the futility of employing gradient corrections to the potential in order to account for non-uniform charge distribution in atoms.

It is inferred from the CC analysis of EC effects in beryllium and its isoelectronic series that terms arising from both ring diagrams and ladder diagrams contribute to the EC correction. This is understandable since the $X\alpha$ model shares some features of both the electron gas and HF models. In the electron gas model, which serves as the basis for $X\alpha$ potential approximation, the ring diagrams alone contribute; and in the HF model, whose shell-structure like characteristic is well reproduced by $X\alpha$ model, only ladder diagrams are

found to be important. In this connection it may be pointed out that for suitable values of α , the $X\alpha$ model overcomes energy divergences encountered through the application of electron gas description to non-uniform charge distributions; at the same time it has a computational simplicity not shared by the HF method. In this sense, many-electron studies with reference $X\alpha$ wavefunctions, can draw upon the merits of both electron gas and HF based many-electron theories.

The application of CC methodology to go beyond the local potential IPA's is not devoid of shortcomings. Firstly, the non-linear equations are not well-behaved; this may well be due to the choice of the $X\alpha$ model to provide the reference state. A detailed analysis of the terms that induce instability in the equations merits study. Also, it is not known, whether a limited virtual orbital basis will suffice to describe the EC effects in larger systems correctly. Limited basis calculations on larger atoms, with "valence only" excitations would throw more light on the use of this approach for many-body calculations.

In conclusion, it may be stated that our study has made an effort to analyse the nature of $X\alpha$ approximation and gauge its use as a starting point in many-body calculations. The results of our analysis clearly indicate the advantage of using the $X\alpha$ local potential model in many-body atomic structure calculations.

BIBLIOGRAPHY

1. H.A. Bethe and E. Salpeter, "Quantum Mechanics of one-and two-electron Atoms" (Academic Press, New York, 1957).
2. D.R. Hartree, Proc. Camb. Phil. Soc., 24, 89 (1928).
3. J.C. Slater, "Quantum Theory of Atomic Structure" (McGraw Hill, New York, 1960), Vol. I.
4. J.C. Slater, Phys. Rev., 35, 509 (1930).
5. P.A.M. Dirac, Proc. Roy. Soc. (Lond.), A 112, 661 (1926).
6. J.C. Slater, Phys. Rev., 34, 1293 (1929).
7. V. Fock, Z. Phys., 61, 126 (1930); 62, 795 (1930).
8. J.C. Slater, Phys. Rev., 81, 385 (1951).
9. D. Pines, "Elementary Excitations in Solids" (W.A. Benjamin Inc., New York, 1963).
10. L.H. Thomas, Proc. Camb. Phil. Soc., 23, 542 (1927).
11. E. Fermi, Z. Phys., 48, 73 (1928); 49, 550 (1928).
12. P.C. Hohenberg and W. Kohn, Phys. Rev. 136, B 864 (1964).
13. N.H. March, "Self-Consistent Field in Atoms" (Pergamon Press, London, 1975).
14. P. Rennert, Acta Phys., 37, 219 (1974).
15. W. Kohn and S.J. Sham, Phys. Rev., 140, A 1133 (1965).
16. P.A.M. Dirac, Proc. Camb. Phil. Soc., 26, 376 (1930).
17. P. Gombas, "Die Statistische Theorie des Atoms und ihre Anwendungen" (Springer-Verlag, Vienna, 1949).
18. P. Gaspar, Acta Phys., 3, 263 (1954).
19. J.C. Slater, Adv. Quantum Chem., 6, 1 (1972).
20. J.C. Slater, "The Self-Consistent Field for Molecules and Solids: Quantum Theory of Molecules and Solids, Volume 4" (McGraw Hill, New York, 1974).

21. K.H. Johnson, Adv. Quantum Chem., 7, 143 (1973).
22. R.P. Feynman, Phys. Rev., 56, 340 (1934).
23. J.C. Slater, J. Chem. Phys., 57, 2389 (1972).
24. K. Schwarz, Phys. Rev., B5, 2466 (1972).
25. E. Clementi and C. Roetti, At. Data Nucl. Data Tables, 14, 177 (1974).
26. P-O. Löwdin, Adv. Chem. Phys., 2, 207 (1959).
27. H.F. Schaefer, III, "The Electronic Structure of Atoms and Molecules" (Addison-Wesley, Massachusetts, 1972).
28. A. Dalgarno, Adv. Phys., 11, 281 (1962).
29. H.J. Silverstone and O. Sinanoglu, J. Chem. Phys., 44, 1899, 3608 (1966).
30. E.A. Hylleraas, Z. Phys., 48, 469 (1928).
31. W. Kutzelnigg, in "Methods of Electronic Structure Theory", edited by H.F. Schaefer, III (Plenum Press, New York, 1977), pp 129-188.
32. E.A. Hylleraas, Z. Phys., 54, 347 (1929).
33. C. Möller and M.S. Plesset, Phys. Rev., 46, 618 (1934).
34. H.P. Kelly, Phys. Rev., 131, 690 (1963).
35. J. Čížek, J. Chem. Phys., 45, 4256 (1966); Adv. Chem. Phys., 14, 35 (1969).
36. R. McWeeny, Rep. Prog. Phys., 43, 68 (1980) and references therein.
37. I. Shavitt, in "Methods of Electronic Structure Theory", edited by H.F. Schaefer, III (Plenum Press, New York, 1977), pp. 189-275.
38. R. Courant and D. Hilbert, "Methods of Mathematical Physics", (Interscience, New York, 1953), Volume 1, pp. 175-6.
39. P-O. Löwdin, Phys. Rev., 97, 1509 (1955).
40. R.K. Nesbet, Phys. Rev., 109, 1632 (1958).

41. O. Sinanoglu, Proc. Roy. Soc. (Lond.), A 260, 379 (1961); J. Chem. Phys., 36, 706, 3198 (1962).
42. H. Primas, in "Modern Quantum Chemistry", edited by O. Sinanoglu (Academic Press, New York, 1965), Vol. 2, pp 45-74.
43. K.A. Brueckner, Phys. Rev., 97, 1353 (1955); 100, 36 (1955).
44. R.J. Yaris and J.I. Musher, J. Chem. Phys., 41, 1701 (1964).
45. W. Kutzelnigg, Topics Curr. Chem., 41, 31 (1973).
46. R.K. Nesbet, Adv. Chem. Phys., 2, 321 (1965).
47. J.C. Slater, Phys. Rev., 32, 349 (1928).
48. R. Jastrow, Phys. Rev., 98, 1479 (1955).
49. L. Szasz, J. Chem. Phys., 35, 1072 (1961); J. Math. Phys., 3, 1147 (1962).
50. J.S. Sims and S.A. Hagstrom, Phys. Rev., A 4, 908 (1971); J. Chem. Phys., 55, 4699 (1971).
51. D.C. Clary and N.C. Handy, Phys. Rev., A 14, 1607 (1976).
52. J.D. Talman, Phys. Rev., A 21, 1805 (1980).
53. P-O. Löwdin, Int. J. Quantum Chem., 2, 867 (1968).
54. L. Brillouin, Actualités Sci. et Ind., 159 (1934).
55. J.S. Binkley and J.A. Pople, Int. J. Quantum Chem., 9, 229 (1975).
56. J. Goldstone, Proc. Roy. Soc. (Lond.), A 239, 267 (1957).
57. B.H. Brandow, Rev. Mod. Phys., 39, 771 (1967).
58. J. Paldus and J. Čížek, Adv. Quantum Chem., 2, 105 (1975).
59. I. Lindgren, Int. J. Quantum Chem., 512, 33 (1978).
60. B.H. Brandow, Adv. Quantum Chem., 10, 187 (1976).
61. S. Reimes, "Many Electron Theory", (North Holland Publishing Company, Amsterdam, 1972).

62. H.P. Kelly, Adv. Theoret. Phys., 2, 75 (1968);
Adv. Chem. Phys., 14, 129 (1969).
63. E.S. Chang, R.T. Pu and T.P. Das, Phys. Rev.,
174, 1 (1968).
64. A. Hibbert, Rep. Prog. Phys., 38, 1217 (1975).
65. F. Coester, Nucl. Phys., 7, 421 (1958).
66. H. Kümmel, in "Lectures in the Many-Body Problem",
edited by E.R. Caianiello (Academic Press, New York,
1962), pp. 265-277.
67. H. Kümmel, K.H. Lührman and J.G. Zabolitsky, Phys.
Rep., C 36, 1 (1978).
68. J.C. Slater, "The Calculation of Molecular Orbitals"
(Wiley-Interscience, New York, 1979).
69. O. Gunnarson and R.O. Jones, Phys. Scripta, 21,
394 (1980).
70. E.P. Wigner, Phys. Rev., 40, 1002 (1934).
71. M. Gell-Mann and K.A. Brueckner, Phys. Rev., 106,
364 (1957).
72. S.K. Ma and K.A. Brueckner, Phys. Rev., 165, 18 (1968).
73. K.S. Singwi, A. Sjölander, M.P. Tosi and R.H. Land,
Phys. Rev., B 1, 1044 (1970).
74. C.M. Singal and T.P. Das, Phys. Rev., B 8, 3675(1973);
B 12, 795 (1975).
75. O. Gunnarson and B.I. Lundqvist, Phys. Rev., B 13,
4274 (1976).
76. H. Stoll, E. Golka and H. Preuss, Theoret. Chim.
Acta, 55, 29 (1980).
77. C.F. von Weisäcker, Z. Phys., 96, 431 (1965).
78. M.S. Gopinathan, M.A. Whitehead and R. Bogdanović,
Phys. Rev., A 14, 1 (1976).
79. J.L. Gásquez and J. Keller, Phys. Rev., A 16, 1358(1977).
80. J.A. Alonso and L.A. Girifalco, Phys. Rev., B 17,
3735 (1978).

81. R.N. Zare, J. Chem. Phys., 45, 1966 (1966); 47, 356 (1967).
82. J. Paldus and J. Cizek, in "Energy, Structure and Reactivity", edited by W.D. Smith and B.M. Walter (John Wiley & Sons, New York, 1973), pp. 198-212.
83. J. Hubbard, Proc. Roy. Soc. (Lond.), A 240, 539(1957).
84. J. da Providencia, J. Nucl. Phys., 46, 401 (1963).
85. T.P. Zivković and H.J. Monkhorst, J. Math. Phys., 19, 1007 (1978).
86. J. Čížek and J. Paldus, Int. J. Quantum Chem., 5, 359 (1971).
87. I. Hubac and P. Čásky, Topics Curr. Chem., 75, 99 (1978).
88. G.H. Weiss and A.A. Maradudin, J. Math. Phys., 3, 771 (1962).
89. J. Paldus, J. Čížek and I. Shavitt, Phys. Rev., A 5, 50 (1972).
90. B.G. Adams, K. Jankowsky and J. Paldus, Chem. Phys. Lett., 67, 144 (1979).
91. H.A. Bethe and J. Goldstone, Proc. Roy. Soc. (Lond.), A 238, 551 (1957).
92. J. Paldus, J. Čížek, M. Saute and A. Laforge, Phys. Rev., A 17, 805 (1978).
93. D. Mukherjee, R.K. Moitra and A. Mukhopadhyay, Molec. Phys., 30, 1861 (1975).
94. F.E. Harris, in "Electrons in Finite and Infinite Structures", edited by P. Phariseau and L. Scheire (Plenum Press, New York, 1977), pp. 274-320.
95. D.L. Freeman, Phys. Rev., B 15, 5512 (1977).
96. C.F. Bunge, Phys. Scripta, 21, 328 (1980).
97. R.K. Nesbet, Phys. Rev., 155, 51 (1967).
98. C.F. Bunge, At. Data Nucl. Data Tables, 18, 293 (1976).
99. R. Latter, Phys. Rev., 99, 510 (1955).

100. F. Herman and S. Skillman, "Atomic Structure Calculations" (Prentice-Hall Inc., New Jersey, 1963).
101. E.U. Condon and G.H. Shortley, "The Theory of Atomic Spectra", (Cambridge University Press, London, 1959).
102. R.N. Zare, JILA, Rept. No. 80 (1966).
103. B. Carnahan, "Applied Numerical Methods" (Wiley Interscience, New York, 1969).
104. F.B. Hildebrand, "Introduction to Numerical Analysis" (McGraw Hill, New York, 1956).
105. J.M. Ortega and W.C. Rheinboldt, "Iterative Solution of Non-linear Equations in Several Variables" (Academic Press, New York, 1976).
106. K.M. Brown, Comm. ACM, 10, 728 (1967); SIAM J. Numr. Anal., 6, 560 (1969).
107. B.Y. Tong and L.J. Sham, Phys. Rev., 144, 1 (1966).
108. N.H. March and J.S. Plaskett, Proc. Roy. Soc. (Lond.), A 235, 419 (1956).
109. D. Pines, Phys. Rev., 92, 626 (1953).
110. U. von Barth and L. Hedin, J. Phys. C, 5, 1629 (1972).
111. N. Elyasher and D.D. Koelling, Phys. Rev., B 15, 3620 (1977).
112. K.A. Brueckner, in "Atomic Physics", edited by B. Bederson, V.M. Cohen and F.M.J. Pichanick (Plenum Press, New York, 1969), pp. 111-130.
113. F. Herman, J.P. van Dyke and I.B. Ortenberger, Phys. Rev. Lett., 22, 807 (1969).
114. E. Kmetko, Phys. Rev., A 1, 37 (1970).
115. F. Herman and K. Schwarz, in "Computational Solid State Physics", edited by F. Herman, N.W. Dalton and T.R. Koehler (Plenum Press, New York, 1972), pp. 245-252.
116. H.P. Kelly, Phys. Rev., 182, 84 (1969).
117. N.C. Dutta, T. Ishihara, C. Matsubara and T.P. Das, Phys. Rev. Lett., 22, 8 (1969).
118. H.J. Monkhorst, Int. J. Quantum Chem., S 11, 421(1977).

*A good notation has a subtlety and suggestiveness
which at times make it seem almost like a
live teacher.*

Bertrand Russell.

APPENDIX A

- A1 The Language of Second Quantisation
- A2 Feynman Diagrams for Perturbation Theory
- A3 Fourth-Order RSPT and Cancellation of
Unlinked Terms
- A4 Hole-Particle Formalism
- A5 Normal Product Operators and Wick's Theorem
- A6 Further Examples of Diagrammatics

A1 THE LANGUAGE OF SECOND QUANTISATION

The wavefunction for an N-Fermion system can be written in the form of a Slater determinant (ϕ) of one-electron functions (ϕ_i). The determinant, on expansion in terms of cofactors yields

$$\phi(1,2, \dots, N) = \frac{1}{\sqrt{N}} \sum_{i \in \phi} \phi_i(1) \phi_i(2, \dots, N) (-1)^{n_i+1} \quad (\text{A1.1})$$

The subscripts refer to the orbital index, the number in the brackets to the electron coordinate index and n_i to the ordinal number of the orbital i in the determinant under consideration; the summation runs over all the orbitals in ϕ . Eqn. (A1.1) can be rewritten in terms of the annihilation operator, which is defined as,

$$\hat{a}_i \phi(1,2, \dots, N) = (-1)^{n_i+1} \phi_i(2, \dots, N) \quad \text{for } \phi_i \in \phi \quad (\text{A1.2})$$

$$\text{and} \quad \hat{a}_i \phi(1,2, \dots, N) = 0 \quad \text{for } \phi_i \notin \phi \quad (\text{A1.3})$$

Eqn. (A1.1) then becomes,

$$\phi(1,2, \dots, N) = \frac{1}{\sqrt{N}} \sum_i \phi_i(1) \hat{a}_i \phi(1',2, \dots, N) \quad (\text{A1.4})$$

where $(1',2, \dots, N)$ is a function of electron coordinates 2 to N and $1'$ is a dummy variable. A second expansion of yields,

$$\phi(1,2, \dots, N) = \frac{1}{\sqrt{N(N-1)}} \sum_{ij} \phi_i(1) \phi_j(2) \hat{a}_j \hat{a}_i \phi(1',2',3, \dots, N) \quad (\text{A1.5})$$

The adjoint of the operator \hat{a}_i is defined as the creation operator, which satisfies

$$\langle \hat{a}_i \phi_A | \phi_B \rangle = \langle \phi_A | \hat{a}_i^\dagger \phi_B \rangle \quad (\text{A1.6})$$

for all ϕ_A and ϕ_B . It follows from the above that ,

$$\hat{a}_i^\dagger \phi(2,3, \dots, N) = (-1)^{n_i+1} \phi_i(1,2, \dots, N) \text{ for } \phi_i \notin \phi(2, \dots, N) \quad (\text{A1.7})$$

$$\hat{a}_i^\dagger \phi(2,3, \dots, N) = 0 \quad \text{for } \phi_i \in \phi(2, \dots, N) \quad (\text{A1.8})$$

The relationships between the \hat{a} 's and \hat{a}^\dagger 's follow from their definition

$$\hat{a}_i \hat{a}_j + \hat{a}_j \hat{a}_i = 0 \quad (\text{A1.9})$$

$$\hat{a}_i^\dagger \hat{a}_j^\dagger + \hat{a}_j^\dagger \hat{a}_i^\dagger = 0 \quad (\text{A1.10})$$

$$\hat{a}_i \hat{a}_j^\dagger + \hat{a}_j^\dagger \hat{a}_i = \delta_{ij} \quad (\text{A1.11})$$

where δ_{ij} is the Kronecker symbol, which implies

$$\delta_{ij} = 1 \quad \text{for } i = j$$

$$= 0 \quad \text{for } i \neq j$$

The Hamiltonian for an N-electron system may be written as

$$\begin{aligned} \hat{H} &= \hat{Z} + \hat{V} \\ &= \sum_{\mu} \hat{z}(\mu) + \sum_{\mu < \nu} \hat{v}(\mu, \nu) \end{aligned} \quad (\text{A1.12})$$

where \hat{z} is the one-electron operator, \hat{v} the two-electron operator and μ, ν are electron indices. For N-electron determinantal functions ϕ_A and ϕ_B .

$$\begin{aligned} \langle \phi_A | \hat{z} | \phi_B \rangle &= \langle \phi_A | \sum_{\mu} \hat{z}(\mu) \phi_B \rangle \\ &= N \langle \phi_A | \hat{z}(1) | \phi_B \rangle \end{aligned} \quad (\text{A1.13})$$

$$\begin{aligned} \langle \phi_A | \hat{v} | \phi_B \rangle &= \langle \phi_A | \sum_{\mu < \nu} \hat{v}(\mu, \nu) | \phi_B \rangle \\ &= \frac{1}{2} N(N-1) \langle \phi_A | \hat{v}(1, 2) | \phi_B \rangle \end{aligned} \quad (\text{A1.14})$$

Rewriting (A1.13) and (A1.14) in terms of eqn. (A1.4) and (A1.5) respectively,

$$\begin{aligned} N \langle \phi_A | \hat{z}(1) | \phi_B \rangle &= \sum_{ij} \langle \phi_i(1) | \hat{z}(1) | \phi_j(1) \rangle \langle \hat{a}_i \phi_A | \hat{a}_j \phi_B \rangle \\ &= \sum_{ij} \langle i | \hat{z} | j \rangle \langle \phi_A | \hat{a}_i^\dagger \hat{a}_j | \phi_B \rangle \end{aligned} \quad (\text{A1.15})$$

$$\begin{aligned} \frac{N(N-1)}{2} \langle \phi_A | \hat{v}(1, 2) | \phi_B \rangle &= \frac{1}{2} \sum_{ijkl} \langle \phi_i(1) \phi_j(2) | \hat{v}(1, 2) | \phi_l(1) \phi_k(2) \rangle \\ &\quad \langle \hat{a}_j \hat{a}_i \phi_A | \hat{a}_l \hat{a}_k \phi_B \rangle \\ &= \frac{1}{2} \sum_{ijkl} \langle ij | \hat{v} | kl \rangle \langle \phi_A | \hat{a}_i^\dagger \hat{a}_j^\dagger \hat{a}_l \hat{a}_k | \phi_B \rangle \end{aligned} \quad (\text{A1.16})$$

where any ϕ_k is represented symbolically by k .

Eqn. (A1.12) can therefore be written as :

$$H = \sum_{ij} \langle i | \hat{z} | j \rangle \hat{a}_i^\dagger \hat{a}_j + \frac{1}{2} \sum_{ijkl} \langle ij | \hat{v} | kl \rangle \hat{a}_i^\dagger \hat{a}_j^\dagger \hat{a}_l \hat{a}_k \quad (\text{A1.17})$$

The second quantisation formalism represents a convenient way of handling the antisymmetry requirement and with its use the need to use a determinantal representation is obviated [1] .

A2 FEYNMAN DIAGRAMS FOR PERTURBATION THEORY

The second quantisation formalism can be used to represent a general RS expansion matrix element,

$$\langle \hat{V} \hat{R} \hat{V} \hat{R} \dots \hat{R} \hat{V} \rangle \quad (\text{A2.1})$$

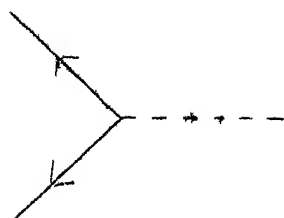
where, \hat{V} is the perturbation and \hat{R} defined in terms of the projection operator is $\hat{P}/(E_0 - \hat{H}_0)$.

In general, if the perturbation \hat{V} contains a one- and a two-body operator, it can be written in terms of creation-annihilation operators as,

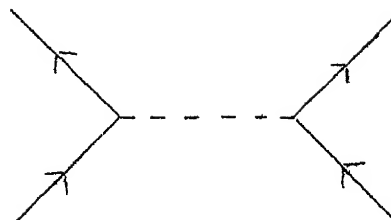
$$\begin{aligned} \hat{V} &= \hat{V}_1 + \hat{V}_2 \\ &= \sum_{ik} \langle i | \hat{V}_1 | k \rangle \hat{a}_i^\dagger \hat{a}_k + \\ &\quad \gamma_2 \sum_{ijkl} \langle ij | \hat{V}_2 | kl \rangle \hat{a}_i^\dagger \hat{a}_j^\dagger \hat{a}_l \hat{a}_k \end{aligned} \quad (\text{A2.2})$$

where \hat{V}_1 and \hat{V}_2 are the one- and two-body components of \hat{V} . The operator \hat{V} can be represented diagrammatically in terms of the one- and two-body operators as shown in Fig. A2.1 .

[1] R. Manne, Int. J. Quant. Chem., Symp. 11, 175 (1977)



one-body diagram



two-body diagram

Fig. A2.1 Feynman-diagram for one- and two-body operators

When the general matrix element eqn. (A2.1) is written in terms of eqn. (A2.2), a sum of 2^n matrix elements are obtained. Each of these is of the type $\langle \hat{V}_{k_1} \hat{R} \hat{V}_{k_2} \hat{R} \dots \hat{R} \hat{V}_{k_n} \rangle$, where any k_i is 1 or 2. The expanded form of the matrix element is very complicated; it is apparent that a general term in this expansion contains products of \hat{V}_1 and \hat{V}_2 matrix elements and creation and annihilation operators.

The operator part of the term has the form

$$\langle \hat{a}_i^\dagger \hat{a}_j^\dagger \hat{a}_l \hat{a}_k \hat{R} \hat{a}_m^\dagger \hat{a}_n^\dagger \hat{a}_q \hat{a}_p \hat{R} \dots \hat{R} \hat{a}_r^\dagger \hat{a}_u \hat{R} \dots \rangle .$$

Since the operator \hat{R} is diagonal in the given basis, the operator indices occur equally in pairs, i.e., corresponding to every creation operator \hat{a}_k^\dagger there must exist an annihilation operator \hat{a}_k . Only such of those summations of 2^n terms where this criterion is met need be considered. The condition on occurrence of the operator indices in pairs can be represented by linking the two operators. For example, a single pair of operators obeys the contraction rule :

$$\langle \hat{a}_i^\dagger \hat{a}_j \rangle = \delta_{ij} \quad (\text{A2.3})$$

and two pairs of operators have the contraction relationship

$$\langle \hat{a}_i^\dagger \hat{a}_j^\dagger \hat{a}_l \hat{a}_k \rangle = \delta_{ik} \delta_{jl} (1 - \delta_{ij}) \quad (\text{A2.4})$$

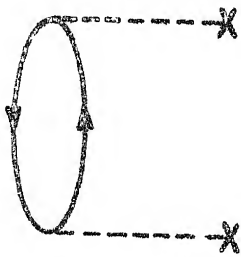
$$\langle \hat{a}_i^\dagger \hat{a}_j^\dagger \hat{a}_l \hat{a}_k \rangle = -\delta_{il} \delta_{jk} (1 - \delta_{ij}) \quad (\text{A2.5})$$

where, the signs follow from the anticommutation relationships between the operators. Diagrammatically this contraction implies the joining of the directed lines such that a creation operator line is joined to an annihilation operator line and further that the indices are matched. The operator $\hat{R} = \hat{P}/(E_0 - \hat{H}_0)$ generates the energy denominators of the RSPT.

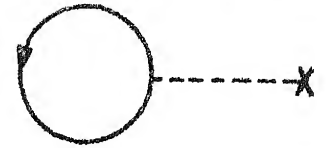
Typical second order RSPT diagrams and the corresponding matrix elements are given in Fig. A2.2. Goldstone showed that when the 2^n terms of a general RSPT matrix element $\langle \hat{V} \hat{R} \hat{V} \hat{R} \dots \hat{R} \hat{V} \rangle$ are expressed diagrammatically, all the unlinked diagrams cancel mutually leaving non-vanishing contributions only from the totally linked diagrams [2]. A diagram is considered linked if all the electron lines are connected to each other either directly or indirectly via interaction lines or other electron lines. Further, all the diagrams representing the matrix elements will be closed due to absence of any uncontracted operators.

[2] J. Goldstone, Proc. Roy. Soc. (Lond.), A 239, 267 (1957)

$$\Sigma \langle i | \hat{v}_1 | j \rangle \langle k | \hat{v}_1 | l \rangle \langle \hat{a}_i^\dagger \hat{a}_j^\dagger \hat{R} \hat{a}_k \hat{a}_l \rangle \quad \Sigma \langle i | \hat{v}_1 | j \rangle \langle k | \hat{v}_1 | l \rangle \langle \hat{a}_i^\dagger \hat{a}_j^\dagger \hat{R} \hat{a}_k \hat{a}_l \rangle$$

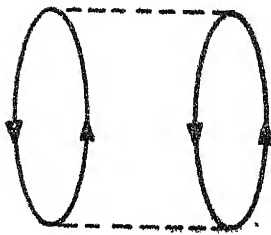


I

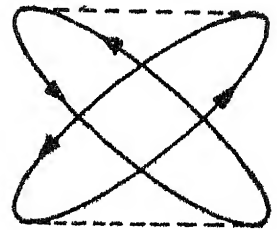


II

$$\frac{1}{4} \Sigma \langle ij | \hat{v}_2 | kl \rangle \langle mn | \hat{v}_2 | pq \rangle \langle \hat{a}_i^\dagger \hat{a}_j^\dagger \hat{a}_l \hat{a}_k \hat{R} \hat{a}_m^\dagger \hat{a}_n^\dagger \hat{a}_q \hat{a}_p \rangle$$

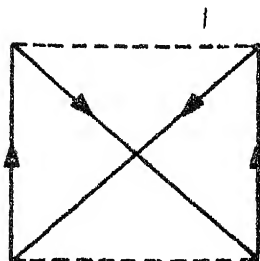


III

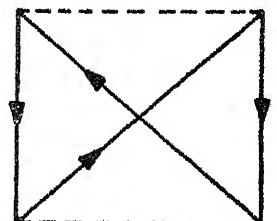
 \equiv 

IV

$$\frac{1}{4} \Sigma \langle ij | \hat{v}_2 | kl \rangle \langle mn | \hat{v}_2 | pq \rangle \langle \hat{a}_i^\dagger \hat{a}_j^\dagger \hat{a}_l \hat{a}_k \hat{R} \hat{a}_m^\dagger \hat{a}_n^\dagger \hat{a}_q \hat{a}_p \rangle$$



V

 \equiv 

VI

Fig. A2.2 Typical second-order RSPT diagrams and matrix elements.

Diagrams I, III and V of Fig. A2.2 are examples of such closed-linked diagrams. Diagram II of Fig. A2.2 is an example of unlinked diagram where there are two disconnected pieces. Such diagrams do not contribute to the energy expansion. The general RSPT term may therefore be written diagrammatically. The rules for constructing the diagrams are as follows [3] :

1. For a given order of perturbation, all the topologically different linked diagrams are drawn.
2. These diagrams are labelled with orbital indices, one corresponding to an orbital in the ground state ϕ_0 (hole lines) and the other corresponding to a virtual orbital (particle lines).
3. The numerator of the term corresponding to the diagram is a product of a combination of one- and two-electron integrals. The denominator is given by a product of the terms $(\sum_{\text{hole lines}} \epsilon_a - \sum_{\text{particle lines}} \epsilon_r)$ between each of the two vertices.
4. For every pair of 'equivalent' lines in the diagram the term is multiplied by a factor of $1/2$. An equivalent pair of lines is defined to be two lines going in the same direction, beginning at one vertex and ending at another, e.g. III of Fig. A2.2 has two such pairs.

[3] B.H. Brandow, Rev. Mod. Phys., 39, 771 (1967).

5. A sign factor of $(-1)^{1+h}$ is associated with the term which has in the corresponding diagram 'h' hole lines and '1' closed loops e.g. III of Fig. A2.2 has two hole lines and two closed loops.
6. The term in each diagram is independently summed for all particle states and hole states. Exclusion principle violating terms [3] arising from these independent summations are to be included.

Application of the above rules to the fourth-order RSPT term is illustrated in the following section.

A3 FOURTH-ORDER RSPT AND CANCELLATION OF UNLINKED TERMS

Use of Feynman's graphical techniques highlights the existence of the size-extensivity problem in limited basis fourth-order RSPT. Limiting, the basis to ground and double-excited functions only, the fourth-order RSPT energy expressions given by eqn. (I.46) can be expressed graphically. Expansion of the terms in eqn. (I.46) yields the terms represented by diagrams A-N of Fig. A3.1 [4]. The diagrams M and N arise from the term $\langle \hat{V} \hat{R} \langle \hat{V} \hat{R} \hat{V} \rangle \hat{R} \hat{V} \rangle$ in eqn. (I.45). These diagrams called as bracketed diagrams are unlinked and by virtue of their being proportional to N^2 , render an unphysical character to the perturbation expansion. As can be seen from the expressions in Table A3.1,

[4] R.J. Bartlett, and G.D. Purvis, Int. J. Quant. Chem., 14, 561 (1978).

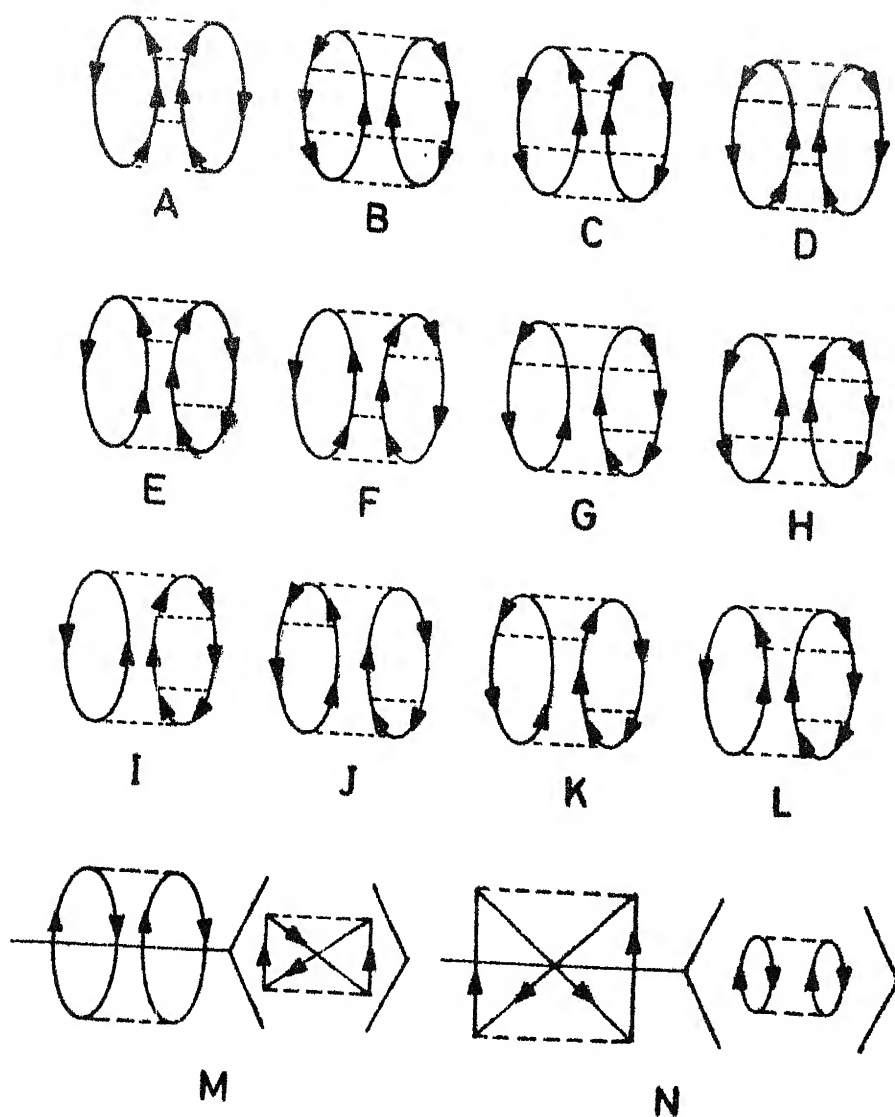


Fig. A3.1 Double excitation and bracketed diagrams of fourth-order perturbation theory.

Table A3.1 Terms corresponding to double-excitation and bracketed diagrams of fourth-order perturbation theory

Diagram	Term
A	$\frac{1}{16} \sum \langle \alpha\beta rs \rangle \langle rs uw \rangle \langle uw xy \rangle \langle xy \alpha\beta \rangle / D_{\alpha\beta rs} D_{\alpha\beta xw} D_{\alpha\beta xy}$
B	$\frac{1}{16} \sum \langle rs \alpha\beta \rangle \langle \alpha\beta \delta\epsilon \rangle \langle \delta\epsilon \eta\xi \rangle \langle \eta\xi rs \rangle / D_{\alpha\beta rs} D_{\delta\epsilon rs} D_{\eta\xi rs}$
C	$\frac{1}{16} \sum \langle rs \alpha\beta \rangle \langle \alpha\beta \delta\epsilon \rangle \langle rs uw \rangle \langle \delta\epsilon uw \rangle / D_{\alpha\beta rs} D_{\delta\epsilon rs} D_{\delta\epsilon uw}$
D	$\frac{1}{16} \sum \langle rs \alpha\beta \rangle \langle uw rs \rangle \langle \alpha\beta \delta\epsilon \rangle \langle \delta\epsilon uw \rangle / D_{\alpha\beta rs} D_{\alpha\beta uw} D_{\delta\epsilon uw}$
E	$-\frac{1}{2} \sum \langle rs \alpha\beta \rangle \langle u\beta s\delta \rangle \langle xy ru \rangle \langle \alpha\delta xy \rangle / D_{\alpha\beta rs} D_{\alpha\delta ru} D_{\alpha\delta xy}$
F	$-\frac{1}{2} \sum \langle rs \alpha\beta \rangle \langle uw rs \rangle \langle y\beta w\delta \rangle \langle \alpha\delta uy \rangle / D_{\alpha\beta rs} D_{\alpha\beta uw} D_{\alpha\delta uy}$
G	$-\frac{1}{2} \sum \langle rs \alpha\beta \rangle \langle u\beta s\delta \rangle \langle \alpha\delta \eta\xi \rangle \langle \eta\xi ru \rangle / D_{\alpha\beta rs} D_{\alpha\delta ru} D_{\eta\xi ru}$
H	$-\frac{1}{2} \sum \langle rs \alpha\beta \rangle \langle \alpha\beta \eta\delta \rangle \langle u\delta s\xi \rangle \langle \eta\xi ru \rangle / D_{\alpha\beta rs} D_{\delta\eta rs} D_{\eta\xi ru}$
I	$\sum \langle rs \alpha\beta \rangle \langle u\beta s\delta \rangle \langle w\delta u\epsilon \rangle \langle \alpha\epsilon rw \rangle / D_{\alpha\beta rs} D_{\alpha\delta ru} D_{\alpha\epsilon rw}$
J	$\sum \langle rs \alpha\beta \rangle \langle u\beta s\delta \rangle \langle \alpha w \epsilon r \rangle \langle \epsilon\delta wu \rangle / D_{\alpha\beta rs} D_{\alpha\delta ru} D_{\alpha\delta wu}$
K	$\sum \langle rs \alpha\beta \rangle \langle u\beta s\delta \rangle \langle \alpha w \epsilon u \rangle \langle \epsilon\delta rw \rangle / D_{\alpha\beta rs} D_{\alpha\epsilon ru} D_{\epsilon\delta rw}$
L	$\sum \langle rs \alpha\beta \rangle \langle u\beta s\delta \rangle \langle w\delta r\epsilon \rangle \langle \alpha\epsilon wu \rangle / D_{\alpha\beta rs} D_{\alpha\delta ru} D_{\alpha\epsilon uw}$
M+N	$-\frac{1}{16} \sum \langle \alpha\beta rs \rangle \langle \alpha\beta rs \rangle \langle \delta\epsilon uw \rangle \langle \delta\epsilon uw \rangle / D_{\alpha\beta rs} D_{\delta\epsilon uw} D_{\alpha\beta rs}$

$\alpha, \beta, \delta, \epsilon, \eta, \xi$ represent the occupied orbitals, and

r, s, u, w, x, y represent the virtual orbitals and

$$\langle ij || kl \rangle = \int d\tau_1 \int d\tau_2 \phi_i^*(1) \phi_j^*(2) \frac{1}{|r_1 - r_2|} (1 - \hat{P}_{12}) \phi_k(1) \phi_l(2)$$

$$D_{ijkl} = e_i + e_j - e_k - e_l.$$

there are no corresponding cancellation terms for M-N from diagrams A-L and this introduces serious errors. However, inclusion of quadruple excitation eliminates the unlinked bracketed terms, M and N of Fig. A3.1, in this order. The fourth-order terms originating from inclusion of quadruple excitations are represented by the diagrams O-W, in Fig. A3.2. The corresponding expressions are given in Table A3.2. The diagrams O to U in Fig. A3.2 are proportional to N and therefore well behaved, while V and W, the unlinked terms, are proportional to N^2 [5]. However, these terms are identical to the unphysical terms arising from the diagrams M and N of Fig. A3.1 and therefore mutually cancel with them. This proves that even in fourth-order RSPT it is necessary to go to quadruple excitations to ensure the cancellation of unphysical terms. The higher order unlinked terms demand the inclusion of correspondingly higher n-tuple excited basis to ensure the well-behavedness of the theory. If only limited basis are used, the unlinked terms escalate as the order increases and book-keeping becomes impossible. This serious shortcoming of RSPT is easily overcome with the application of the linked-cluster theorem to the expansion. The main premise of the linked-cluster theorem is that no unlinked terms figure in the summation; and the linked terms are well behaved with respect to N-dependence and cause no breakdown of the theory. With

[5] K.A. Brueckner, Phys. Rev., 100, 36 (1955)

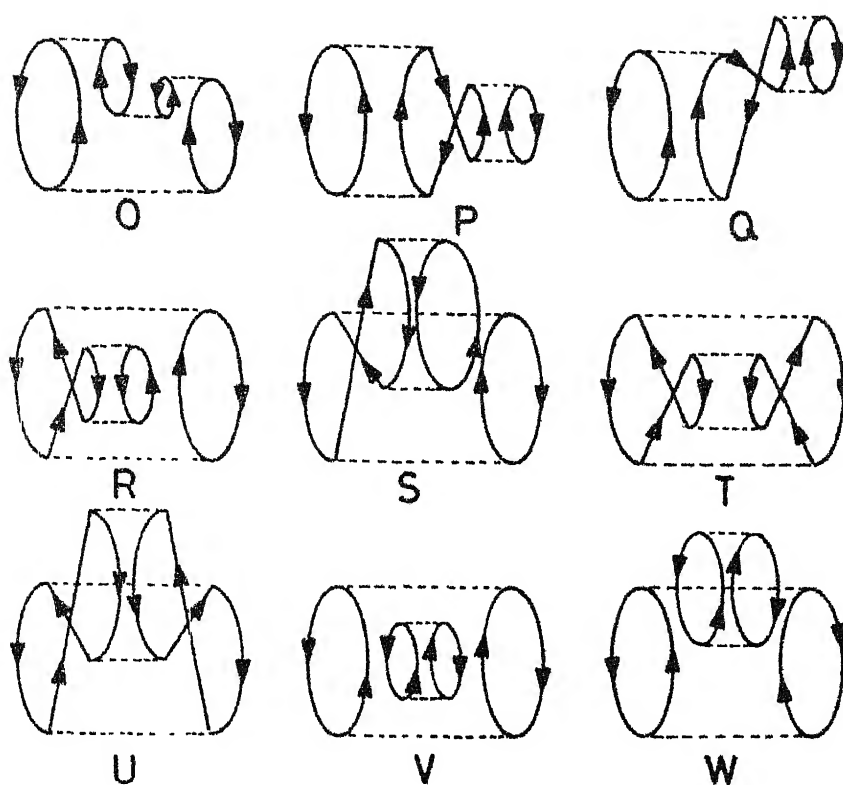


Fig. A3.2 Quadruple excitation diagrams of fourth-order perturbation theory.

Table A3.2 Terms corresponding to quadruple-excitation diagrams of fourth-order perturbation theory

Diagram	Term
O	$\frac{1}{2} \sum \langle rs \alpha\beta \rangle \langle uw \delta\epsilon \rangle \langle \epsilon\beta ws \rangle \langle \alpha\delta ru \rangle / D_{\alpha\beta rs} D_{\epsilon\beta ws} D_{\alpha\delta ru}$
P+Q	$-\frac{1}{4} \sum \langle rs \alpha\beta \rangle \langle uw \delta\epsilon \rangle \langle \beta\epsilon uw \rangle \langle \alpha\delta rs \rangle / D_{\alpha\beta rs} D_{\beta\epsilon uw} D_{\alpha\delta rs}$
R+S	$-\frac{1}{4} \sum \langle rs \alpha\beta \rangle \langle uw \delta\epsilon \rangle \langle \delta\epsilon rw \rangle \langle \alpha\beta us \rangle / D_{\alpha\beta rs} D_{\delta\epsilon rw} D_{\alpha\beta us}$
T+U	$\frac{1}{16} \sum \langle rs \alpha\beta \rangle \langle uw \delta\epsilon \rangle \langle rs \delta\epsilon \rangle \langle \alpha\beta uw \rangle / D_{\alpha\beta rs} D_{\delta\epsilon rs} D_{\alpha\beta uw}$
V+W	$\frac{1}{16} \sum \langle rs \alpha\beta \rangle^2 \langle \delta\epsilon uw \rangle^2 / D_{\alpha\beta rs}^2 D_{\delta\epsilon uw}^2$

$\alpha, \beta, \delta, \epsilon, n, \xi$ represent the occupied orbitals and

r, s, u, w, x, y represent the virtual orbitals and

$$\langle ij || kl \rangle = \int d\tau_1 \int d\tau_2 \phi_i^*(1) \phi_j^*(2) \frac{1}{|r_1 - r_2|} (1 - \hat{P}_{12}) \phi_k(1) \phi_l(2)$$

$$D_{ijkl} = \epsilon_i + \epsilon_j - \epsilon_k - \epsilon_l.$$

the linked-cluster expansion, therefore, neither unlinked bracketed diagrams like M and N of Fig. A3.1 nor the unlinked quadruple excited diagrams V and W of Fig. A3.2 are ever considered, and the theory is rigorously size-extensive upto any order for any n-tuple excitation.

A4 HOLE-PARTICLE FORMALISM

The idea of a vacuum state with no electrons is tacitly implied in the preceding discussion. When dealing with ground states it is convenient to redefine the 'vacuum' to represent the occupied ground state instead of the 'true vacuum' consisting of no particles. This vacuum is referred to as the Fermi vacuum. Use of this representation results in a considerable decrease in the number of creation-annihilation operators that need be considered. The Fermi vacuum state is then

$$|\Phi_0\rangle = \hat{a}_1^\dagger \hat{a}_2^\dagger \dots \hat{a}_n^\dagger |0\rangle \quad (\text{A4.1})$$

where $|0\rangle$ is the true vacuum.

In the Fermi vacuum representation, states occupied in $|\Phi_0\rangle$ are referred to as hole states, while these unoccupied are referred to as particle states. In this hole-particle formalism, the creation and annihilation operators \hat{a}_i^\dagger and \hat{a}_j can be reexpressed in terms of the hole-particle operators \hat{b}_i^\dagger , \hat{b}_j as,

$$\begin{aligned}
\hat{a}_r^\dagger &= \hat{b}_r^\dagger && \text{(creates particles)} \\
\hat{a}_r &= \hat{b}_r && \text{(destroys particle)} \\
\hat{a}_\alpha^\dagger &= \hat{b}_\alpha && \text{(destroys hole)} \\
\hat{a}_\alpha &= \hat{b}_\alpha^\dagger && \text{(creates hole)}
\end{aligned} \tag{A4.2}$$

α, β , etc. represent hole states while r, s , etc. represent particle states. i, j etc. are general indices and can be either hole or particle states. The contraction relationships between a 's and b 's are as below :

$$\begin{aligned}
\overbrace{\hat{a}_i \hat{b}_j} &= 0 \\
\overbrace{\hat{a}_i^\dagger \hat{b}_j} &= 0 \\
\overbrace{\hat{a}_i \hat{b}_j^\dagger} &= \delta_{ij} \quad \text{if } i = r, s, \text{ etc.} \\
&= 0 \quad \text{if } i = \alpha, \beta, \text{ etc.} \\
\overbrace{\hat{a}_i \hat{a}_j} &= 0 \\
\overbrace{\hat{a}_i^\dagger \hat{a}_j} &= \delta_{ij} \quad \text{if } i = \alpha, \beta, \dots \\
&= 0 \quad \text{if } i = r, s, \dots \\
\overbrace{\hat{b}_i \hat{a}_j} &= \delta_{ij} \quad \text{if } i = \alpha, \beta, \dots \\
&= 0 \quad \text{if } i = r, s, \dots \\
\overbrace{\hat{b}_i^\dagger \hat{a}_j} &= 0 \\
\overbrace{\hat{b}_i \hat{a}_j^\dagger} &= \delta_{ij} \quad \text{if } i = r, s, \dots, \quad \text{where } \delta_{ij} = \langle i | j \rangle \\
&= 0 \quad \text{if } i = \alpha, \beta, \dots \\
\overbrace{\hat{b}_i^\dagger \hat{a}_j^\dagger} &= 0
\end{aligned} \tag{A4.3}$$

A5 NORMAL PRODUCT OPERATORS AND WICK'S THEOREM

A normal product of operators $(\hat{c}_{1_1}, \hat{c}_{1_2}, \dots, \hat{c}_{1_k})$ where \hat{c}_i are either creation or annihilation operators is defined such that, all the creation operators are arranged to the left of all the annihilation operators in the product, i.e.,

$$N [\hat{c}_{k_1} \hat{c}_{k_2} \dots \hat{c}_{k_n}] = (-1)^p \hat{a}_{1_1}^\dagger \hat{a}_{1_2}^\dagger \dots \hat{a}_{1_r}^\dagger \hat{a}_{1_{r+1}} \dots \hat{a}_{1_n} \quad (\text{A5.1})$$

where p is the parity of permutation

$$p = \begin{pmatrix} k_1 & k_2 & \dots & k_n \\ 1_1 & 1_2 & \dots & 1_n \end{pmatrix}$$

The contraction of two operators \hat{c}_1 and \hat{c}_2 is then defined as

$$\overbrace{\hat{c}_1 \hat{c}_2} = \hat{c}_1 \hat{c}_2 - N [\hat{c}_1 \hat{c}_2] \quad (\text{A5.2})$$

All contractions vanish except for the case :

$$\overbrace{\hat{a}_i \hat{a}_j^\dagger} = \delta_{ij} \quad \text{or} \quad \overbrace{\hat{b}_i \hat{b}_j^\dagger} = \delta_{ij} \quad (\text{A5.3})$$

The normal product with contractions is defined as :

$$\begin{aligned} N [\hat{c}_1 \hat{c}_2 \dots \hat{c}_{1_1} \dots \hat{c}_{1_2} \dots \hat{c}_{k_1} \dots \hat{c}_{k_2} \dots \\ \hat{c}_{m_1} \dots \hat{c}_{m_2} \dots \hat{c}_{n_1} \dots \hat{c}_{n_2} \dots \hat{c}_k] \\ = (-1)^p \overbrace{\hat{c}_{1_1} \hat{c}_{k_2}} \overbrace{\hat{c}_{1_2} \hat{c}_{k_1}} \dots \overbrace{\hat{c}_{m_2} \hat{c}_{n_2}} \dots \dots \dots \\ N [\hat{c}_1 \hat{c}_2 \dots \hat{c}_{1_1-1} \dots \hat{c}_k] \end{aligned} \quad (\text{A5.4})$$

where p is the total parity of permutation.

Wick's theorem [6] is stated here without proof :

$$\hat{c}_1 \dots \hat{c}_k = N[\hat{c}_1 \dots \hat{c}_k] + \sum N[\underbrace{\hat{c}_1 \dots \hat{c}_i}_{\text{contracted}} \dots \underbrace{\hat{c}_{i+1} \dots \hat{c}_k}_{\text{contracted}}] \quad (\text{A5.5})$$

where the summation extends over normal products with all possible contractions of two operators, of four operators, etc. \hat{c}_i 's can be either second-quantised creation, annihilation operators or hole-particle operators.

The Hamiltonian $\hat{H} = \hat{Z} + \hat{V}$ can be expressed in the normal product form, using Wick's theorem.

$$\hat{Z} = \sum_{ik} \langle i | \hat{Z} | k \rangle \hat{a}_i^\dagger \hat{a}_k \quad (\text{A5.6})$$

The operator product in this expression can be written in normal product form as :

$$\begin{aligned} \hat{a}_i^\dagger \hat{a}_k &= N[\hat{a}_i^\dagger \hat{a}_k] + \overbrace{\hat{a}_i^\dagger \hat{a}_k}^{\text{contracted}} \\ &= N[\hat{a}_i^\dagger \hat{a}_k] + \langle i | k \rangle_{i,k \in \alpha, \beta \dots} \end{aligned} \quad (\text{A5.7})$$

Therefore,

$$\hat{Z} = \sum_{ik} \langle i | \hat{Z} | k \rangle N[\hat{a}_i^\dagger \hat{a}_k] + \sum_{i \in \alpha, \beta \dots} \langle i | \hat{Z} | i \rangle \quad (\text{A5.8})$$

The second term in the above equation is nothing but

$\langle \phi_0 | \hat{Z} | \phi_0 \rangle$. Eqn. (A5.8) may therefore be written as :

$$\hat{Z} = \langle \phi_0 | \hat{Z} | \phi_0 \rangle + \hat{Z}_N \quad (\text{A5.9})$$

where,

$$\hat{Z}_N = \sum_{ik} \langle i|\hat{Z}|k\rangle N[\hat{a}_i^\dagger \hat{a}_k] \quad (A5.10)$$

$$\hat{V} = \sum_{ijkl} \langle ij|\hat{V}|kl\rangle \hat{a}_i^\dagger \hat{a}_j^\dagger \hat{a}_l \hat{a}_k \quad (A5.11)$$

The operator product in this expression can be written in the normal product form as :

$$\begin{aligned} \hat{a}_i^\dagger \hat{a}_j^\dagger \hat{a}_l \hat{a}_k &= N[\hat{a}_i^\dagger \hat{a}_j^\dagger \hat{a}_l \hat{a}_k] + N[\overbrace{\hat{a}_i^\dagger \hat{a}_j^\dagger \hat{a}_l}^{\quad} \hat{a}_k] + \\ &\quad N[\overbrace{\hat{a}_i^\dagger \hat{a}_j^\dagger \hat{a}_k}^{\quad} \hat{a}_l] + N[\overbrace{\hat{a}_i^\dagger \hat{a}_j^\dagger \hat{a}_l}^{\quad} \hat{a}_k] + \\ &\quad N[\overbrace{\hat{a}_i^\dagger \hat{a}_j^\dagger \hat{a}_k}^{\quad} \hat{a}_l] + N[\overbrace{\hat{a}_i^\dagger \hat{a}_j^\dagger \hat{a}_l}^{\quad} \hat{a}_k] + \\ &\quad N[\overbrace{\hat{a}_i^\dagger \hat{a}_j^\dagger \hat{a}_l \hat{a}_k}^{\quad}] \\ &= N[\hat{a}_i^\dagger \hat{a}_j^\dagger \hat{a}_l \hat{a}_k] + N[\hat{a}_j^\dagger \hat{a}_l] \langle i|k\rangle_{i,k \in \alpha, \beta \dots} \\ &\quad - N[\hat{a}_j^\dagger \hat{a}_k] \langle i|l\rangle_{i,l \in \alpha, \beta} + N[\hat{a}_i^\dagger \hat{a}_k] \langle j|l\rangle_{j,l \in \alpha, \beta \dots} \\ &\quad - N[\hat{a}_i^\dagger \hat{a}_l] \langle j|k\rangle_{j,k \in \alpha, \beta} + [\langle i|k\rangle \langle j|l\rangle - \langle i|l\rangle \langle j|k\rangle] \\ &\quad \quad \quad i, j, k, l \in \alpha, \beta \dots \end{aligned} \quad (A5.12)$$

Substituting (A5.12) in (A5.11), we get

$$\begin{aligned} \hat{V} &= \frac{1}{2} \sum_{ijkl} \langle ij|\hat{V}|kl\rangle \{ N[\hat{a}_i^\dagger \hat{a}_j^\dagger \hat{a}_l \hat{a}_k] + N[\hat{a}_j^\dagger \hat{a}_l] \delta_{ik} + \\ &\quad N[\hat{a}_i^\dagger \hat{a}_k] \delta_{jl} - N[\hat{a}_j^\dagger \hat{a}_k] \delta_{il} - N[\hat{a}_i^\dagger \hat{a}_l] \delta_{jk} + \delta_{ik} \delta_{jl} - \delta_{il} \delta_{jk} \} \\ &= \hat{V}_N + \hat{G}_N + \langle \hat{\psi}_0 | \hat{V} | \hat{\psi}_0 \rangle \end{aligned} \quad (A5.13)$$

where,

$$\hat{V}_N = \gamma_2 \sum_{ijkl} \langle ij | \hat{V} | kl \rangle N[\hat{a}_i^\dagger \hat{a}_j^\dagger \hat{a}_l \hat{a}_k] \quad (\text{A5.14})$$

$$\hat{G}_N = \sum_{ik} \langle i | \hat{g} | k \rangle_A N[\hat{a}_i^\dagger \hat{a}_k] \quad (\text{A5.15})$$

with

$$\langle i | \hat{g} | k \rangle_A = \sum_{\xi} 2 \langle i\xi | \hat{V} | k\xi \rangle - \langle i\xi | \hat{V} | \xi k \rangle \quad (\text{A5.16})$$

the subscript A represents the antisymmetrisation of the matrix element.

The Hamiltonian in normal product form is therefore,

$$\begin{aligned} \hat{H} = & \langle \phi_0 | \hat{H} | \phi_0 \rangle + \sum_{ik} \langle i | \hat{f} | k \rangle N[\hat{a}_i^\dagger \hat{a}_k] + \\ & \gamma_2 \sum_{ijkl} \langle ij | \hat{V} | kl \rangle N[\hat{a}_i^\dagger \hat{a}_j^\dagger \hat{a}_l \hat{a}_k] \end{aligned} \quad (\text{A5.17})$$

where

$$\langle i | \hat{f} | k \rangle = \langle i | \hat{z} | k \rangle + \langle i | \hat{g} | k \rangle \quad (\text{A5.18})$$

A6 FURTHER EXAMPLES OF DIAGRAMMATICS

The applicability of Feynman-Goldstone diagrammatics extends well beyond perturbation theories. The diagrams and the rules for setting up matrix elements for non-perturbative theories are exactly analogous to those described earlier. The diagrams for the wavefunction, unlike the energy diagrams are open, and as discussed in Chapter II, a linked-cluster theorem can be proved for the wavefunction expansion as well. The elementary diagrams encountered in the non-perturbative

method are the "H" and "T" diagrams; these are presented in Fig. A6.1. Linking of these diagrams invokes the same set of rules prescribed earlier. Examples of such linking are illustrated in Fig. A6.2. Since in both "H" and "T" diagrams particle-hole operators occur in pairs, the linking results in none, one or two open-paths.

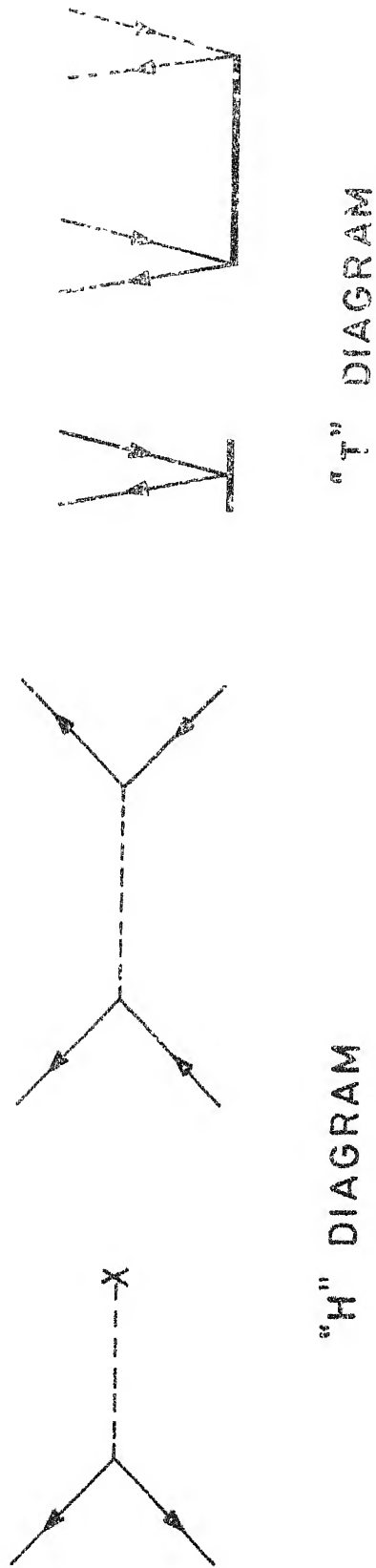


Fig. A 6.1 Examples of "H" and "T" diagrams.

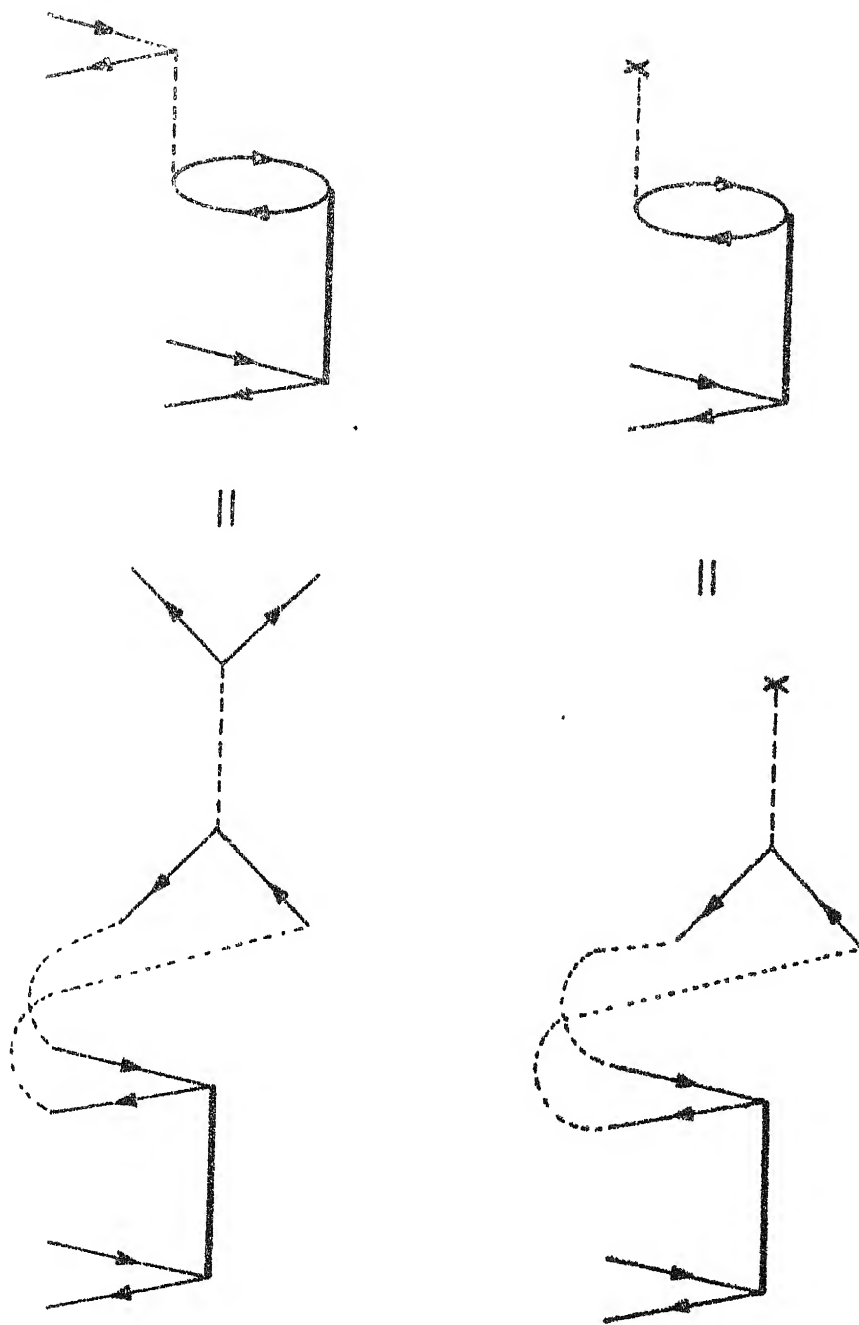


Fig. A6.2 Examples of "R" diagrams with one and two open-paths obtained by linking of "H" and "T" diagrams.

APPENDIX B

LISTINGS OF SOME PROGRAMS USED IN THIS THESIS

- I. Routine for General Matrix Element Evaluation
- II. Program for the Solution of Linear CC Equations
- III. Program for the Evaluation of r, r^2 and $1/r$
Expectation Values

CALCULATE THE GENERAL INTEGRAL R (JA,JB,JC,JD)

~~~~~  
 This subroutine evaluates the general matrix element over the wavefunctions from the Xalpha program. The subroutine has in common the radial wavefunctions of the main Xalpha program. Part of the program is adapted from the routines of Zare (vide - JILA Report 80, 1966). The 3J symbols necessary are generated by a separate program and input into this program. The routine calls the intes routine in which the integration is done  
 ~~~~~

The 3J coefficients are converted into the required CG matrix for multiplication of the radial integrals.

READ *, ((CG(I,J,K),K=1,3),J=1,4),I=1,4)

DO 22 I=1,4

DO 22 J=1,3

KA(I,J)=0.0

KA(1,1)=1

KA(1,2)=2

KA(1,3)=6

KA(2,1)=3

KA(2,2)=7

KA(3,1)=4

KA(3,2)=8

KA(4,1)=5

KA(4,2)=9

DO 198 JK=1,3

DO 199 I=1,4

DO 199 J=1,3

DO 199 M=1,4

DO 199 N=1,3

JA=KA(I,J)

JB=KA(M,N)

IF (JA.EQ.0) GO TO 199

IF (JB.EQ.0) GO TO 199

CON(JA,JB,JK)=CG(I,M,JK)

CONTINUE

CONTINUE

DO 110 J=2,441

SNN(1,J)=SNL(1,J)

SNN(2,J)=SNL(2,J)

DO 111 K=3,5

SNN(K,J)=SNL(3,J)

SNN(6,J)=SNL(4,J)

DO 112 K=7,9

SNN(K,J)=SNL(5,J)

CONTINUE

ML(1)=0

ML(2)=0

```

      ML(3)=1
      ML(4)=0
      ML(5)=-1
      ML(6)=0
      ML(7)=1
      ML(8)=0
      ML(9)=-1
      DO 114 JA=1,9
      DO 114 JB=1,9
      DO 114 JC=1,9
      DO 114 JD=1,9
      VEE(JA,JB,JC,JD)=0.0
      IF((ML(JA)+ML(JB)-ML(JC)-ML(JD)).NE.0) GO TO 114
      DO 115 JK=1,3
      JL=JK-1
      CALL INTEG(JA,JB,JC,JD,JL,RESULT,H)
129    CGS=CGN(JA,JC,JK)*CGN(JD,JB,JK)
115    VEE(JA,JB,JC,JD)=VEE(JA,JB,JC,JD)+RESULT*CGS
114    CONTINUE
      WRITE(2,*) (((VEE(JA,JB,JC,JD),JD=1,9),JC=1,9),JB=1,9),JA=1,9)
      RETURN
      END
      -----
c
c      This subroutine computes the matrix elements using the
c      method given in 'The Theory of Atomic Spectra' by
c      F.U.Condon and G.H.Shortely.
c
c      SUBROUTINE INTEG(JA,JB,JC,JD,JK,RESULT,H)
c      Titles subroutine computes R***K integrals.
c
c      RESULT R (JA,JB,JC,JD)
c      COMMON XNUM , RSVALE , RSATOM
c      COMMON V , SNLO , R , RU , RUEXCH , XI
c      COMMON XJ , SNL ,>NNLZ , WWNL , NKKK , EE
c      COMMON RU2 , RU3 , RUINL1 , RUFNL1 , RUINL2 , RUFNL2
c      COMMON/KONST/MESH,NCSPVS,Z,NBLOCK
c      DIMENSION X(441),RSCORE(441),RU2(441),RU(441),>NNLZ(5),R(441),
c      1RSVALE(441),RU3(441),XI(441),WWNL(5),V(441),RSATOM(441),
c      2 XJ(441),NKKK(5),EE(5),RUEXCH(441),DENM(441),
c      3 SNL(5,441),SNLO(441),A(5,5),OLNS(441),XNUM(441)
c      DIMENSION RUINL1(441),RUFNL1(441),RUINL2(441),RUFNL2(441)
c      EQUIVALENCE(RSCORE,XNUM),(RSVALE,DENM),(X,R)
c      DIMENSION SNN(9,441)
c      COMMON/RAD/SNN
c      -----
c      XI(1)=0.0
c      DO 70 I=2,MESH
c      XI(I)=1.0
c      CONTINUE
70

```

```

71      IF(JK) 2000,74,71
        DO 73 J=1,JK

          DO 72 I=2,MESH
            XI(I)=XI(I)*R(I)
72      CONTINUE
73      CONTINUE
C       XI(I) NOW CONTAINS THE ARRAY R(I)**JK
74      CONTINUE
        XJ(1)=0.0
        SNI0(I)=0.0
        OLNS(I)=0.0
        DO 75 I=2,MESH
          SNI0(I)=SNN(JA,I)*SNN(JI,I)
          OLNS(I)=SNN(JB,I)*SNN(JD,I)
C       SET UP ARRAYS OF REPEATEDLY USED WAVE FUNCTION PRODUCTS
C       XJ(I) NOW CONTAINS ARRAY 1/R(I)**JK+1
75      CONTINUE
        RSCORE(I)=0.0
10      DO 15 I=2,MESH
          RSCORE(I)=OLNS(I)
15      CONTINUE
        IF(JK) 20,30,20
20      DO 25 I=2,MESH
          RSCORE(I)=RSCORE(I)*XI(I)
25      CONTINUE
30      CONTINUE
        CALL SMP5N(RSCORE,RSVALF,H,NBLOCK,40)
        RSVALF(1)=0.0
        DO 35 I=2,MESH
          RSVALF(I)=RSVALF(I)*SNI0(I)*XJ(I)
35      CONTINUE
        CALL SJNT(RSVALF,H,RESUL1,NBLOCK)
        RSCORE(1)=0.0
        DO 40 I=2,MESH
          RSCORE(I)=OLNS(I)*XJ(I)
40      CONTINUE
        CALL SJNT(RSCORE,H,TOTINT,NBLOCK)
        CALL SMP5N(RSCORE,RSVALF,H,NBLOCK,40)
        RSVALF(1)=0.0
        DO 45 I=2,MESH
          RSVALF(I)=SNI0(I)*(TOTINT-RSVALF(I))
45      CONTINUE
        IF(JK) 50,60,50
50      DO 55 I=2,MESH
          RSVALF(I)=RSVALF(I)*XI(I)
55      CONTINUE
60      CONTINUE
        CALL SJNT(RSVALF,H,RESUL2,NBLOCK)

```

```

      RESULT=1.0*(RESUM1+RESUM2)
1000  RETURN
2000  WRITE(21,2001) JK
2001  FORMAT(' PROGRAM INTERNO NEG. J ',J3)
      STOP
      END
      SUBROUTINE SMPSN (Y,YI,DX,NB,NIN)
      DIMENSION Y(441), YI(441)
      ASUM=0.
      BSUM=0.
      YI(1)=0.
      H=DX/3.
      I=1
      G=H/4.
      KMAX=NIN/2.
      NIN MUST BE AN EVEN INTEGER
      DO 500 J=1,NB
      DO 400 K=1,KMAX
      J=I+2
      BSUM=BSUM+H*(Y(1-2)+4.*Y(I-1)+Y(1))
      YI(1)=ASUM+BSUM
400    YI(1-1)=YI(I-2)+G*(5.*Y(I-2)+8.*Y(I-1)-Y(I))
      ASUM=YI(1)
      BSUM=0.
      H=H+H
      G=G+G
500    CONTINUE
      RETURN
      END
      SUBROUTINE SINT(X,H,VALUE,NIN)
      SINT=EXTENDED SIMPSONS RULE INTEGRATION FORMULA
      OBTAINS INTEGRAL FROM 0 TO INFINITY OF X AND CALLS IT VALUE
      DIMENSION X(441)
      CURSUM=0.0
      RUNSUM=0.0
      HESH=H
      I=1
      DO 10 J=1,NIN
      C** NIN IS THE NUMBER OF FORTY POINT BLOCKS OVER WHICH THE INTEGRATION
      IS BEING CARRIED
      CURSUM=X(I)
      I=I+1
      DO 5 K=1,19
      CURSUM=CURSUM+4.*X(I)+2.*X(I+1)
      I=I+2
5      CONTINUE
      CURSUM=CURSUM+4.0*X(I)+X(I+1)

```

```
RUNSUM= RUNSUM+HMF GH*CURSUM  
CURSUM=0.0  
HMF GH=2.0*HMF SH  
I=I+1  
CONTINUE  
  
VALUE=RUNSUM/3.0  
RETURN  
END
```

10

C

```

c --- This program solves the linear part of the
c      coupled cluster equations. The linear equations
c      arising from one open-path diagrams are first
c      listed in the serial order 1 to M(N-M) and then
c
c      are listed the two open-path diagram equations
c      in the continuing sequential order M(N-M)+1 to
c      (N-M)*(N-M)*M*M. The latter are then reduced using the
c      symmetry  $t(Al,Bl,K,S)=t(Bl,Al,S,K)$ .
c      The inverse of the coefficient matrix is calculated and
c      multiplied by the coefficient vector.

```

```

COMMON/LABEL/IND(2,2,9,9)
INTEGER AL,BL,R,S,U,W,DL,EL,Z1
COMMON N,M,NM,M1
DIMENSION XX(210),TT(2,2,9,9),V(9,9,9,9),EN(9)
DIMENSION X(119),ML(9)
DIMENSION VL(9,9)
DIMENSION AX(119)
DIMENSION A(119,119),B(119)
OPEN(UNIT=20,DEVICE='DSK',FILE='LIN.DAT')
OPEN(UNIT=21,DEVICE='DSK',FILE='MET.DAT')
OPEN(UNIT=22,DEVICE='DSK',FILE='MET.OUT')
N = 9
M = 2
M1=M+1
NM=N-M
NOLD=210
NEQ=119
DO 10 J=1,NEQ
  B(1)=0.
  DO 10 J=1,NEQ
    A(1,J)=0.
c --- Input data for the linear equations -- the V,VL and En
c --- Matrix elements calculated from the Xalpha program.
  10 CONTINUE
  WRITE (22,999)
999  FORMAT(10X,'/// COUPLED CLUSTER EQUATION RESULTS ///')
  READ(20,9000)
9000  FORMAT (1H1,
1 60H
2
)
  READ(20,*) ALPHA,BETA
  READ(20,*)(((V(I,J,K,L),L=1,N),K=1,N),J=1,N),I=1,N)

```

```

READ(20,*)((VL(I,J),J=1,N),I=1,N)
READ(20,*)LO
READ(20,*)(EN(I),I=1,N)
WRITE(22,9000)
WRITE(22,99) ALPHA,BETA
99  FORMAT(5X,' ALPHA =',F15.9,10X,' BETA =',F15.9//)
WRITE(22,9001)
9001 FORMAT(' THE ORBITAL ENERGIES IN THE SEQUENCE 1S,2S,2P,3S,3P,3D')
WRITE(22,*)(EN(I),I=1,9)

c .....
c Indexing the t2 coefficients in proper order
K=15
DO 15 AL=1,M
DO 15 BT=1,M
DO 15 R=M1,N
DO 15 S=M1,N
IF ((AL.EQ.BT.AND.R.LT.S).OR.AL.LI.BT) GO TO 13
GO TO 14
13  IND(AL,BT,R,S)=K
K=K+1
GO TO 15
14  IND(AL,BT,R,S)=0
15  CONTINUE

c .....
c one open-path diagram equations with t1 and t2 coefficients
c .....
I=0
DO 20 AL=1,M
DO 20 R=M1,N
I=I+1
DO 21 ZI=1,2
B(I)=B(I)+VL(R,AL)-2.*V(R,ZI,AL,ZI)+V(R,ZI,ZI,AL)
21  CONTINUE
A(I,I)=A(I,1)+EN(R)-FN(AL)
DO 22 S=M1,N
DO 22 ZI=1,M
IF (S.EQ.R) GO TO 22
J=INDEX2(AL,S)
A(I,J)=A(I,J)+2.*V(R,ZI,S,ZI)-V(R,ZI,ZI,S)-VL(R,S)
22  CONTINUE
DO 23 BT=1,M
DO 23 ZI=1,M
IF(BT.EQ.AL) GO TO 23
J=INDEX2(BT,R)
A(I,J)=A(I,J)-(2.*V(BT,ZI,AL,ZI)-V(BT,ZI,ZI,AL)-VL(BT,AL))
23  CONTINUE
DO 30 BT=1,M
DO 30 S=M1,N
J=INDEX2(BT,S)

```

```

A(I,J)=A(I,J)+2.*V(R,BT,AL,S)-V(R,BT,S,AL)
30  CONTINUE
    DO 40 BT=1,M
    DO 40 S=M1,N
    DO 40 U=M1,N
    J=INDEX4(BT,AL,S,U)
    A(I,J)=A(I,J)+2.*V(R,BT,U,S)-V(R,BT,S,U)
40  CONTINUE
    DO 50 BT=1,M
    DO 50 DL=1,M
    DO 50 S=M1,N
    J=INDEX4(BT,DL,S,R)
    A(I,J)=A(I,J)-(2.*V(DL,BT,AL,S)-V(DL,BT,S,AL))
50  CONTINUE
    DO 52 DL=1,M
    DO 52 U=M1,N
    DO 53 ZI=1,M
    J=INDEX4(AL,DL,R,U)
    A(I,J)=A(I,J)+2.*(2.*V(DL,ZI,U,ZI)-V(DL,ZI,ZI,U)-VL(DL,U))
53  CONTINUE
52  CONTINUE
    DO 54 DL=1,M
    DO 54 U=M1,N
    DO 54 ZI=1,M
    J=INDEX4(AL,DL,U,R)
    A(I,J)=A(I,J)-(2.*V(DL,ZI,U,ZI)-V(DL,ZI,ZI,U)-VL(DL,U))
54  CONTINUE
    20  CONTINUE
C--- ..... two open-path diagram equations with t1 and t2 coefficients .....
C--- .....
C--- .....
I=14
DO 60 AL=1,M
DO 60 BT=1,M
DO 60 R=M1,N
DO 60 S=M1,N
K=INDEX4(AL,BT,R,S)
IF ((AL.EQ.BT.AND.R.LE.S).OR.AL.LT.BT) GO TO 777
GO TO 60
777 CONTINUE
I=I+1
R(1)=-V(R,S,AL,BT)
A(1,I)=A(1,I)+EN(R)+LN(S)-EN(AL)-EN(BT)
DO 61 U=M1,N
DO 61 ZI=1,M
J=INDEX4(AL,BT,U,S)
IF (U.EQ.R) GO TO 61
A(I,J)=A(I,J)+(2.*V(R,ZI,U,ZI)-V(R,ZI,ZI,U)-VL(R,U))
61 CONTINUE

```

```

DO 62 U=M1,N
DO 62 Z1=1,M
J=INDEX4(BT,AL,U,R)
IF (U.EQ.S) GO TO 62
A(I,J)=A(I,J)+(2.*V(S,Z1,U,Z1)-V(S,Z1,Z1,U)-VL(S,U))
62 CONTINUE
DO 63 DL=1,M
DO 63 Z1=1,M
J=INDEX4(DL,BT,R,S)
IF (DL.EQ.AL) GO TO 63
A(I,J)=A(I,J)-(2.*V(AL,Z1,DL,Z1)-V(AL,Z1,Z1,DL)-VL(AL,DL))
63 CONTINUE
DO 64 DL=1,M
DO 64 Z1=1,M
J=INDEX4(DL,AL,S,R)
IF (DL.EQ.BT) GO TO 64
A(I,J)=A(I,J)+(2.*V(BT,Z1,DL,Z1)-V(BT,Z1,Z1,DL)-VL(BT,DL))
64 CONTINUE
DO 70 U=M1,N
DO 70 DL=1,M
J=INDEX4(DL,BT,U,S)
A(I,J)=A(I,J)+2.*V(R,DL,AL,U)-V(R,DL,U,AL)
J=INDEX4(DL,AL,U,R)
A(I,J)=A(I,J)+2.*V(S,DL,BT,U)-V(S,DL,U,BT)
J=INDEX4(DL,BT,S,U)
A(I,J)=A(I,J)-V(R,DL,AL,U)
J=INDEX4(DL,BT,R,U)
A(I,J)=A(I,J)-V(S,DL,U,AL)
J=INDEX4(DL,AL,R,U)
A(I,J)=A(I,J)-V(S,DL,BT,U)
J=INDEX4(DL,AL,S,U)
A(I,J)=A(I,J)-V(R,DL,U,BT)
70 CONTINUE
DO 80 U=M1,N
DO 80 W=M1,N
J=INDEX4(AL,BT,U,W)
A(I,J)=A(I,J)+0.5*V(R,S,U,W)
J=INDEX4(BT,AL,U,W)
A(I,J)=A(I,J)+0.5*V(S,R,U,W)
80 CONTINUE
DO 90 DL=1,M
DO 90 EP=1,M
J=INDEX4(DL,EP,R,S)
A(I,J)=A(I,J)+0.5*V(AL,BT,DL,EP)
J=INDEX4(DL,LP,S,R)
A(I,J)=A(I,J)+0.5*V(BT,AL,DL,EP)
90 CONTINUE
DO 91 U=M1,N
J=INDEX2(AL,U)

```

```

      A(I,J)=A(I,J)+V(R,S,U,BI)
      J=INDEX2(BI,U)
      A(I,J)=A(I,J)+V(S,R,U,AL)
91    CONTINUE
      DO 92 DL=1,M
      J=INDEX2(DL,R)
      A(I,J)=A(I,J)-V(DL,S,AL,BI)
      J=INDEX2(DL,S)
      A(I,J)=A(I,J)-V(DL,R,BI,AL)
92    CONTINUE
60    CONTINUE

```

```

c- call the routine for the solution of the system of equations
CALL LICQ(A,NLQ,B,X)
c- check if the solutions satisfy the equation to 1.e 7 accuracy
DO 19 I=1,119
  AX(I)=0.
  DO 27 J=1,119
27  AX(I)=AX(I)+A(I,J)*X(J)
    DIFF=AX(I)-B(I)
    IF(DIFF,LT,1.E-7) GO TO 19
    WRITE (22,*)DIFF,I
19  CONTINUE
c- reconversion of the reduced number to the original number
c- coefficients. for the case Be series the conversion takes
c- the 119 coefficients to 210 coefficients.
  I=14
  DO 150 AL=1,M
  DO 150 RT=1,M
  DO 150 R=M1,N
  DO 150 S=M1,N
    I=I+1
    II=INDEX4(AL,BI,R,S)
    XX(I)=X(II)
150  CONTINUE
c- call the routine that evaluates the exchange-correlation
c- corrections using the coefficients and matrix elements.
CALL COREN(XX,V,EN,N,F0,M)
c- output from this program to be used as input in the
c- nonlinear program.
WRITE(21,*)((V(I,J,K,L),L=1,9),K=1,9),J=1,9),I=1,9)
WRITE(21,*)((V(I,J),J=1,9),I=1,9)
WRITE(21,*)(EN(I),I=1,9)
WRITE (21,*) (XX(I),I=1,210)
STOP
END
c- ordering the ti coefficients sequentially

```

```

FUNCTION INDEX2(AL,K)
COMMON N,M,NM,M1
INDEX2 = NM*(AL-1)+(K M)
RETURN
END
c-- ordering the t2 coefficients sequentially
FUNCTION INDEX4(AL,BT,R,S)
COMMON N,M,NM,M1
COMMON/LABEL/INI(2,2,9,9)
INTEGER AL,BT,R,S
IF ((AL.EQ.BT.AND.R.LL.S).OR.AL.LT.BT) GO TO 11
INDEX4=IND(BT,AL,S,R)
RETURN
11 INDEX4=1ND(AL,BT,R,S)
RETURN
END
c-- routine for solving the linear system of equations.
c-- this routine is based on the LU decomposition algorithm.
SUBROUTINE LIEQ(A,NN,R,X)
c Master program to coordinate the subroutines:
c Decomp,Solve,Impruv and Sing.
DIMENSION A(NN,NN),B(NN),X(NN)
COMMON/AREA1/UL(119,119)
CALL DECOMP(NN,A)
CALL SOLVE(NN,R,X)
CALL IMPRUV(NN,A,R,X,DIGITS)
RETURN
END
SUBROUTINE DECOMP(NN,A)
DIMENSION A(NN,NN),SCALES(119)
COMMON/AREA1/UL(119,119)
COMMON/AREA2/IPS(119)
N=NN
c-- initialize IPS,UL,AND SCALES.
DO 5 I=1,N
  IPS(I)=I
  ROWNRM=0.0
  DO 2 J=1,N
    UL(I,J)=A(I,J)
    IF(ROWNRM-ABS(UL(I,J))) 1,2,2
1 ROWNRM=ABS(UL(I,J))
2 CONTINUE
  IF(ROWNRM) 3,4,3
3 SCALES(I)=1.0/ROWNRM
  GO TO 5
4 CALL SING(1)
  SCALES(I)=0.0
5 CONTINUE
c-- Gaussian elimination with partial pivoting.

```

```

NM1=N-1
DO 17 K=1,NM1
BIG=0.0
DO 11 I=K,N
IP=IPS(I)
SIZE=ABS(UL(IP,K))*SCALE3(IP)
IF(STE-BIG) 11,11,10
10 BIG=SIZE
IDXP1V=I
11 CONTINUE
IF(BIG) 13,12,13
12 CALL SING(2)
GO TO 17
13 IF(IDXP1V-K) 14,15,14
14 J=IPS(K)
IPS(K)=IPS(IDXP1V)
IPS(IDXP1V)=J
15 KP=IPS(K)
PIVOT=UL(KP,K)
KP1=K+1
DO 16 I=KP1,N
IP=IPS(I)
EM=UL(IP,K)/PIVOT
UL(IP,K)=-EM
DO 16 J=KP1,N
UL(IP,J)=UL(IP,J)+EM*UL(KP,J)
16 CONTINUE
17 CONTINUE
KP=IPS(N)
IF(UL(KP,N)) 19,18,19
18 CALL SING(2)
19 RETURN
END

SUBROUTINE SOLVE(NN,B,X)
DIMENSION B(NN),X(NN)
COMMON/AREA1/UL(119,119)
COMMON/AREA2/IPS(119)
N=NN
NP1=N+1
IP=IPS(1)
X(1)=B(IP)
DO 2 I=2,N
IP=IPS(I)
IM1=I-1
SUM=0.0
DO 1 J=1,IM1
1 SUM=SUM+UL(IP,J)*X(J)
2 X(I)=B(IP)-SUM
IP=IPS(N)

```

```

X(N)=X(N)/UL(IP,N)
DO 4 IBACK=2,N
  I=NP1-IBACK
C   I GOES (N-1),...,1
  IF=IPS(I)
  TP1=I+1
  SUM=0.0
  DO 3 J=IF1,N
3    SUM=SUM+UL(IP,J)*X(J)
4    X(I)=(X(I)-SUM)/UL(IP,I)
  RETURN
END
SUBROUTINE IMPROV(NN,A,B,X,DIGITS)
  DIMENSION A(NN,NN),B(NN),X(NN),R(119),DX(119)
  COMMON/AREA1/UL(119,119)
  DOUBLE PRECISION SUM
  N=NN
  EPS=1.0E-8
  ITMAX=16
  XNORM=0.0
  DO 1 I=1,N
1    XNORM=AMAX1(XNORM,ABS(X(I)))
  IF(XNORM) 3,2,3
2  DIGITS=-A10G10(EPS)
  GO TO 10
3  DO 9 ITER=1,ITMAX
  DO 5 J=1,N
  SUM=0.0
  DO 4 J=1,N
4    SUM=SUM+A(I,J)*X(J)
  SUM=B(I)-SUM
5  R(I)=SUM
  CALL SOLVE(N,R,DX)
  DXNORM=0.0
  DO 6 I=1,N
  T=X(I)
  X(I)=X(I)+DX(I)
  DXNORM=AMAX1(DXNORM,ABS(X(I)-T))
6  CONTINUE
  IF(ITER=1) 8,7,8
7  DIGITS=-A10G10(AMAX1(DXNORM/XNORM,EPS))
8  IF(DXNORM-EPS*XNORM) 10,10,7
9  CONTINUE
  CALL SING(3)
10 RETURN
  END
SUBROUTINE SING(IWHY)
11  FORMAT(10X,'MATRIX WITH ZERO ROW IN DECOMPOSE.'/)
12  FORMAT(10X,'SINGULAR MATRIX IN DECOMPOSE. ZERO DIVIDE IN SOLVE.'/)

```

```

13  FORMAT(10X,'NO CONVERGENCE IN IMPROV. MATRIX IS NEARLY SINGULAR.')
    GO TO (1,2,3),TWHY
1   PRINT 11
    GO TO 10
2   PRINT 12
    GO TO 10
3   PRINT 13
10  RETURN
    END

```

```

C -----
C This routine calculates the exchange-correlation corrections.
C -----

```

```

SUBROUTINE COREN(XX,V,I,N,N+EO,M)
  INTEGER AL,BT,R,S
  DIMENSION XX(210),FN(9),V(9,9,9,9)
  DIMENSION I(2,2,9,9),IX(2,9)
  DIMENSION L(2,2,9,9)
  NM=N-M
  M1=M+1
  WRITE (22,28)
  L=0
  DO 19 AL=1,M
    DO 19 R=M1,N
      L=I+1
      TX(AL,R)=XX(1)
19  CONTINUE
      DO 23 AL=1,M
        DO 23 BT=1,M
          DO 23 R=M1,N
            DO 23 S=M1,N
              I=NM*(NM*(AL-1)+NM*(BT-1)+(R-M-1))+(S-M)+14
              T(AL,BT,R,S)=XX(I)
              WRITE (22,24) R,S,AL,BT,XX(I)
              E(AL,BT,R,S)=0.
23  CONTINUE
28  FORMAT( / 'The t2 coefficients obtained from linear equation')
24  FORMAT( / '<',11,11,'t2',11,11,'>',5X,F15.8)
      CELE=0.
      DO 100 AL=1,M
        DO 100 BT=1,M
          DELE=0.
          DO 90 R=M1,N
            DO 90 S=M1,N
              E(AL,BT,R,S)=0.5*V(R,S,AL,BT)*(2.*T(AL,BT,R,S)-T(AL,BT,S,R))
              DELE=DELE+E(AL,BT,R,S)
              EONE=EONE+(2.*V(R,S,AL,BT)-V(R,S,BT,AL))*TX(AL,R)*TX(BT,S)
90  CONTINUE
      CELE=CELE+DELE

```

```

26      WRITE (22,26) AL,RI,IELF
      FORMAT( ' exchange-correlation correction for the pair',12,'s',
112,'s',3X,'=',F15.9,5X,'HARTREES')
100     CONTINUE
      WRITE(22,46) EONE
46      FORMAT( ' The one electron contribution =',5X,F15.8)
      WRITL (22,27) CELE
27      FORMAT( ' The total exchange-correlation correction =',5X,
1F15.9,5X,'HARTREES')
      ETOT=CELE+E0*0.5
      WRITE(22,33) FTO1
33      FORMAT( ' THE TOTAL ENERGY WITH EXCHANGE-CORRELATION CORRECTION',
15X,'-',F15.9,3X,'HARTREES')
      WRITE(22,29)
29      FORMAT( ' NOW FOLLOW THE PAIRWISE EXCITATION CONTRIBUTIONS ')
      DO 30 AL=1,M
      DO 30 RI=1,M
      DO 30 R=M1,N
      DO 30 S=M1,N
      IF(E(AL,RI,R,S).EQ.0.) GO TO 30
      WRITE(22,31) AL,RI,R,S,E(AL,RI,R,S)
31      FORMAT(10X,' E(',J1,',',I1,',',I1,',',I1,') =',5X,F15.9)
30      CONTINUE
      CALL ANAL(F)
      RETURN
      END

```

```

c -----
c The following routine does the partial-wave analysis of the
c exchange-correlation corrections.

```

```

      SUBROUTINE ANAL(F)
      DIMENSION E(2,2,9,9)
      WRITE (22,6)
6      FORMAT( 20X,'// PARTIAL WAVE ANALYSIS OF EX-COR ENERGY //',/)
      WRITE (22,7)
7      FORMAT(15X,'-----',/)
      1-----',/)
      WRITE(22,14)
14      FORMAT( 11X,'PAIK',20X,'SS',28X,'PP',/)
      WRITE (22,7)
      DO 8 I=1,2
      DO 8 J=1,2
      IF (I.GT.J) GO TO 8
      PWEN=0.
      DO 12 K=3,9
      DO 12 L=3,9
      IF(K.EQ.6.AND.L.EQ.6) GO TO 10
      PWEN=PWEN+E(I,J,K,L)
      GO TO 12
10      PWEN1=E(I,J,K,L)
12      CONTINUE

```

```

      IF (I.EQ.1.AND.J.EQ.1) GO TO 21
      IF (I.EQ.1.AND.J.EQ.2) GO TO 22
      IF (I.EQ.2.AND.J.EQ.2) GO TO 23
21    WRITE (22,31) PWEN1,PWEN
      GO TO 8
22    PWEN=2.*PWEN
      PWEN1=2.*PWEN1
      WRITE (22,32) PWEN1,PWEN
      GO TO 8
23    WRITE (22,33) PWEN1,PWEN
31    FORMAT(11X,'1s2',15X,F15.9,15X,F15.9,/)
32    FORMAT(10X,'1s2s',15X,F15.9,15X,F15.9,/)
33    FORMAT(11X,'2s2',15X,F15.9,15X,F15.9,/)
      WRITE (22,40)
40    FORMAT(15X,'.-----'//
      1-----'//)
      8    CONTINUE
      RETURN
      END

```

PROGRAM TO EVALUATE THE EXPECTATION VALUES OF THE OPERATORS
 R^{-2} , R AND $1/R$ USING THE CLUSTER EXPANDED WAVE FUNCTION
 FOR BERYLLIUM ISOELECTRONIC SERIES OF ATOMIC SYSTEMS

INPUT IS FROM TWO DISK FILES AND THE TTY
 THE TTY INPUT (ACCEPT STATEMENT) IS ENTERED INTO THE
 CONTROL FILE IN THE BATCH MODE
 THE FILE DSK:IVAL.DAT CONTAINING $\alpha_1, \alpha_2, \alpha_3, \alpha_4$ VALUES
 IS OUTPUT FROM THE CLUSTER EQUATIONS PROGRAM
 THE FILE DSK:FOR04.DAT CONTAINING THE MATRIX ELEMENTS OF
 THE OPERATORS OVER THE HF'S NUMERICAL ORBITALS IS GENERATED VIA
 THE MODIFIED "ZARK" PROGRAM. THESE VALUES ARE, HOWEVER,
 ONLY OVER THE RADIAL PARTS. ANGULAR FACTORS ARE INTRODUCED
 WITHIN THIS ROUTINE.

THE OUTPUT IS WRITTEN ONTO THE FILE
 DSK:ONEINT.OUT
 WHICH IS APPENDED TO ON EVERY SUBSEQUENT RUN
 OF THIS PROGRAM

```

DIMENSION T(2,2,3,9,3,9)
DIMENSION AOINT(9,9)
INTEGER AL,BT,R,S,K(9)
LOGICAL HI,LO
DOUBLE PRECISION PROP1(3),CASE
DATA PROP1/' R ' 2 ' , ' R ' , ' 1 / R ' /

```

```

OPEN(UNIT=4,DEVICE='DSK')
OPEN(UNIT=5,DEVICE='DSK',FILE='IVAL.DAT')
OPEN(UNIT=6,DEVICE='DSK',FILE='ONEINT.OUT',ACCESS='APPEND')

```

A TITLE OF 10 CHARACTER LENGTH IS READ IN

```
ACCEPT 109,CASE
```

```
FORMAT(A10)
```

```
WRITE(6,209)CASE
```

```

209 FORMAT(//////////, ' *****',//
1 ' * CASE: ', A10, ' *',//
2 ' *****')

```

```

READ(5,*) (((((AL,BT,R,S),S=3,9),R=3,9),BT=1,2),AL=1,2)
DO 9999 IPR=1,3

```

```

READ(4,*) ((AOINT(I,J),I=1,9),J=1,9)
WRITE(6,888)PROP1(IPR)

```

```

888 FORMAT(//// '==== 1- LI PROPERTY : ',A10,'====')

```

ANGULAR FACTORS FOR AO INTEGRALS ARE INTRODUCED

```

DO 1 I=1,9
K(I)=I

```

```

1      IF(I.GT.6)K(I)=I-4
      IF (I.EQ.1.OR.J.EQ.2.OR.I.EQ.6) K(I)=0
      CONTINUE

      DO 2 I=1,9
      DO 2 J=1,9
      IF(K(I).EQ.K(J))GO TO 2
      AOINT(I,J)=0.
2      CONTINUE

      WRITE(6,400)((AOINT(I,J),J=1,9),I=1,9)
400    FORMAT(/// ***** 1-11 INT OVER A0'S ***** '/( '9F10.6)
      IF(JPR.NE.1)GO TO 86

C      THE "1" VALUES ARE CONVERTED TO THE CORRESPONDING
C      CT COEFFICIENTS
C
      DO 3 AL=1,2
      DO 3 BT=1,2
      DO 3 R=3,9
      DO 3 S=3,9
      T(AL,BT,R,S)=T(AL,BT,R,S)/4.0
3      CONTINUE

C
86     CONTINUE

C      CALCULATION FOR REFERENCE STATE SINGLE DET
C
67     CONTINUE
      SUM=0
      DO 10 I=1,2
10     SUM=SUM+2*AOINT(I,I)

      BASE=SUM

      WRITE(6,200) SUM
200    FORMAT(/// ' EXPECTATION VALUE= '9F12.5,
1' FOR REFERENCE S DET')

C      EVALUATION OF NORMALISATION FACTOR

C      ANORM=1.
      THE FACTOR PRE ACCOUNTS FOR SPINS
      DO 20 AL=1,2
      DO 20 BT=1,2
      DO 20 R=3,9
      DO 20 S=3,9
      PRE=6.

```

```

      IF (AL.EQ.BT.OR.R.EQ.S)PRL=2.
      IF (AL.EQ.BT.AND.R.EQ.S)PRL=1.
      ANORM=ANORM+I(AL,BT,R,S)*I(AL,BT,R,S)*PRL
20    CONTINUE

C      EVALUATE THE CONTRIBUTIONS FROM OTHER DETERMINANTS

      DO 100 AI=1,2
      DO 100 BI=1,2
      DO 100 R=3,9
      DO 100 S=3,9

      DO 99 IAL=1,2
      DO 99 IBT=1,2
      DO 99 IR=3,9
      DO 99 IS=3,9
      FAC=I(AL,BT,R,S)*I(IAL,IBT,IR,IS)

C      COMPARE THE SETS { AL,BT,R,S } AND { IAL,IBT,IR,IS }

      LO=(R.EQ.IR.AND.S.EQ.IS).OR.(R.EQ.IS.AND.S.EQ.IR)
      HI=(AL.EQ.IAL.AND.BT.EQ.IBT).OR.(AL.EQ.IBT.AND.BT.EQ.IAL)
      IF(.NOT.(HI.OR.LO))GO TO 91
      IF(LO.AND.HI)GO TO 51
      IF(LO)GO TO 41

C      NON-IDENTITY AMONG { R,S } AND { IR,IS }
C      CHECK IF ONLY ONE DIFFERENCE EXISTS AND BRANCH

      IF (R.EQ.IR) GO TO 32
      IF (S.EQ.IS) GO TO 33
      IF (R.EQ.IS) GO TO 34
      IF (S.EQ.IR) GO TO 35
      GO TO 91
32    M=S
      N=IS
      GO TO 80
33    M=R
      N=IR
      GO TO 80
34    M=IS
      N=R
      GO TO 80
35    M=IR
      N=S
      GO TO 80
41    CONTINUE

C      NON-IDENTITY AMONG { AL,S } AND { IAL,IS }
C      CHECK IF ONLY ONE DIFFERENCE EXISTS AND BRANCH

```

```

      IF (AL.EQ.IAL) GO TO 42
      IF (BT.EQ.TBT) GO TO 43
      IF (AL.EQ.TBT) GO TO 44
      IF (BT.EQ.JAL) GO TO 45
      GO TO 91
42    M=BT
      N=TBT
      GO TO 80
43    M=AL
      N=JAL
      GO TO 80
44    M=TBT
      N=AL
      GO TO 80
45    M=IAL
      N=BT
      GO TO 80

C      INDEX SETS IDENTICAL

51    CONTINUE
      CONTR=BASF+ADINT(K,R)+ADINT(S,S)-ADINT(AL,AL)-ADINT(BT,BT)
      PRE=-6.
      IF(AL.EQ.BT.OR.R.EQ.S)PRE=-2.
      IF(AL.EQ.BT.AND.R.EQ.S)PRE=-1.
      SUM=SUM+IAC*CONTR*PRE
      GO TO 99

C      ONE DIFFERENCE IN INDEX SET

80    SUM=SUM+IAC*ADINT(M,N)
      GO TO 99

C
C      THE INDEX SETS DIFFER BY MORE THAN ONE
C
91    CONTINUE
C
99    CONTINUE
C
100   CONTINUE

C      NORMALISE THE RESULT AND OUTPUT

      SUM=SUM/ANORM
      WRITE(6,300) SUM
300   FORMAT(/// '      EXPECTATION VALUE= ',F12.5,

```

1 ' ALL CONFES INCLUDED')

9999 CONTINUE
 STOP
 END